National Library of Canada
Bibliothèque nationale du Canada

Acquisitions and Bibliographic Services Branch
Direction des acquisitions et des services bibliographiques

395 Wellington Street
Ottawa, Ontario
K1A 0N4

395, rue Wellington
Ottawa (Ontario)
K1A 0N4

Your file Votre référence

Our file Notre référence

NOTICE

The quality of this microform is heavily dependent upon the quality of the original thesis submitted for microfilming. Every effort has been made to ensure the highest quality of reproduction possible.

If pages are missing, contact the university which granted the degree.

Some pages may have indistinct print especially if the original pages were typed with a poor typewriter ribbon or if the university sent us an inferior photocopy.

Reproduction in full or in part of this microform is governed by the Canadian Copyright Act, R.S.C. 1970, c. C-30, and subsequent amendments.

AVIS

La qualité de cette microforme dépend grandement de la qualité de la thèse soumise au microfilmage. Nous avons tout fait pour assurer une qualité supérieure de reproduction.

S'il manque des pages, veuillez communiquer avec l'université qui a conféré le grade.

La qualité d'impression de certaines pages peut laisser à désirer, surtout si les pages originales ont été dactylographiées à l'aide d'un ruban usé ou si l'université nous a fait parvenir une photocopie de qualité inférieure.

La reproduction, même partielle, de cette microforme est soumise à la Loi canadienne sur le droit d'auteur, SRC 1970, c. C-30, et ses amendements subséquents.

Canada

CORTICAL FUNCTION IN VISIBLE PERSISTENCE: EVIDENCE FROM VISUAL EVOKED POTENTIALS

by

Blake W. Johnson

B.Sc., University of Alberta, 1985 (With Distinction)

M.A., Simon Fraser University, 1987

THESIS SUBMITTED IN PARTIAL FULFILLMENT OF THE REQUIREMENTS

FOR THE DEGREE OF DOCTOR OF PHILOSOPHY

in the Department

of

PSYCHOLOGY

© Blake W. Johnson, 1992

SIMON FRASER UNIVERSITY

August, 1992

All rights reserved. This work may not be reproduced in whole or in part, by photocopy or other means, without permission of the author.

National Library of Canada
Bibliothèque nationale du Canada

Acquisitions and Bibliographic Services Branch
Direction des acquisitions et des services bibliographiques

395 Wellington Street
Ottawa, Ontario
K1A 0N4

395, rue Wellington
Ottawa (Ontario)
K1A 0N4

Your file Votre référence

Our file Notre référence

The author has granted an irrevocable non-exclusive licence allowing the National Library of Canada to reproduce, loan, distribute or sell copies of his/her thesis by any means and in any form or format, making this thesis available to interested persons.

L'auteur a accordé une licence irrévocable et non exclusive permettant à la Bibliothèque nationale du Canada de reproduire, prêter, distribuer ou vendre des copies de sa thèse de quelque manière et sous quelque forme que ce soit pour mettre des exemplaires de cette thèse à la disposition des personnes intéressées.

The author retains ownership of the copyright in his/her thesis. Neither the thesis nor substantial extracts from it may be printed or otherwise reproduced without his/her permission.

L'auteur conserve la propriété du droit d'auteur qui protège sa thèse. Ni la thèse ni des extraits substantiels de celle-ci ne doivent être imprimés ou autrement reproduits sans son autorisation.

ISBN 0-315-91068-2

Canada

APPROVAL

NAME: Blake Warren Johnson

DEGREE: Doctor of Philosophy

TITLE OF PROJECT: Cortical Function In Visible Persistence: Evidence From Visual Evoked Potentials

EXAMINING COMMITTEE:

Chair: Dr. J. Koepke

Dr. H. Weinberg
Professor
Senior Supervisor

Dr. R. Koopman
Associate Professor

Dr. V. Modigliani
Professor

Dr. C. MacKenzie
Associate Professor

Dr. D.B. MacDonald
Director, EEG Laboratory
Faculty of Medicine
University of British Columbia
External Examiner

DATE APPROVED: August 26, 1992

PARTIAL COPYRIGHT LICENSE

I hereby grant to Simon Fraser University the right to lend my thesis, project or extended essay (the title of which is shown below) to users of the Simon Fraser University Library, and to make partial or single copies only for such users or in response to a request from the library of any other university, or other educational institution, on its own behalf or for one of its users. I further agree that permission for multiple copying of this work for scholarly purposes may be granted by me or the Dean of Graduate Studies. It is understood that copying or publication of this work for financial gain shall not be allowed without my written permission.

Title of Thesis/Project/Extended Essay

Cortical function in visible persistence: Evidence from visual evoked potentials.

Author: _____
(signature)

[redacted] Blake Johnson
(name)

September 1, 1992
(date)

ABSTRACT

Two major theoretical accounts of visible persistence ("storage" and "processing" hypotheses) assign crucially different roles to the neural activity associated with the onset and offset of visual stimuli. Visual evoked potentials (VEPs) were measured from three human observers in a temporal integration of form parts paradigm. In support of a processing model, the temporal patterning of VEPs was found to be strikingly related to stimulus onset asynchrony. VEP components were localized to extrastriate regions of visual cortex by means of equivalent dipole estimations. Taken together, the temporal and spatial characteristics of the VEPs associated with temporal integration support the interpretation that visible persistence may be identified more fittingly with ongoing neural processes than with the decaying contents of a sensory store.

ACKNOWLEDGMENTS

I would like to thank the members of my committee, particularly my supervisor, Hal Weinberg, as well as Vito Modigliani and Ray Koopman, for their advice in the development of this thesis, and the external examiners, Dr. D.B. MacDonald and Dr. Christine MacKenzie for their helpful criticisms and comments.

I would also like to express thanks to my past and present colleagues in the Brain Behavior Laboratory: Tony Robertson, Doug Cheyne, Dianne Crisp and Giselle Carriere, for their help and encouragement over the last six years.

Finally, I would like to thank my wife, Sandra, and my daughter, Tara, for their love and support through the writing of this thesis.

TABLE OF CONTENTS

Approval ii

Abstract iii

Acknowledgments iv

Table of Contents v

List of Tables viii

List of Figures ix

Introduction 1

- Visible Persistence 1
- Theoretical Background 2
  - Iconic Memory 2
  - Classification of Persistence Effects 4
  - Theories of Visible Persistence 6
    - Storage Hypothesis 7
    - Processing Hypothesis 9
  - The Locus of Visible Persistence 13
- Present study 15
  - Psychophysical Measures 16
  - Visual Evoked Potentials: Temporal Properties 17
  - Visual Evoked Potentials: Source Localization 19
    - Source Derivation 20
    - Dipole Source Potential Analysis 22
    - The Volume Conductor 24
- Conceptual Outline of the Present Study 25

Part 1: Temporal Patterning of Visual Evoked Potentials 26

Experiment 1 26

Introduction 26

Method 26

Results and Discussion 30

Experiment 2 43

Introduction 43

Methods 46

Results and Discussion 49

Part 2: Spatial patterning of visual evoked potentials 67

Introduction 67

1. Scalp Topography 68

Method 68

Results 69

Discussion 89

2. Source Localization 89

Previous VEP Source Localization Studies 89

Source Localization in the Present Study 91

Method 91

Results 95

Discussion 131

Summary and Conclusions 132

Appendix 1: Sources and Source localization 136

Sources In the Brain 136

Static Fields 136

Electrostatic Fields 137

Electric Potential Energy 138

Neuronal Current Sources 140

Morphological Considerations 143

Cortical Histology 143

Open and Closed Fields 145

Criticisms of the Open-Field Model 148

Physiological Considerations: Action Potentials and Postsynaptic Potentials 150

Source Localization 153

The Forward and Inverse Problems 153

Model of the Source: The Current Dipole 156

Physiological Significance of the Dipole Model 158

Models of the Volume Conductor 159

References 161

LIST OF TABLES

Table

1. Single moving dipole source estimates (left hemifield stimulation). 116

2. Single moving dipole source estimates (right hemifield stimulation). 117

3. Single moving dipole source estimates (lower hemifield stimulation). 118

4. Single moving dipole source estimates (upper hemifield stimulation). 119

5. Two dipole spatio-temporal source estimates (left hemifield stimulation) 123

6. Two dipole spatio-temporal source estimates (right hemifield stimulation) 124

A-1. Features of synaptic and action potentials 152

LIST OF FIGURES

Figure

1. Example of the stimulus sequence 12
2. Percentage of correct responses for each of the six interstimulus intervals 32
3. Visual evoked responses to sequential visual stimuli plotted for each of six interstimulus intervals (Subject J.S.) 33
4. Visual evoked responses to sequential visual stimuli plotted for each of six interstimulus intervals (Subject D.L.) 34
5. Visual evoked responses to sequential visual stimuli plotted for each of six interstimulus intervals (Subject W.P.) 35
6. Grand average visual evoked responses to sequential visual stimuli plotted for each of six interstimulus intervals (Subject J.S.) 36
7. Grand average visual evoked responses to sequential visual stimuli plotted for each of six interstimulus intervals (Subject D.L.) 37
8. Grand average visual evoked responses to sequential visual stimuli plotted for each of six interstimulus intervals (Subject W.P.) 38
9. Labeling of peaks of visual evoked responses elicited by the dot matrix stimuli 41
10. Hypothesized neural responses to sequential visual stimuli. 45
11. Temporal patterning of stimuli in Experiments 1 and 2 48
12. Percent correct responses as a function of duration of the leading display 52
13. Visual evoked responses to sequential dot matrix stimuli plotted for each of the six durations of the leading display (Subject J.S.) 53
14. Visual evoked responses to sequential dot matrix stimuli plotted for each of the six durations of the leading display (Subject D.L.) 54

15. Visual evoked responses to sequential dot matrix stimuli plotted for each of the six durations of the leading display (Subject W.P.) 55

16. Grand average visual evoked responses to sequential dot matrix stimuli plotted for each of the six durations of the leading display (Subject J.S.) 56

17. Grand average visual evoked responses to sequential dot matrix stimuli plotted for each of the six durations of the leading display (Subject D.L.) 57

18. Grand average visual evoked responses to sequential dot matrix stimuli plotted for each of the six durations of the leading display (Subject W.P.) 58

19. Comparison of visual evoked responses from Experiments 1 and 2 (Subject J.S.) 59

20. Comparison of visual evoked responses from Experiments 1 and 2 (Subject D.L.) 60

21. Comparison of visual evoked responses from Experiments 1 and 2 (Subject W.P.) 61

22. Visual evoked responses to a singly presented half of the dot matrix display (Subject J.S.) 62

23. Visual evoked responses to a singly presented half of the dot matrix display (Subject W.P.) 63

24. International 10-20 System of Electrode Placement 71

25. VEP topography: 10 msec ISI dot matrix stimuli (Subject J.S.) 72

26. VEP topography: 10 msec ISI dot matrix stimuli (Subject E.R.) 73

27. VEP topography: 500 msec ISI dot matrix stimuli (Subject J.S.) 74

28. VEP topography: 500 msec ISI dot matrix stimuli (Subject E.R.) 75

29. VEP topography: 10 msec ISI checkerboard stimuli (Subject J.S.) 76

30. VEP topography: 10 msec ISI checkerboard stimuli (Subject E.R.) 77

31. VEP topography: 500 msec ISI checkerboard stimuli (Subject J.S.) 78

32. VEP topography: 500 msec ISI checkerboard stimuli (Subject E.R.) 79

33. Laplacian derivation: 10 msec ISI dot matrix stimuli (Subject J.S.) 81

34. Laplacian derivation: 10 msec ISI dot matrix stimuli (Subject E.R.) 82

35. Laplacian derivation: 500 msec ISI dot matrix stimuli (Subject J.S.) 83

36. Laplacian derivation: 500 msec ISI dot matrix stimuli (Subject E.R.) 84

37. Laplacian derivation: 10 msec ISI checkerboard stimuli (Subject J.S.).....85

38. Laplacian derivation: 10 msec ISI checkerboard stimuli (Subject E.R.).....86

39. Laplacian derivation: 500 msec ISI checkerboard stimuli (Subject J.S.).....87

40. Laplacian derivation: 500 msec ISI checkerboard stimuli (Subject E.R.).....88

41. Posterior Electrode Montage 97

42. Head Centered Coordinate System 98

43. Visual evoked responses to left hemifield presentation of dot matrix stimuli (Subject J.S.) 99

44. Visual evoked responses to left hemifield presentation of dot matrix stimuli (Subject W.P.).....100

45. Visual evoked responses to left hemifield presentation of dot matrix stimuli (Subject E.R.).....101

46. Visual evoked responses to right hemifield presentation of dot matrix stimuli (Subject J.S.) 102

47. Visual evoked responses to right hemifield presentation of dot matrix stimuli (Subject W.P.).....103

48. Visual evoked responses to right hemifield presentation of dot matrix stimuli (Subject E.R.).....104

49. Visual evoked responses to lower hemifield presentation of dot matrix stimuli (Subject J.S.) 105

50. Visual evoked responses to lower hemifield presentation of dot matrix stimuli (Subject W.P.).....106

51. Visual evoked responses to lower hemifield presentation of dot matrix stimuli (Subject E.R.).....107

52. Visual evoked responses to upper hemifield presentation of dot matrix stimuli (Subject J.S.) 108

53. Visual evoked responses to upper hemifield presentation of dot matrix stimuli (Subject W.P.) 109

54. Visual evoked responses to upper hemifield presentation of dot matrix stimuli (Subject E.R.) 110

55. Top: Retinotopic organization of visual cortex. Bottom: Jeffrey's and Axford's (1972) model of C.II generators in extrastriate cortex 112

56. Single dipole parameter estimates for all three subjects 120

57. Two dipole spatio-temporal source estimates: Left hemifield stimulation (Subject J.S.) 125

58. Two dipole spatio-temporal source estimates: Left hemifield stimulation (Subject W.P.) 126

59. Two dipole spatio-temporal source estimates: Left hemifield stimulation (Subject E.R.) 127

60. Two dipole spatio-temporal source estimates: Right hemifield stimulation (Subject J.S.) 128

61. Two dipole spatio-temporal source estimates: Right hemifield stimulation (Subject W.P.) 129

62. Two dipole spatio-temporal source estimates: Right hemifield stimulation (Subject E.R.) 130

A-1. Electric field vectors 139

A-2. Electric field lines for two simple charge distributions 139

A-3. Equipotential line 140

A-4. Theoretical extracellular fields generated by pyramidal cell depolarization 143

A-5. Open and closed extracellular fields 146

INTRODUCTION

Visible Persistence

It is well-known that an observer's perception of a brief visual display may continue for a short time after the physical termination of the stimulus, a phenomenon referred to as visible persistence. An everyday example of visible persistence is given by the phenomenal appearance of a television screen. The physical display is made up of phosphor dots that emit light for less than a millisecond and are refreshed only about every 17 ms. Thus, most of the screen is blank at any given instant. However, an integrated image is seen because of the visible persistence of the individual phosphor dots.

Two hypotheses have been put forward to account for visible persistence: the storage hypothesis and the processing hypothesis. The storage hypothesis regards visible persistence as the decaying contents of a sensory store, which Neisser (1967) called "iconic memory". According to this view, the sensory store is charged while the stimulus is on view, but its contents begin to decay as soon as the stimulus is turned off, in the manner of a leaky capacitor. A possible neuroanatomical locus for such a store, suggested by Sakitt (1976), is in the retinal photoreceptors. On this view, the duration of visible persistence is determined by the decay of photoreceptor activity after stimulus offset.

In contrast, the processing hypothesis (Di Lollo, 1980) states that visible persistence is an outcome of the activity of sensory coding mechanisms at an early stage of visual information processing. The onset of a stimulus is said to initiate a period of encoding activity that continues for a duration that is independent of the duration of the inducing stimulus. The duration of visible persistence would thus be determined by the difference between the duration of the encoding process and the duration of the inducing stimulus.

In practice, the most salient difference between the two accounts is whether the onset or offset of a stimulus is regarded as the critical event for visible persistence. Persistence is time-locked to stimulus offset according to the storage hypothesis, but to stimulus onset according to the processing hypothesis. Thus, the two hypotheses assign crucially different roles to the neural activity associated with the onset and offset of stimuli.

Although psychophysical investigations of visible persistence have been both numerous and extensive (Coltheart listed over 100 pertinent papers up to 1980, and many more have appeared since), little is known of the corresponding course of neural activity in human observers. As will be seen, knowledge of such activity can play an important role in establishing constraints and in defining limiting conditions for theoretical accounts of visible persistence. The present research is intended as a step toward redressing this gap in knowledge of the neurophysiological concomitants of visible persistence.

The aim of the present study was to employ a method for the study of visible persistence and to compare the pattern of results obtained psychophysically with visual evoked potentials obtained with the same method, stimuli, and observers. These data bear directly upon the viability of several alternative theoretical interpretations of this phenomenon.

Theoretical Background

Iconic Memory

Visible persistence has long been of interest as a sensory phenomenon (see Long, 1980, and Breitmeyer, 1984, for historical reviews of persistence research since the 19th century). The modern era of research can be dated to 1960, when Sperling initiated a "cognitive revolution" in the conceptual status of persistence effects in vision. Since Sperling's (1960) report, persistence phenomena have played an important role in theories of visual information processing.

Sperling's (1960) invention of the partial report method allowed him to demonstrate that, for a short time after the termination of a brief visual display, observers may selectively access a highly accurate representation of the display. It had long been known that if asked to report the characters of a brief display of 6 to 18 or more characters, observers could correctly report an average of 4-5 items (the full report, or FR condition). Sperling's innovation was to restructure the traditional display of, say, one long line of twelve characters, into a display that had three rows of four characters each. Observers were required to report only one of the lines, cued by a distinctive auditory tone presented after the display offset (the partial report, or PR, condition).

In order to compare the PR and FR performance, Sperling assumed that, for example, if a subject could report 3 of 4 characters in a cued row, it must be that the same number of characters were available to the subject in the two uncued rows. Partial report performance was then scored as the average number of correct items in a row multiplied by the number of rows in the display: in this example, PR performance would be 9 out of 12.

Sperling (1960) demonstrated that at zero cue delay, PR performance was close to perfect while FR performance never rose above 4.5 correct out of 12. In addition, the PR superiority effect was degraded with increasing cue delay: by a cue delay of one second, PR performance was equivalent to FR performance. Sperling's (1960) interpretation was that the PR technique tapped a distinct form of memory, characterized by a large capacity and rapid decay. He called this form of memory a "visual information store" and tentatively suggested that this store be identified with the sensory (visible) persistence following the offset of the display. He suggested that visible persistence could be likened to a rapidly fading visual image of the stimulus, containing a brief representation of most or perhaps all of the information contained in the visual display. Neisser (1967) coined the term "iconic memory" to refer the visual information store, and this term was widely adopted.

The formulation of the concept of iconic memory was to have a broad impact on the study of visual perception. Sperling's (1960; 1963) pioneering studies coincided with the advent of information-processing approaches to the study of visual perception, and iconic memory was

seen to fit naturally within this type of conceptual framework. Haber (1969) outlined the main assumptions underlying the information processing approach (in extract):

> 1. A perceptual response is assumed not to be an immediate consequence of stimulation, but one which has gone through a number of stages or processes, each of which takes time to organize or traverse.
> 2. Processing is limited by the capacities of information-handling channels, the information content of the stimulus, and the prior experiences and condition of the perceiver.
> 3. Perceptual processes cannot be studied or analyzed independently of memorial ones, since recoding and preservation of information occurs at all stages of information processing.
> (Haber, 1969, pp. 3-4).

In essence, an information processing approach advocates the study of those points in time where recoding of visual information occurs, in order to map out the stages involved in the processing of the retinal image into perceptual experience. A number of prominent models of visual information processing (e.g. Atkinson & Shiffrin, 1968; Neisser, 1967; Turvey, 1973) incorporated iconic memory as the first stage of visual information processing - as a brief store of essentially "unencoded" (as evidenced by its large capacity and precategorical properties) information. Higher level processes could access the visual information stored therein as long as the iconic representation persisted in the visual system.

Classification of Persistence Effects

When Neisser (1967) originally coined the term "iconic memory", he used it to refer to a photographlike representation of the visual stimulus that remained perceptually available for a brief time after the offset of the inducing stimulus. Iconic memory was equated with the sensory persistence following offset of a visual display, and was initially regarded as a unitary phenomenon. As studies of iconic memory accumulated, however, it became apparent that not one but several processes were involved in visual persistence.

In an extensive review of the empirical literature, Coltheart (1980) marshaled considerable evidence to support his thesis that there are in fact three kinds of "visual persistence", which can be distinguished both conceptually and procedurally. Further, he pointed out that the

interrelationships among the three types of visual persistence are not at all obvious and remained to be demonstrated empirically, although it was common practice to regard the three types as manifestations of a common phenomenon.

Coltheart began by making a conceptual distinction among three types of visual persistence. He argued that there are three senses in which a visual stimulus may be conceived to persist psychologically after its offset, as follows (in extract):

> First, neural activity in the visual system evoked by the stimulus may continue after stimulus offset ("neural" persistence) . Second, the visual stimulus may continue to be phenomenally present, or visible, for some time after its physical offset ("visible" persistence). Finally, information about visual properties of the stimulus may continue to be available to an observer for some time after stimulus offset ("informational" persistence).

The three concepts can be distinguished procedurally, in that they are investigated with the following different techniques:

> One may make neurophysiological recordings of events occurring in the visual system after the offset of a visual stimulus; or one could ask subjects to describe what they see after the offset of a visual stimulus; or one could require them to perform tasks which require that specifically *visual* properties of the stimulus are accessible after the onset of the stimulus. (Coltheart, 1980, p. 184).

Having defined neural, visible and informational persistence in this manner, Coltheart proceeded to point out that many investigators have implicitly or explicitly equated the different types of persistence, in the face of a nearly complete absence of empirical justification for this equation. In the case of the relationship between neural and visible persistence, Coltheart concluded that, while much suggestive evidence exists for relating the two, a conclusive demonstration has not yet been performed. Since little attention has thus far been paid to the distinction between the various types of persistence, studies of neural persistence and studies of visible persistence have been carried out in separate experimental conditions, making it difficult to rigorously test hypotheses about the relationship between the two. In the case of the relation between visible and informational persistence, on the other hand, Coltheart asserted that the available evidence conclusively demonstrates that they are not the same entity - informational and visible persistence are distinct phenomena with fundamentally different properties.

Coltheart proposed, on the basis of extensive empirical evidence obtained with a variety of experimental paradigms, that visible persistence and informational persistence[1] behave quite differently with respect to two stimulus parameters: stimulus duration and stimulus intensity. Specifically, duration of visible persistence is inversely related to both the duration (the "inverse duration effect") and the intensity (the "inverse intensity effect") of the inducing stimulus, while informational persistence is not affected by variations in either parameter. Since the two types of persistence have different properties, they cannot refer to the same entity.

Of several proposed classification schemes, that of Coltheart (1980) has perhaps been the most influential. However, this classification has not met universal acceptance. In a review published the same year, Long reached conclusions directly contrary to those of Coltheart (1980). He argued that the experimental evidence supports a direct, rather than an inverse relation between stimulus intensity and duration, and the duration of "visual" persistence. Further, Long (1980) concluded that the available empirical evidence supports the assertion of Sakitt (1976) that the icon is not only visible, but neural, having a locus in the photoreceptors of the retina.

Theories of Visible Persistence

The present work, adopting the terminology of Coltheart (1980) is concerned specifically with the neuronal processes underlying "visible persistence", denoting "the fact that the *sine qua non* of this entity is that it can be *seen*" (Coltheart, 1980, p. 185, italics Coltheart's). In practice, visible persistence is considered to be tapped in experimental paradigms which require subjects to make a phenomenological judgment about the appearance of a visual display. Sakitt, whose work is discussed in detail below, does not discriminate between neural, visible and informational persistence, referring to all three as "visual persistence".

---

[1] Coltheart (1980) equates informational persistence with Neisser's (1967) original definition of iconic memory, and uses the two terms interchangeably.

Two main hypotheses have been put forward to account for visible persistence: the storage hypothesis and the processing hypothesis.

Storage Hypothesis

The storage hypothesis was originally formulated (by e.g. Sperling, 1960; Neisser, 1967) to account for iconic memory. On this account, visible persistence is regarded as the decaying contents of a sensory store. The store is replenished while the stimulus is on view, but its contents begin to decay as soon as the stimulus is turned off. An often used-metaphor is that of a simple resistance-capacitance circuit, whose charge begins to decay as soon as the charging agent is removed. A storage account of visible persistence has perhaps been most explicitly articulated by Sakitt (1976), who suggested a locus for the sensory storage in the retinal photoreceptors.

Sakitt's (1976) argument for a photoreceptor locus rested on several converging lines of evidence. With a rod monochromat as a subject, she first demonstrated that rods are sufficient, if not necessary, to obtain a partial report superiority in a standard Sperling task. In her second, crucial, experiment, she utilized the fact that the rod system saturates at background intensities above about 1000 scotopic trolands[2]. In normal vision, rod saturation is not noticed since the cones can still operate, but a rod monochromat is essentially blind at saturating intensities. With a display of white letters on a white background at saturating intensities, the rod monochromat's performance was zero at all cue delays in the Sperling task. However, when this subject closed her eyes after the stimulus, a persisting image of the display could be seen and a PR superiority was obtained which decayed over increasing cue delays. Sakitt interpreted this result to mean

---

[2] Saturation refers to the fact that rod output is maximal at this level of illumination. The troland (td) is a measure of retinal illuminance and is given by the product of stimulus luminance (in candelas per square meter) and pupil area (in square millimeters).

that all of the information about the persisting image (icon) must have been stored prior to the first saturable stage of vision.

On Sakitt's reasoning, a uniformly maximum signal is being transmitted to higher perceptual centers at rod saturation. Since the icon eventually appeared, the information must have been stored prior to the point of saturation. Drawing on electrophysiological evidence that saturation occurs as early as the photocurrent in rod photoreceptors in the rat, Sakitt concluded that iconic storage must occur prior to the photocurrent, either inside the rod or at the rod membrane. The experimental results are explained if the rods recover upon the subject closing her eyes, reducing the photoreceptor response below the saturation level. The rods that were exposed to the display letters would then have a larger output than the rods exposed only to the background.

In a third experiment with dark-adapted, normally sighted subjects, Sakitt measured the relative sensitivity for producing an iconic image of a given duration as a function of the spectral wavelength of the light illuminating the letter display. Specifically, for each wavelength, the subject was required to adjust the intensity of the stimulus until the offset of the iconic image seemed coincident with the presentation of an auditory probe, presented either 500 msec or 1000 msec after the onset of the stimulus. The results showed that the spectral sensitivity for producing both the 500 msec and 1000 msec icons fit the scotopic curve much better than the photopic curve, supporting the conclusion that iconic memory in normal vision is dominated by the rods.

In a subsequent series of experiments, Sakitt and Long (1978, 1979) used dark-adapted subjects who were required to detect a spatial gap between two luminous rectangles which were presented successively with a temporal gap. This was considered to be a measure of the duration of the "icon", since performance required that the two stimuli be phenomenally simultaneous (a measure of "visible persistence" according to Coltheart's, 1980, criteria). Their results were consistent with the interpretation that gap detection was performed by the cones for ISIs of up to about 100-200 msec, but by the rods for longer ISIs. They concluded that both cone

and rod icons exist, but that the rod persistence is robust and long-lasting in comparison to cone persistence, and is thus the major contributor to iconic memory.

Processing Hypothesis

The view of visible persistence as a simple sensory store, whose contents fade quickly upon offset of the inducing stimulus, has been challenged by Di Lollo (1980). Di Lollo (1980) proposed an alternative theoretical framework which he called a "sensory-coding", or "processing" approach. In this framework, persistence is equated, not with the decaying contents of a sensory store, but rather with the activity of sensory coding mechanisms at an early stage (which Di Lollo called the "recruiting phase") of visual information processing:

> The mechanisms in this phase would be activated by the onset of a display, and activity would continue to the end of the phase whether or not the inducing stimulus was still on display. Thus, visual persistence would be available only for inducing stimuli whose duration did not exceed the period of early sensory coding activity, and its duration would correspond to the difference between the duration of the inducing stimulus and the duration of the encoding process. On this account, the extent to which two sequential stimuli are seen to overlap temporally would depend on the period for which the two stimuli are concurrently active within the recruiting phase. (Di Lollo, 1980, p. 79).

In Di Lollo's model, the end result of visual information processing is the encoding of the stimulus to a level that permits comparison with long-term memories. This is accomplished in two phases of coding: the recruiting phase and a succeeding "interpreting phase". The recruiting phase operates to code stimulus features (such as dots, bars, edges and discontinuities). The resulting "feature-encoded" representations are then identified and categorized in the interpreting phase. Higher level processes, and higher level memory, may then operate upon the "meaning-encoded" representations that emerge from the interpreting phase.

The recruiting and interpreting phases of visual information processing are distinguished by a number of characteristics in this model. The recruiting phase is characterized by:

1. faithful maintenance of stimulus geometry with initial retinal configuration;
2. virtually unlimited processing capacity;
3. mainly parallel processing;
4. masking through integration of contours (as distinct from interruption of processing); and

5. sensory persistence (namely, the maintenance of physical, as distinct from informational, aspects of the display). (Di Lollo, 1980, p. 93).

The interpreting phase is characterized by:

1. mainly serial processing;
2. little if any correspondence between stimulus geometry and initial retinal configuration;
3. masking by interruption of processing;
4. maintenance of informational rather than physical aspects of the display. (Di Lollo, 1980, pp. 93-94).

Di Lollo's model is a modification of earlier stage models in several important respects. First "visual persistence" (referring, in this context, to phenomenal continuity of the visual display) results from the activity of sensory coding mechanisms (in the recruiting phase), rather than from the decaying contents of a sensory store. Second, the model predicts that different kinds of persistence may result from activity in different stages of information processing, the particular type of persistence reflecting the predominant type of processing that is occurring in that phase. For example, while the phenomenal persistence examined in this type of study was assumed to arise from activity in the recruiting phase, the interpreting phase may be expected to generate a persistence based on informational rather than physical aspects of the display, and thus need not necessarily be visible. This type of nonvisible persistence had previously been suggested by Turvey (1978), who referred to it as "schematic persistence".

Empirical support for the processing hypothesis is found in what has come to be known as the "inverse duration effect" (Coltheart, 1980), the finding that the duration of visible persistence decreases as a function of increasing stimulus duration.

Di Lollo (1980) employed a "temporal integration of form parts" paradigm (Coltheart, 1980) in which two halves of a visual display were flashed successively on an oscilloscope screen. Subjects were required to perform a task on the basis of the visual integration of the two halves of the display. Visible persistence in this paradigm is indexed by the fact that successful performance of the task requires that the two sequential stimuli must be perceived as temporally coextensive.

The complete visual display was a 5 by 5 square matrix of dots presented as two temporally successive frames (see Figure 1). The leading frame (F1) consisted of 12 randomly chosen dots and the trailing frame (F2) of another 12 dots, so that if presented simultaneously, one dot was missing from the complete matrix. The task required of the subjects was to identify the missing dot on each trial. In this experiment (Di Lollo, 1980) the interstimulus interval (ISI)[3] and the duration of the trailing display were held constant at 10 msec each, while the duration of the leading display was varied (but matched for brightness) from 10 to 200 msec. The results of this experiment showed that performance was nearly perfect for leading display durations of up to 80 msec, but declined rapidly thereafter.

[3] Interstimulus interval (ISI) is a measure of the temporal distance between the offset of the leading stimulus and the onset of the trailing stimulus.

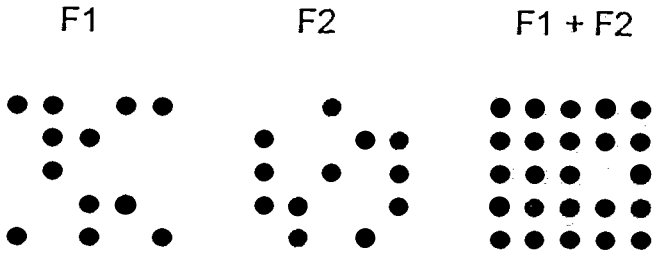

Figure 1. Example of the stimulus sequence employed in the temporal integration of form parts paradigm. F1 = first frame of 12 dots. F2 = second frame of 12 dots. F1 + F2 shows the integrated matrix perceived when the two sets of dots are displayed simultaneously.

Di Lollo (1980) concluded that his results could not be explained within the framework of a sensory storage hypothesis. If visible persistence were due to the decaying contents of a sensory store, performance would not have been affected by the experimental manipulation, since the temporal gap between the offset of the leading stimulus and the onset of the trailing stimulus was held constant. Di Lollo (1980) suggested that his results were consistent with the alternative hypothesis that persistence is initiated by the onset of the leading stimulus, and continues for a fixed duration (some 100-150 msec) independently of the inducing stimulus duration.

This interpretation was supported by the results of a further experiment (Di Lollo, 1980; Experiment 4) which examined the effect of stimulus duration on forward masking. In this experiment a test stimulus (an alphabetic character) was displayed in the same spatial location and immediately upon the termination of a masking stimulus (an aggregate of parts of alphabetic characters). The test stimulus was displayed for 20 msec, while the duration of the masking stimulus was varied from 20 to 640 msec. The author's rationale was that perception of a temporally trailing test stimulus should be enhanced if the persistence of a leading mask is reduced. From the perspective of a storage hypothesis, this could be accomplished by increasing the ISI between the leading mask and the trailing test stimuli. On the basis of the results described above, however, a counterintuitive prediction was that increasing the duration of the leading mask should reduce its post-offset persistence and thus its interference with the trailing test stimulus. The results bore out this prediction: identification of the test character improved dramatically as the duration of the mask was increased.

The Locus of Visible Persistence

As discussed above, the properties of visible persistence are defined by its sensitivity to the physical aspects of the stimulus (in particular, duration and intensity). On the basis of these stimulus-bound properties, it is generally agreed that the neurophysiological locus of visible persistence must reside within relatively early stages of the visual system - the retino-geniculo-striate projection system and regions of the extrastriate cortex involved in low-level processing of

physical aspects of the stimulus (Breitmeyer, 1984; Coltheart, 1980; Uttal, 1981). However, the precise locus within this general region is still strongly debated.

The issue of the locus of visible persistence is central to current theoretical accounts of the phenomenon. The issue may be dichotomized as thus: Is visible persistence determined largely or entirely by "peripheral" structures at the level of the retina (as suggested by Sakitt, 1976), or are more central structures involved, including visual cortex? The problem is a complex one, for several reasons. Although it is obvious that visual cortex must be involved if a stimulus is perceived ("visible"), it may be that the duration of visible persistence is determined by photoreceptor properties and that central persistence merely reflects this peripheral persistence. On the other hand, if there are central determinants of visible persistence, the total duration of persistence likely reflects both central and peripheral components. Peripheral persistence will inevitably be passed on to central structures and be manifest in perception unless there exists some central mechanism which discounts or removes the peripheral portion of persistence. For these reasons, it is quite difficult to empirically disentangle the relative contributions of peripheral and central determinants.

There are a number of cogent reasons for believing that there exist specifically central (cortical) sources of visible persistence. The existence of central sources is inferred from studies which have established that the duration of visible persistence is appreciably affected by stimulus variables, such as binocular viewing (Engel, 1970), spatial frequency (Meyer, Lawson & Cohen, 1975; Meyer & Maguire, 1977) and orientation (Lovegrove et al., 1981), which do not substantially affect cells below the level of visual cortex.

Despite the numerous psychophysical studies of visible persistence there have been surprisingly few attempts to study its neurophysiological basis. One of the few relevant studies is that of Duysens, Orban, Cremieux and Maes (1985), who identified a specific subpopulation of cells in area 17 of cat visual cortex whose "On" responses were independent of stimulus duration. For these cells, the portion of the On discharge occurring in the period following the physical termination of the stimulus increased in amplitude and duration as the stimulus was

shortened, in a manner closely paralleling the inverse duration effect of visible persistence. These authors concluded that this group of cells (which they identified as "A and S families" of cells) were the most likely cortical substrates for visible persistence, and that their temporal properties were consistent with the predictions of Di Lollo's processing hypothesis: their responses had a finite latency and duration, the sum of which exceeded stimulus duration when the latter was short. The maximum duration of neural persistence in these cells, about 100 msec, is approximately the same range as that reported for visible persistence, 100-150 msec (Coltheart, 1980; Di Lollo, 1980).

Present study

To summarize to this point, two hypotheses have been put forward to account for visible persistence: the storage hypothesis and the processing hypothesis. The storage hypothesis regards visible persistence as the decaying contents of a sensory store. In contrast, the processing hypothesis states that visible persistence is an outcome of the activity of sensory coding mechanisms at an early stage of visual information processing.

In practice, the most salient difference between the two accounts is whether the onset or offset of a stimulus is regarded as the critical event for visible persistence. Persistence is time-locked to stimulus offset according to the storage hypothesis, but to stimulus onset according to the processing hypothesis. Thus, the two hypotheses assign crucially different roles to the neural activity associated with the onset and offset of visual stimuli. At present, little is known of the patterns of neural activity corresponding to visible persistence in human observers.

Few options are available for the routine investigation of neural activity in normal human subjects. One such option is EEG, which measures the potential fields of the brain from recording electrodes placed on the scalp overlying visual cortex. In the context of brain activity elicited by visual stimuli, the fields measured by this methodology are referred to as visual evoked potentials (VEPs).

Brain potentials elicited by visual stimuli are typically very small amplitude waves (10-15 microvolts) embedded within the much larger amplitude (60-70 microvolt) fluctuations of the spontaneous EEG. As such, a VEP is typically not identifiable in the EEG record. Commonly, signal averaging techniques (Dawson, 1951) are employed to extract the small transient "signals" from the noise of the ongoing EEG. The rationale of signal averaging is simple: If a stimulus is identically presented over a number of successive trials, and the EEG recorded for some definite epoch of time following stimulus onset, then averaging of the successive EEG epochs will result in the maintenance of activity that is time-locked to the onset of the inducing stimulus and the cancellation of activity that is not so related to the stimulus. Spontaneous EEG will thus average to zero over successive samples. Typically, some 100-200 samples are required to produce a suitably noise-free VEP.

A transient VEP is recorded as a plot of voltage fluctuation over time and consists of a series of positive and negative-going deflections. VEPs are quantified in terms of the latency (from stimulus onset), amplitude and polarity of the various peaks in the waveform. In common practice, peaks are identified with a label indicating polarity (positive or negative) and latency. For example, the label "P100" refers to a positive deflection with a peak latency of 100 msec.

The general approach of the studies described here was to employ a method for the study of visible persistence, and to compare the pattern of results obtained psychophysically with visual evoked potentials obtained with the same method, stimuli, and observers. Following the argument outlined at the beginning of this section, the results thus obtained would bear directly on the predictions of the two alternative theoretical interpretations of visible persistence.

Psychophysical Measures

Temporal integration of form parts was introduced as a technique for the study of visible persistence by Eriksen and Collins (1967). The underlying rationale is simple. A visual pattern is divided to produce two component patterns (S1 and S2) which, in isolation, contain no usable information about the identity of the overall pattern. S1 and S2 are presented in sequence,

separated by an adjustable ISI. If the visible persistence of S1 can span the temporal gap, there is perceptual simultaneity of S1 and S2 and the overall pattern can be identified. On the other hand, identification is impossible if the ISI exceeds the visible persistence of S1. Therefore, the maximum duration of visible persistence is indexed by the maximum ISI at which identification of the pattern is possible.

The temporal integration of form parts technique employed in the following experiments was one used by Di Lollo (1980) and described in detail previously. To reiterate, Di Lollo (1980) found that performance in this temporal integration task became progressively impaired as the duration the leading stimulus was increased to about 200 msec. This effect, referred to as the inverse duration effect, has been extensively replicated in a variety of experimental paradigms (see Coltheart, 1980, for a review of relevant studies).

In essence, the inverse duration effect shows that temporal integration of two sequential stimuli is governed by stimulus onset to onset asynchrony (SOA[4]), rather than interstimulus interval (ISI). This result is consistent with the predictions of the processing hypothesis but cannot be explained within the framework of a storage hypothesis. This line of reasoning suggests the basic approach of the following experiments: to determine if ISI or SOA is the critical variable for VEPs elicited by the two sequential stimuli.

Visual Evoked Potentials: Temporal Properties

There have been no previous VEP studies directly concerned with the inverse duration effect of visible persistence. However, a number of VEP studies have addressed the temporal resolution of visual evoked responses to patterned and unpatterned light. Several relevant results, discussed below, suggest the viability of the present experiments.

---

[4] Stimulus onset to onset asynchrony (SOA) refers to the temporal distance between the onset of the leading stimulus and the onset of the trailing stimulus. In contrast, interstimulus interval (ISI) is a measure of the temporal distance between the offset of the leading stimulus and the onset of the trailing stimulus.

VEPs elicited by the onset and offset of patterned light have been intensively investigated. Pattern onset and offset responses have been most extensively characterized with checkerboard stimuli, although numerous other patterned stimuli such as one-dimensional gratings and polka-dot stimuli have also been employed.

The pattern onset response commonly consists of three peaks of alternating polarity (negative, positive, negative; or positive, negative, positive, depending on the particular experimental conditions). The offset response is more variable in morphology, but commonly has only one or two peaks of opposite polarity. The shapes of both onset and offset responses to checkerboard patterns are critically dependent upon a number of experimental variables, including electrode position, check size, contrast, and the region of the visual field stimulated. Onset and offset responses are elicited with a variety of patterned stimuli other than checkerboards, including one-dimensional gratings and polka-dot stimuli.

Jeffreys (1977) described three components of the VEP elicited by pattern onset stimuli: a positive component at a latency of about 70 msec from pattern onset; a negative component with a peak latency of about 100 msec; and a positive component with a peak latency of about 120 msec. He called these components C(omponent) I, C.II and C.III, respectively. Jeffrey's terminology has become widely accepted as a description of the various components of the pattern pulse and pattern onset VEPs. However, as mentioned previously, the latency, amplitude and polarity of a particular component is critically dependent upon a number of different stimulus and recording parameters.

Several VEP studies have examined the temporal interactions between onset responses to successive presentations of two patterned stimuli to spatially discrete locations in the visual field. Riemslag, Spekreijse and van Wessem (1985) used a circular stimulus field of radius 4.2 degrees containing 20 minute checks. The circular field was divided into eight octants. A double presentation series consisted of a 300 msec presentation of four separate octants, followed, after an adjustable SOA (ranging from 8 to 83 msec), by a 300 msec presentation of the remaining octants.

With these stimuli, Riemslag et al. (1985) reported a limiting SOA of 40-50 msec for resolving separate onset responses to the successive stimuli. Their analysis, restricted to the C.II component of the onset response, suggested complete inhibition of the second onset response at SOAs of less than 40 msec, with a transition to complete algebraic summation of the separate responses at SOAs greater than 50 msec.

A comparable temporal resolution was reported for the C.I component of the onset response by Jeffreys and Musselwhite(1986). In a study of the VEP concomitants of metacontrast masking, these authors used multielement target and masking stimuli consisting of 24 minute squares with an interelement separation of 36 minutes (a multi-element version of the classical single square target and two flanking squares mask employed in many psychophysical studies). Target-mask presentations consisted of a 10 msec target stimulus followed, after an adjustable SOA (ranging from 20 to 100 msec) by a 10 msec masking stimulus. Under these conditions, the responses to the second pattern could be differentiated at SOAs of 30 msec and greater, and completely discrete responses to the successive stimulus were observed at SOAs of 70 msec and greater.

Visual Evoked Potentials: Source Localization

The locus of visible persistence is a matter of some controversy at present. Current theories of visible persistence invoke either a peripheral (photoreceptor) or a central (cortical) locus. Evidence for a peripheral locus is based on the correlation between properties of visible persistence and the known psychophysical properties of rod and cone vision. Evidence for a cortical locus derives from the effect of stimulus variables such as binocular viewing, spatial frequency and orientation, since lower level neurons are not sensitive to these variables to any significant extent.

The issue of the locus of visible persistence is therefore central to current theories of the phenomenon. In the present context, it would be of considerable interest to characterize the cortical generators of the VEPs elicited by the stimuli in a temporal integration of form parts

paradigm. For a variety of reasons, discussed below and in detail in Appendix 1, it is not possible to directly infer the location of cerebral generators on the basis of the potential fields recorded at the surface of the scalp.

Source Derivation

One difficulty in interpreting scalp recorded potential fields derives from the referential nature of EEG recording. In monopolar EEG recording, potential differences are recorded between an "active" electrode and a supposedly "inactive" reference electrode, often placed on the earlobes, mastoid processes, or nose. The assumption of an inactive reference electrode is generally not supportable, for several reasons. First, since potential fields generated by sources in the brain are confined to the head, the reference electrode must also be on the head. Little or no current flows through the volume constriction of the neck, and so there is no potential difference between the neck and the body due to the source in the head: a reference electrode anywhere below the neck will effectively be equivalent to a reference on the neck. Placing the reference on the body will have no advantage over a cephalic reference, but may have the disadvantage of introducing electrocardiogram (ECG) artifact into the EEG recording (Nunez, 1981). Secondly, since scalp evoked potentials are likely to be generated by active brain regions of substantial size, there is no point within the dimensions of the head which is far enough away from the current source to be truly indifferent (Nunez, 1981). The implications of the foregoing are that the scalp recorded potential is dependent upon the locations of both the active and reference electrodes, and the potential fields recorded may be strongly influenced by the choice of reference electrode.

Reference invariant analysis techniques have recently been introduced which produce more readily interpretable field patterns by calculating spatial gradients and derivatives of the referential potentials. One such reference-invariant technique is that of two-dimensional current source-density analysis (Laplacian transformation). This technique, also referred to as "source"

derivation (Hjorth, 1980), involves estimating the change in potential gradient over the scalp (i.e. the second spatial derivative of the potential field) using approximations of the mathematical Laplacian operator.

Since source derivation techniques measure the average radial gradient directed at a particular electrode position from the surrounding electrodes, they provide a means of estimating the strength of sources (or sinks) of current flow acting as the local generators of the field potentials around the electrode. In the implementation of this technique for the scalp EEG (e.g. Hjorth, 1980), a "source" is understood to represent the rate of change of the potential gradient in two orthogonal directions at each electrode position, which in turn may reflect current flow vertically through the scalp below each electrode (Hjorth, 1975; 1980; Nunez, 1981). This transformation, implemented as a derivation of the potential difference between the center electrode and a weighted average of the potentials at surrounding electrodes, provides a better measure of "source" current flow vertically through the skull, since volume-conducted artifact currents flowing transversely to the scalp (i.e. originating outside of the measurement area) are suppressed. Source derivation therefore provides the twin advantages of a reference-free representation of the scalp fields and an improved topographic selectivity as compared to a referential derivation.

The technique used for calculating potential gradients in the present study is an approximation of the Laplacian operator introduced by Hjorth (1975; 1980), calculated by deriving the potential difference between a given electrode and a weighted average of the potentials at surrounding electrodes, the weighting being proportional to the reciprocal of the distance to the center electrode. An unavoidable drawback of this technique is that reliable source estimates cannot be calculated for electrodes at the outer edge of a recording montage, since fewer surrounding electrodes are used in their derivation.

Dipole Source Potential Analysis

While the use of Laplacian-based spatial enhancement techniques simplifies the interpretation of scalp potential field patterns by providing a reference-free representation of current "sources" directed vertically through the scalp, they do not provide an unambiguous means of localizing the active neural tissues that are the generators of the scalp potential field. In fact, the determination of the location of brain generators is fundamentally obscured by the principle of linear superposition of fields (see Appendix 1). The implication of the superposition of potential fields is that any given potential field can be generated identically by an infinite number of configurations of sources. Since there is no unique solution, the problem of localizing the generators of scalp-recorded fields is considered to be an "ill-posed" problem.

Since there are an infinite number of possible solutions, one must ultimately appeal to information outside of the strict logic of the problem to solve an ill-posed problem. The approach taken in the bioelectromagnetic inverse problem is to use this outside information to greatly restrict the number of possible generator configurations which can give rise to empirically observed fields. There are three major types of constraints which may be imposed on the inverse problem in EEG: (1) The type of source is constrained to those capable of generating extracerebral fields. For theoretical and empirical reasons (discussed in Appendix 1), only one type of source - the current dipole- is generally considered in the inverse problem. (2) The number of sources is generally constrained to a few or only one current dipole. (3) The possible spatial locations of sources are constrained by anatomical or physiological considerations. For example the known anatomy of sensory pathways and cerebral cortex greatly limits the number of plausible locations for dipole sources. Given these considerations, the inverse problem can be restated as that of choosing among a finite, even small, number of possible source configurations (Vaughn & Arrezzo, 1988).

Even a severely constrained inverse problem has no unique solution and can be "solved" only in an iterative, least-squares sense. The classic dipole localization method (DLM) uses such an interative strategy. For a given instant in time, a current source configuration is chosen arbitrarily and the scalp potential fields computed for that configuration. The surface field predicted from the "forward solution" is compared to the observed field using goodness of fit statistics. The source parameters are then altered slightly and the process repeated, using numerical minimization techniques to ensure convergence, until a goodness of fit criterion is reached. DLM was first developed for the EEG by Schneider (1972) and Henderson Butler & Glass (1975) and applied to empirical evoked potential by Darcey et al. (1980) and Sidman et al. (1978).

Visual evoked potentials are plots of voltage fluctuations over time, and an additional question of interest in the interpretation of evoked potential fields is that of the patterning of activity of generator structures over time. In recent years, several authors (Baumgartner, Sutherling & Barth, 1989; Scherg 1989) have advocated a combined "spatiotemporal" approach to the modeling of dipole sources. The fundamental assumption of the spatiotemporal model is that of stationary dipole sources whose only time-varying parameters are the temporal variation of the dipole strength (dipole-moment). An advantage of the spatiotemporal approach over the moving dipole approach is that a greatly increased number of degrees of freedom is obtained in the estimation of equivalent sources by incorporating the information contained over a period of time, and by restricting the parameter estimation problem to that of the estimation of the dipole strength parameter. The spatiotemporal approach thus makes feasible the localization of multiple sources, while the "time-slice", or "moving dipole " DLM is limited by the fact that the number of dipole sources that can be accurately modeled is restricted by the number of recording channels, since the number of independent parameters is less than or equal to the number of recording channels. Since a single equivalent dipole has seven coordinates (three for position, and three for orientation, and one for "source-strength" or dipole-moment), no more

than one or two equivalent dipoles can be extracted with confidence with this procedure (Fender, 1987).

As a departure from the traditional moving dipole approach, the spatiotemporal approach represents a change in emphasis in the interpretation of scalp-recorded potentials: While the moving dipole approach necessarily emphasizes the calculation of the spatial parameters of one or a few extremely circumscribed generator regions at some defined instant time (usually defined by a peak or component of the evoked potential), the spatiotemporal approach emphasizes the extraction of the compound activity of a circumscribed brain area and the temporal course of activity in each of the generating structures. Essentially, it makes the plausible assumption that the generators of evoked potentials are circumscribed brain regions which vary, not in spatial location, but in activity over time. Since the spatiotemporal approach makes possible the estimation of multiple sources, it allows the analysis and separation of the compound activities of temporally overlapping activities of distinct brain regions.

The Volume Conductor

Another important consideration in the analysis of scalp potentials is the fact that the EEG, by its nature, is sensitive to currents flowing in conductive media. Since current follows the path of least resistance, and since the media of the brain and its coverings are not uniformly conductive, the path for current flow in the volume between the current source and the extracerebral recording site is not a direct one. Therefore, the potential fields at the scalp will present a somewhat smeared and distorted picture of the underlying generator sites. Accurate source localization requires that volume current distortions be accounted for by modeling the geometries and impedance characteristics of the conductive media. In the present study, forward solutions were calculated using a modification of the forward solution provided by Stok (1986) for electric potential on the surface of a spherical volume conductor fitted to the surface of the occipital region of the head. To correct for conductive inhomogeneities, the head was modeled

as four concentric spheres, with radii corresponding to the surface of the brain, the inner surface of the skull, the outer surface of the skull, and the surface of the scalp. representing the radii of the brain, cerebrospinal fluid (CSF), skull and scalp.

Conceptual Outline of the Present Study

The overall aim of the present study was to gather neurophysiological evidence bearing on the major theoretical accounts of visible persistence. The general approach taken was to employ a method for the study of visible persistence (temporal integration of form parts) and to compare the pattern of results obtained psychophysically with the corresponding cortical evoked potentials obtained with the same method, stimuli, and observers. The temporal patterning of VEPs was the focus of interest in the first set of experiments, with the goal of establishing what correspondences, if any, existed between the VEP measures and the pattern of results obtained psychophysically. The focus of interest then turned to the spatial patterning of VEPs in the second set of experiments, with the goal of drawing inferences concerning their cerebral generator structures.

PART 1: TEMPORAL PATTERNING OF VISUAL EVOKED POTENTIALS

Experiment 1

Introduction

Temporal integration was studied in Experiment 1 using the dot-matrix task outlined above. The display sequence consisted of two images of 12 dots each, separated by an ISI whose duration was varied systematically. When temporally integrated, the two images formed a 5x5 square matrix with one missing element whose location had to be identified (See Figure 1). The experiment was designed to elucidate two basic issues. First, since each stimulus pattern consisted of only 12 dots displayed briefly under mesopic luminance and adapting conditions, it was necessary to determine if measurable potentials would be evoked and, if so, whether they would be related systematically to the temporal pattern of stimulation. Second, Experiment 1 was designed to assess the temporal dynamics and resolution of the transient evoked responses as a basis for establishing functional relationships with corresponding perceptual outcomes such as temporal integration of the two component patterns.

Method

Subjects

Three right-handed male subjects, ranging in age from 29-42 (mean = 33.2) with normal or corrected-to-normal vision took part in Experiment 1.

Visual Stimuli

All visual stimuli were generated by an IBM-compatible personal computer and displayed on a Hewlett-Packard 1333A oscilloscopic point-plotter equipped with fast P15 phosphor. Rapid plotting speeds were achieved with the use of a point-plotting buffer (Finley, 1985). The plotting

buffer stored arrays of coordinates for the points in each image and moved these points to the oscilloscope-controlling digital to analog converters (DAC) at high speed (1,000 points/msec) without the intervention of the main computer. In the context of the displays used in these experiments, a refresh rate of 1.0 msec was obtained.

Temporal integration was studied using the temporal integration of form parts paradigm (Di Lollo, 1980). In this paradigm, subjects were required to perform a task based on the perceptual integration of two halves of a display presented sequentially, and separated by an interstimulus interval (ISI) varied from 10 to 500 msec. The duration of visible persistence in this paradigm is indexed by the maximum ISI at which the subjects can still perform the behavioral task.

The basic display sequence consisted of two images of 12 dots each, separated by an adjustable ISI. When temporally integrated, the two images formed a 5 x 5 square dot matrix with one missing element. One side of the dot matrix subtended a visual angle of two degrees at a viewing distance of 57 cm (horizontal and vertical interdot separation was 0.5 degrees). Each frame of 12 dots was displayed for a duration of 10 msec, separated by a variable ISI ranging from 10 to 500 msec.

On each trial, the subject fixated in the middle of four fixation dots arranged around the perimeter of the location of the matrix display. A trial was initiated by the press of a button on a hand-held button box. Upon a button press, the fixation dots disappeared, and the display sequence appeared.

The subject's task was to identify the missing element by keying its coordinates on a button box connected to the controlling computer. The button box contained five response buttons arranged vertically. Responses were keyed in the following manner: after the display appeared, the subject would first key in the row coordinate of the missing dot (for example, the third row of the matrix would be indicated by pressing the third button from the top) and then the column coordinate (for example, the fourth column would be indicated by the fourth button from the top). Once the coordinates had been keyed in, subjects had an opportunity to confirm their responses (a matrix with a missing dot corresponding to the position coordinates keyed in by the subject

appeared on the oscilloscope). If a mistake had been made, the subject pressed any of the five response buttons: the confirmation matrix then disappeared and the subject could re-key in the coordinates. Note that this procedure did not give feedback to the subject: rather it allowed for the correcting of mistakes in keying in the subject's intended response. If no correction was required, then the subject pressed a button to the side of the five response buttons to initiate a new trial.

Subjects held the button box in the left hand and made button presses with the right hand. Subjects typically had to look down at the button box to key in the coordinates.

Upon pressing the button to initiate a trial, the display sequence appeared after a random delay of between 1 and 100 msec. Subjects were instructed to maintain fixation for a brief (approximately one second) interval before keying in the response coordinates.

Subjects viewed the display in a room illuminated by a light source providing ambient luminance of 10 cd/m^2, as measured from the blank surface of the display oscilloscope by a Tektronix J16 digital photometer.

A calibration procedure was employed to ensure that the luminous intensity of the oscilloscope remained constant from day to day. Briefly, the procedure involved plotting a test patch in the center of the oscilloscopic display surface and measuring its luminance with a Tektronix J16 digital photometer. The patch consisted of 961 points embedded in a plotting table containing the coordinates of 1000 points, 39 of which were null. Using the 1 MB plotting buffer, each point of the test patch was refreshed every millisecond. The gain of the oscilloscope was adjusted daily so that the test patch produced a constant reading of 26.3 cd/m^2 on the photometer.

Luminous intensity of the matrix points was controlled through a 12-bit DAC on the *z*-axis of the oscilloscope.

All button press responses were collected and scored by computer. For each set of trials, the computer recorded the total number of correct responses, the number of "f1 errors" (incorrect

identification of a dot that was actually present in the first frame of the display), and the number of "f2 errors" (incorrect identification of a dot that was actually present in the second frame).

VEPs

VEPs were recorded using a Biologic Brain Atlas 20-channel EEG machine. A recording epoch of 1024 msec was used to encompass the range of stimulus durations and ISIs to be employed in the visual displays, digitized at a rate of 250 Hz. Filter bandwidth was 0.1 to 100 Hz, and amplifier gain was set at 20,000. Electrodes were silver/silver chloride, previously shorted in normal saline to drain DC sources. A single recording electrode was placed at Oz (International 10-20 System of Electrode Placement; Jasper, 1958) and referenced to linked ears.

Trials were self-paced, initiated by the subject via a button press. EEG recording was triggered by the onset of the visual stimulus. Each average VEP was collected as two sets of 50 trials to provide reliability data and to break up the recording time minimize strain on subjects. The separate averages were later combined off-line to produce grand average VEPs of 100 trials each.

Pilot Experiments

Since the visual stimuli employed in this experiment were entirely novel in the context of traditional VEP studies, a number of pilot experiments were performed to determine the effect of various aspects of the experimental paradigm that may have been expected to affect the interpretation of the results.

One unique requirement of the present experimental procedure was that subjects were required both to initiate successive stimulus trials (by pressing a button on a hand-held button box) and to enter a response based on the information contained in the visual display (by entering the coordinates of the missing dot on the same button box). Movement artifact was therefore a matter of concern. It was found in preliminary measurements that these artifacts were eliminated by simply instructing the subject to maintain fixation on the oscilloscope screen for a second or two after the display offset.

Another notably unique aspect of the temporal integration of form parts paradigm is that the successive visual displays of 12 dots are randomly selected from a set of from the complete set of 25 dots on each trials. This meant that, although the total area of the retina stimulated on each trial by the two successive stimuli was nearly identical (with the exception of a single dot location) a different set of retinal locations was stimulated on each trial, a departure from traditional VEP studies since the validity of the averaging procedure depends on the presentation of identical stimuli on each successive trial. A preliminary study was carried out to determine if any difference was obtained when the identical dot patterns were presented on each successive trial, versus when the successive patterns were randomly chosen on each trial. It was found that the evoked waveforms in both cases were nearly identical, with the exception that when identical stimuli were monotonously presented, the amplitude of the evoked waveform was somewhat reduced. On the basis of this pilot experiment, it was concluded that the temporal integration of form parts display elicited better fixation and attentiveness to the visual display than the monotonously presented display of traditional VEP experiments. Because of the nearly identical morphology of waveforms in both cases, it was concluded that if there were any differences in the successive brain responses elicited by identical versus nonidentical stimulus presentation, they were not large enough to be manifest in the averaged waveform. This finding is not surprising, since as mentioned, the spatial configuration of the total visual display presented on each trial was identical except for one dot location.

Results and Discussion

Figure 2 illustrates the psychophysical results. Performance of all three observers is seen to be nearly errorless at the shortest ISI, but to decline rapidly to an asymptotic level that is closely approached at an ISI of 80 ms. This pattern of results is entirely in agreement with earlier findings obtained with similar stimuli (Di Lollo, 1980; Hogben & Di Lollo, 1974). Clearly, temporal integration of the two portions of the display was possible only at ISIs shorter than 80 ms. This outcome matches the phenomenological appearance of the displays: the two

components were seen as a single, integrated pattern at the shortest ISI, but as distinct, temporally sequential stimuli at ISIs beyond 80 ms.

Figures 3-5 show the corresponding VEPs for each subject plotted over each interstimulus interval. Two averages of 50 trials each are superimposed to show intraindividual reliability. The superimposed waveforms of Figures 3-5 were subsequently averaged to produce the grand averaged waveforms shown in Figures 6-8.

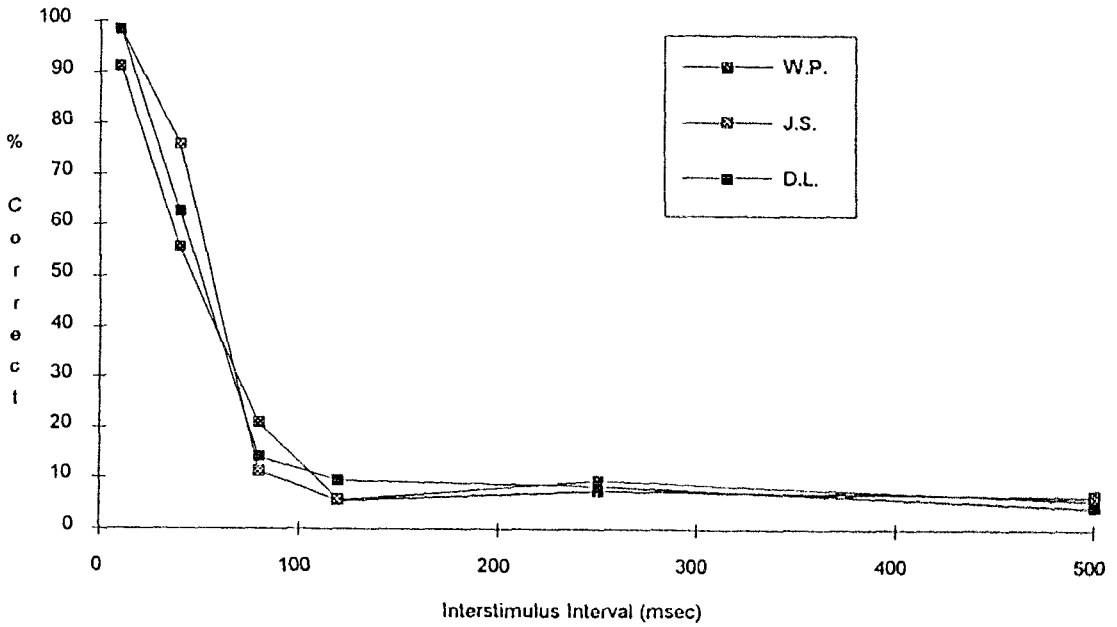

Figure 2. Percentage of correct responses plotted separately for each subject at each of the six interstimulus intervals employed in Experiment 1.

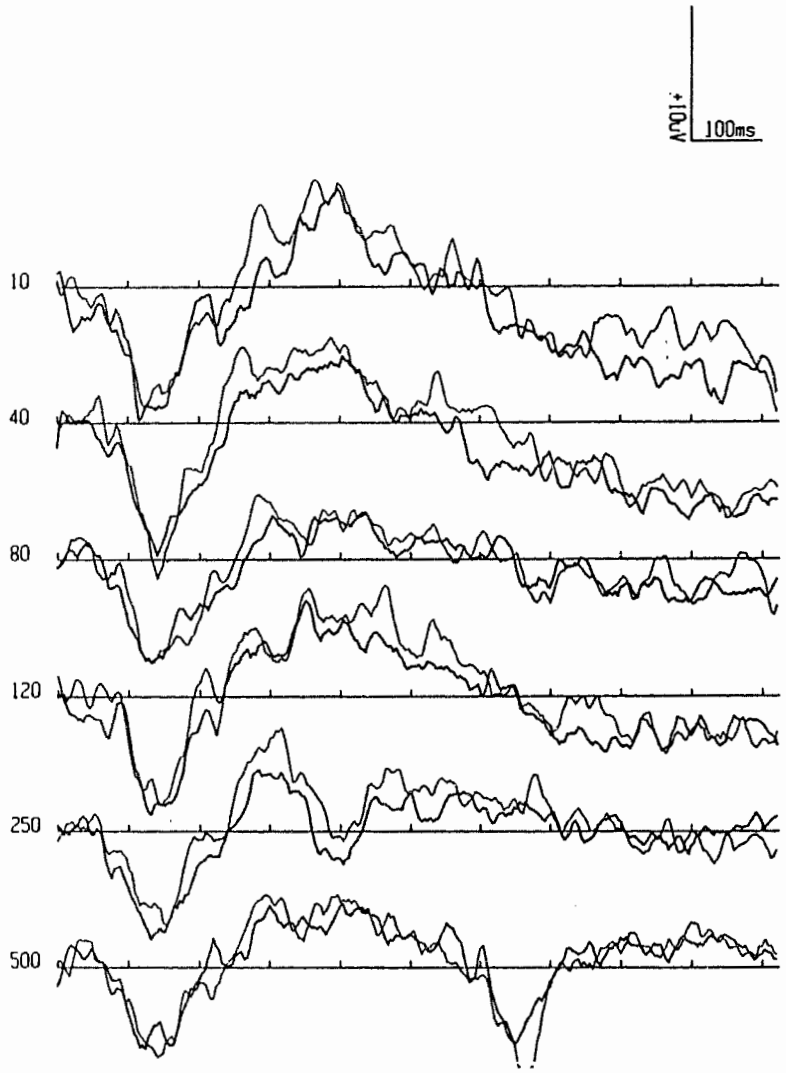

Figure 3. Visual evoked responses to sequential dot matrix stimuli plotted for each of six interstimulus intervals (Subject J.S., Replications, Oz recording).

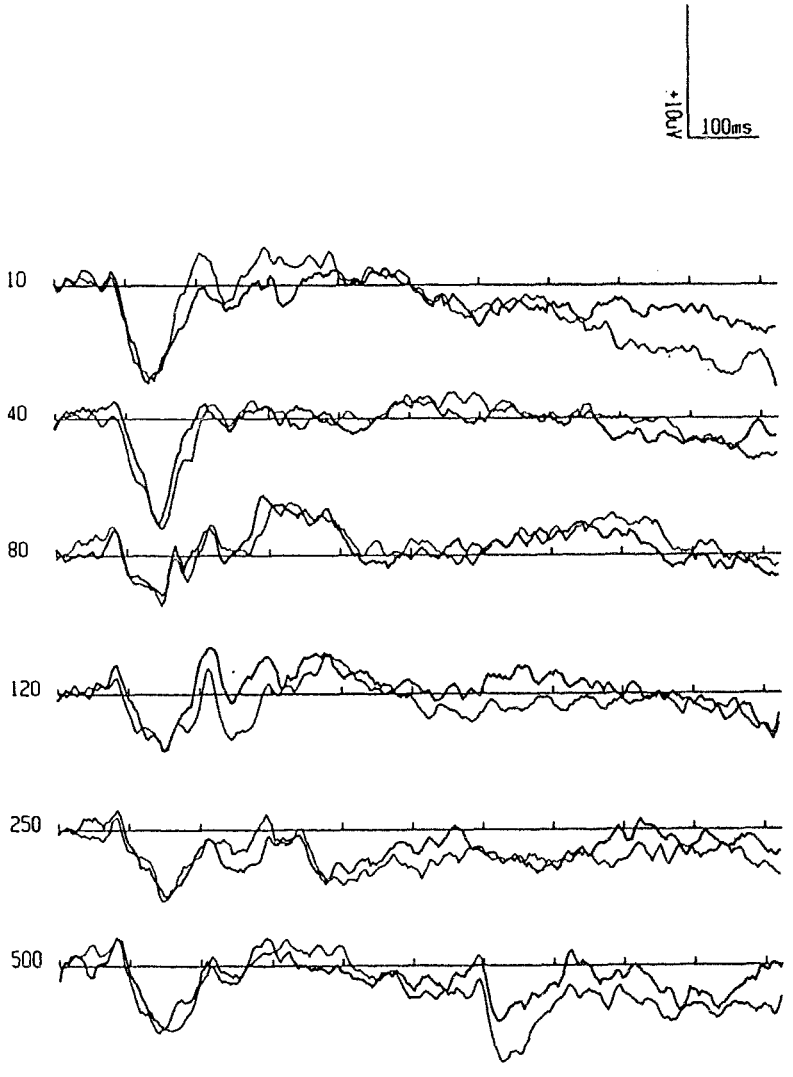

Figure 4. Visual evoked responses to sequential dot matrix stimuli plotted for each of six interstimulus intervals (Subject D.L., Replications, Oz recording).

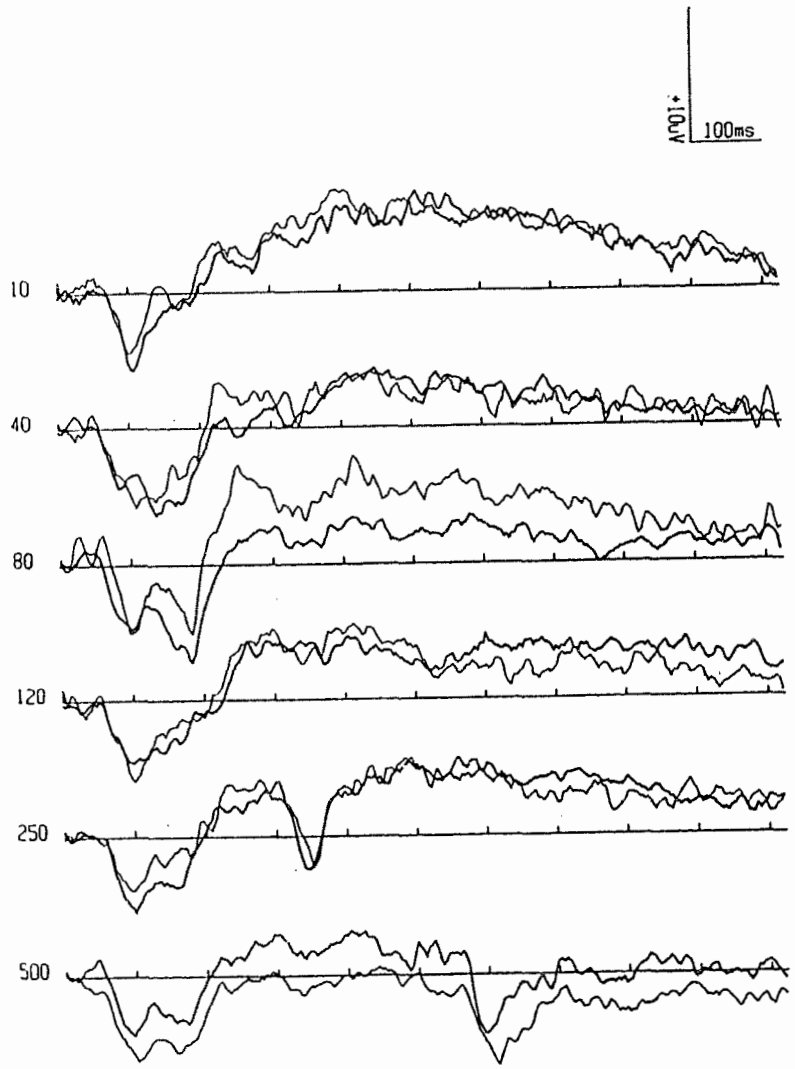

Figure 5. Visual evoked responses to sequential dot matrix stimuli plotted for each of six interstimulus intervals (Subject W.P., Replications, Oz recording).

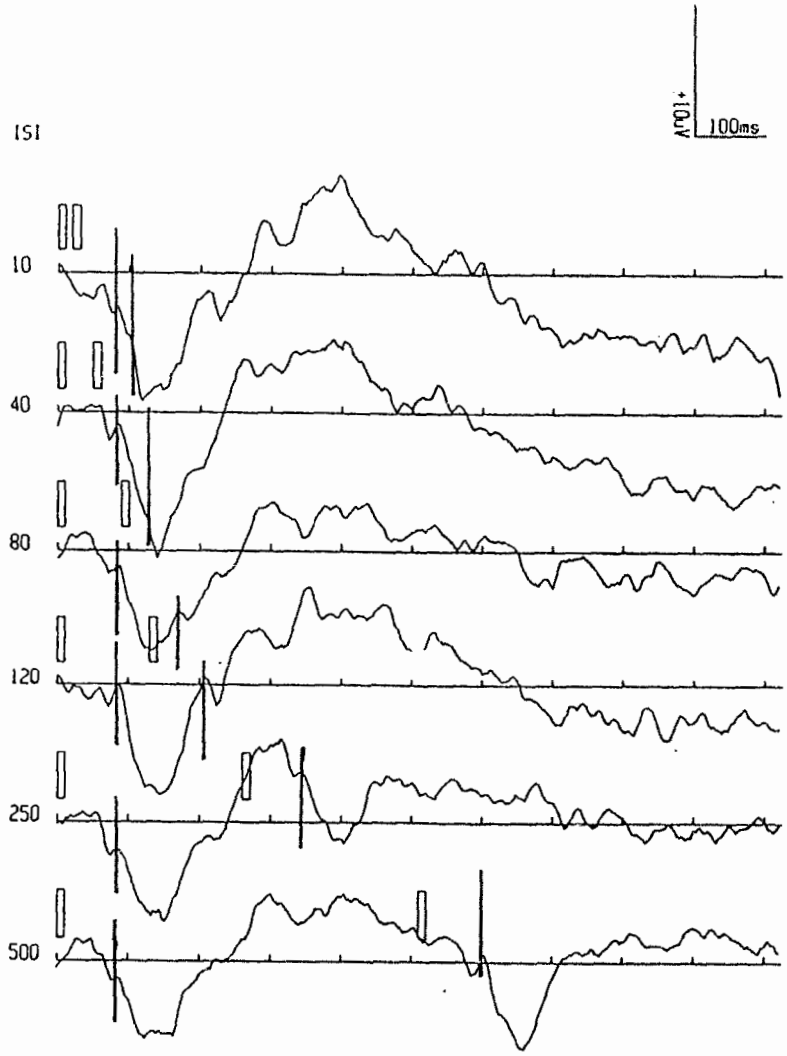

Figure 6. Grand average visual evoked responses to sequential dot matrix stimuli plotted for each of six interstimulus intervals, shown with stimulus markers (Subject J.S.).

Vertical lines: First line indicates the position of P1 or the initial point of the N1; Second line indicates the time point obtained by adding the SOA for that condition to the latency of the P1 or initial point of the N1.

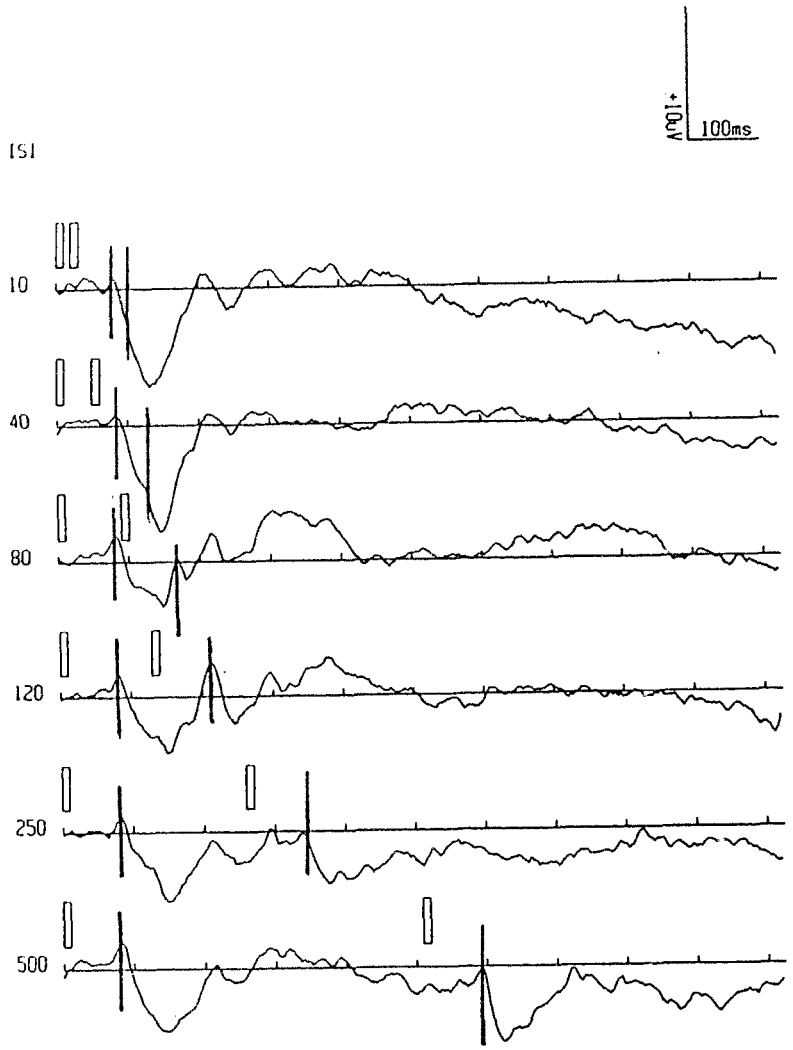

Figure 7. Grand average visual evoked responses to sequential dot matrix stimuli plotted for each of six interstimulus intervals, shown with stimulus markers (Subject D.L.).

Vertical lines: First line indicates the position of P1 or the initial point of the N1; Second line indicates the time point obtained by adding the SOA for that condition to the latency of the P1 or initial point of the N1.

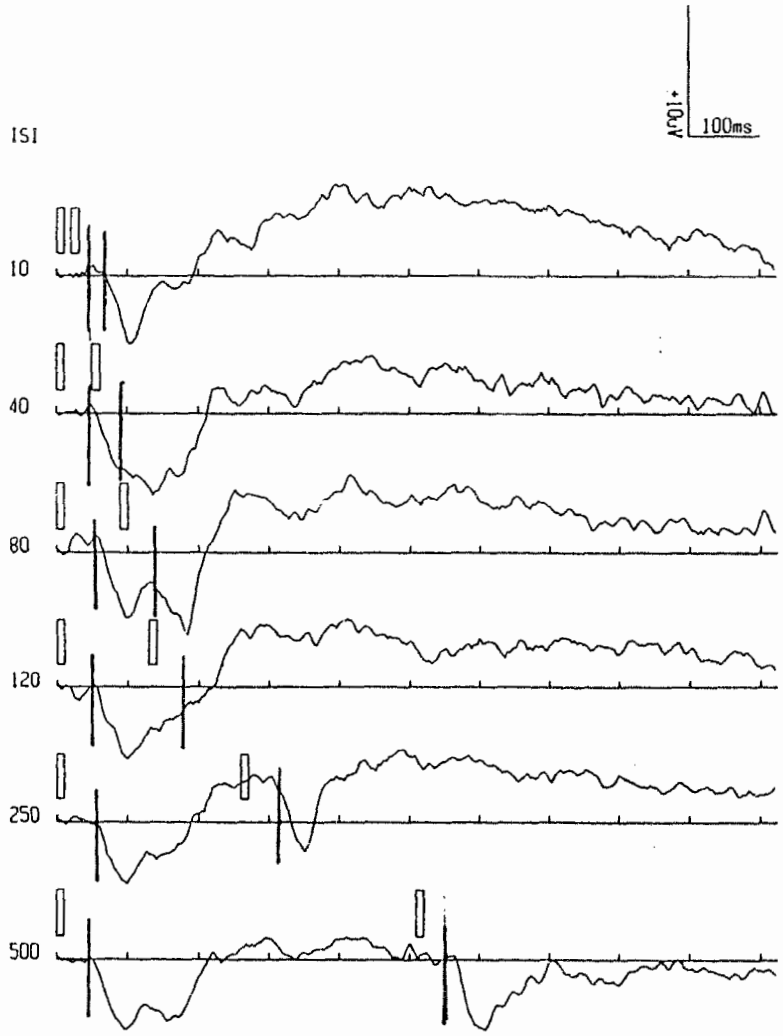

Figure 8. Grand average visual evoked responses to sequential dot matrix stimuli plotted for each of six interstimulus intervals, shown with stimulus markers (Subject W.P.).

Vertical lines: First line indicates the position of P1 or the initial point of the N1; Second line indicates the time point obtained by adding the SOA for that condition to the latency of the P1 or initial point of the N1.

Before considering the correspondence between the psychophysical and VEP data, it is necessary to digress to describe the morphology of the waveforms to provide a frame of reference to these complex voltage plots.

With reference to the initial, small positive deflections of the successive responses at an ISI of 500 msec (indicated by lines) (Figure 6), the inter-peak difference, averaged for the three observers, was 509 ms, corresponding to the SOA of 510 msec. The initial positive deflections are chosen here purely as a convenient point of reference and because they are relatively consistent in latency at each ISI (average latency: 88 msec for Subjects J.S. and D.L. over all stimulus conditions). However, the initial positive peak is entirely missing under most conditions for Subject W.P. In this subject, the onset of the broad, negative deflection seen in all subjects begins at a latency some 40 msec earlier than in the other two subjects. Clearly, it is not plausible to establish strict homologies in terms of peak latencies across all three subjects. What is consistent over all three subjects and all conditions, is the broad negative deflection that dominates the appearance of each waveform, although it too is not consistent in latency or duration across subjects or conditions.

Since a strict correspondence of waveform peaks between subjects and conditions cannot plausibly be established, the approach taken in the description of the waveforms was a purely pragmatic one: it was assumed that the onset of the response evoked by the leading display was marked by the small initial positivity, or if none was present, by the initial point of the negative-going deflection. When no initial positivity could be distinguished (as for most of the conditions for subject W.P.), the initial onset of the broad negative-going deflection was taken as a marker. Then, the time point determined by the latency of the initial marker plus the SOA for the condition was marked with a vertical line as the expected position of the onset of the response to the trailing stimulus. For the sake of reference, each peak of the response is described by its polarity (P) and temporal position (P1, N1 and P2).

The labeling scheme, and the method of identification of the expected position of the response to the trailing stimulus is illustrated for the VEPs of Subject J.S. in Figure 9. Comparing

the initial major deflections obtained at an ISI of 10 ms with the waveform obtained at an ISI of 500 msec, a good correspondence is seen in the latencies of the small initial positive peaks (P1), and in the initial negative peak of the broad negative deflection (N1). Referring to the second PNP complex for the 500 msec ISI waveform, the vertical lines indicate that the P1 of the response evoked by the trailing stimulus falls at exactly the expected time - 510 msec later than the P1 of the response evoked by the leading display. N1s do not exactly correspond, and distinct P2s cannot be distinguished in either of the first or the second response. As will be seen, the identification of the initial marker proved to be a reliable means of identifying the onset of the response to the trailing display.

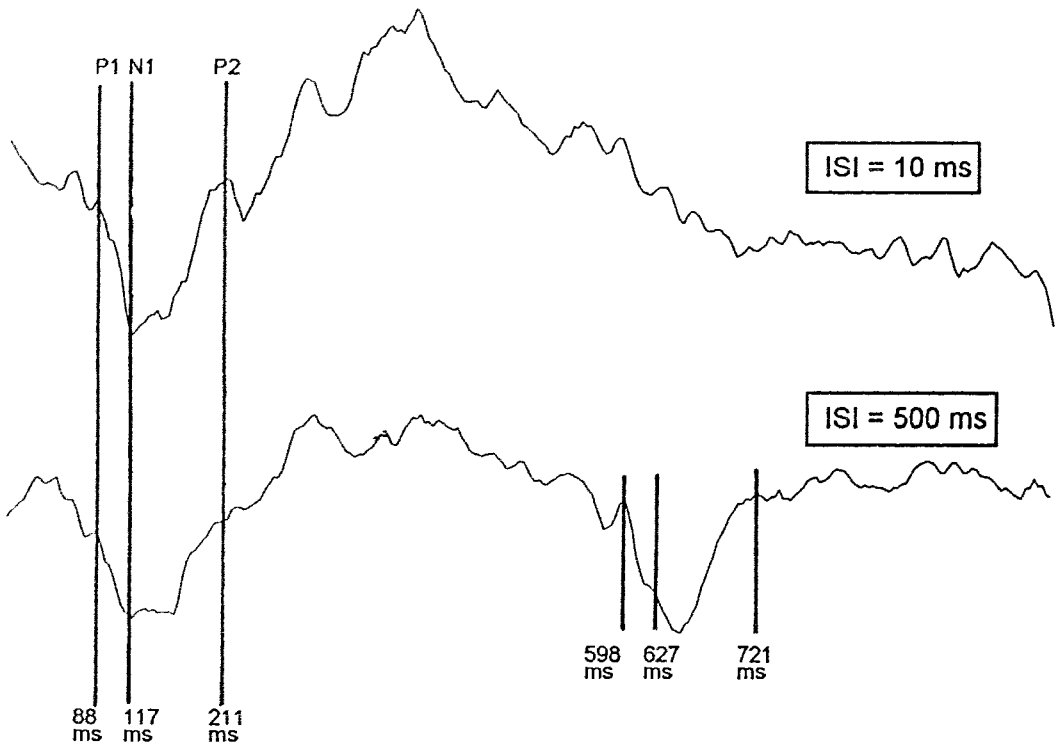

Figure 9. Labeling of peaks of visual evoked responses elicited by the dot matrix stimuli (Subject J.S.).

Referring to Figures 6-8: The first vertical line marks the position of the P1, or if a P1 could not be identified, the initial point of the negative-going deflection. The second vertical line marks the position of the expected onset of the response to the trailing stimulus. For Subjects J.S. and D.L. a small P1 can be reliably identified at a latency of 88 msec at all ISIs. In Subject W.P., the P1 is apparently completely absent at most ISIs and in addition, the major negative-going deflection is initiated and peaks in amplitude at a latency some 20 msec earlier than in the other two subjects. At an ISI of 500 msec, taking the P1 of subjects J.S. and D.L. and the initiation of the negative-going deflection for Subject W.P. as references, very similar PNP deflections can be seen 510 msec later, corresponding to the SOA. At an ISI of 500 msec, therefore, discrete and independent responses are evoked by the successive visual stimuli.

Distinct evoked responses, corresponding to the SOA, can also be seen at ISIs of 250 ms (average inter-P1 difference of 256 ms) for all three subjects, and at ISIs of 130 ms (128 ms), and at ISIs of 90 ms (84 ms) for subjects J.S. and D.L. No such distinct peaks can be seen in the VEP records obtained at the two shortest SOAs. For all three subjects, however, the N1 peak at an ISI of 40 ms is about 34 msec later than the N1 peak at an ISI of 10 msec, a displacement that corresponds to the difference in time of onset of the second stimulus between the two conditions (30 msec).

To summarize, two separate, distinct visual evoked responses can be identified at ISIs of 500 and 250 msec in all three subjects. For Subjects J.S. and D.L., a temporally distinct PNP complex can be identified at an ISI of 120 ms. At the 80 msec ISI, a smaller PNP complex can be identified which is overlapping with the rising limb of the major N1 deflection. In all three subjects, a single, integrated PNP complex is seen at an ISI of 10 msec. The N1 peak at 40 msec ISI is displaced about 30 msec relative to the N1 peak at the 10 msec ISI.

From the results of Experiment 1, it can be concluded that the psychophysical and physiological outcomes exhibit a notable correspondence: perceptual integration of the matrix form was obtained only with ISIs at which a single, integrated evoked response was observed. By contrast, at longer ISIs, when separate peaks were observed in the evoked potentials,

perceptual integration was no longer possible and the component stimuli were seen as separate and temporally sequential. The sole exception to this pattern of results is observed in the VEP of Subject W.P. at an ISI of 120 msec: Unlike the other two subjects, a separate evoked response cannot be discerned in the waveform. With this single exception, the temporal patterning of VEPs is clearly in excellent agreement with the perceptual outcomes measured by the psychophysical results.

It should be noted here that the morphology of the VEPs elicited by the dot matrix stimuli in this experiment corresponds well to the morphology of the classic pattern-onset response described in the introductory section. At the levels of adapting luminance and contrast employed in the present study, the latencies of the pattern onset response are similar to those reported here (Spekreijse, Van der Tweel and Zuidema, 1973), and with foveal stimulation the morphology of the waveforms is quite close, since the foveal pattern onset response lacks a prominent C.I component (Drasdo, 1980). A more detailed comparison of the dot matrix response and the pattern onset response will be made in Part 2 of this study.

Experiment 2

Introduction

Having demonstrated a temporal correspondence between the psychophysical and neurophysiological data of Experiment 1, Experiment 2 was designed to provide a critical test of the storage and processing hypotheses, which assign crucially different roles to the neural activity associated with the onsets and offsets of visual stimuli. As outlined in the introduction, the most salient difference between the two accounts is whether the onset or offset of a stimulus is regarded as the critical event for visible persistence. According to the storage hypothesis, the neural activity underlying visible persistence should decay as function of time from stimulus offset, while the processing hypothesis predicts that the relevant neural activity is initiated at

stimulus onset, and proceeds to completion regardless of whether or not the stimulus remains on view.

Experiment 2 was designed to provide a critical test of the two hypotheses: the underlying rationale of this test is schematically illustrated in Figure 10. Shown are two sets of stimuli separated by an identical ISI but with a nonidentical SOA: the leading frame of the second set of stimuli is of longer duration than the leading frame of the first set of stimuli. According to a storage account of visible persistence, the temporal overlap of neural activity should be identical in both cases. In contrast, a processing account predicts that the manner of temporal overlap of the neural responses underlying visible persistence should be quite different in the two conditions.

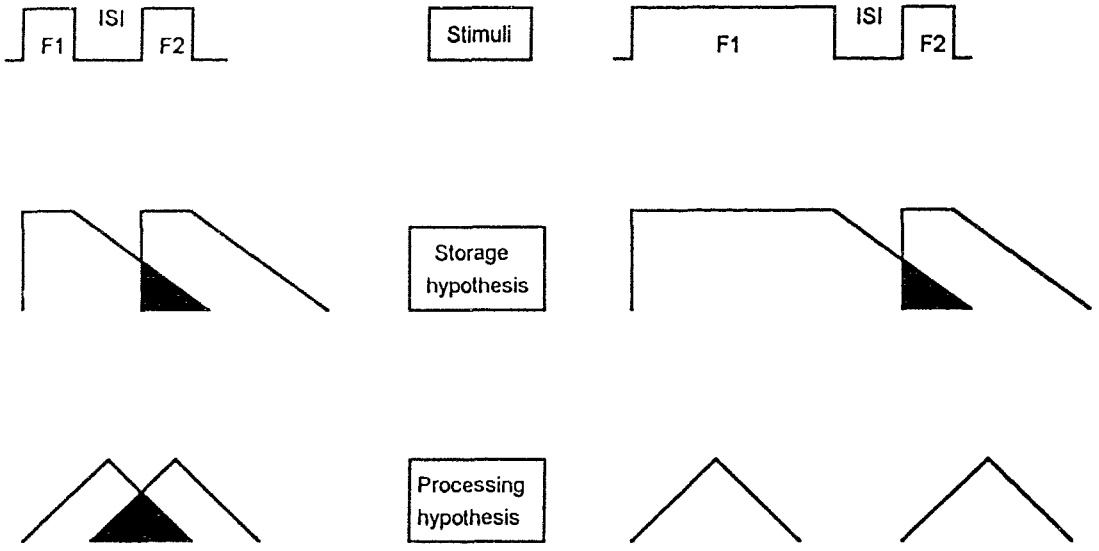

Figure 10. Schematic diagram of hypothesized neural responses to sequential visual stimuli. The stimulus sequences have an identical interstimulus interval but a nonidentical stimulus onset asynchrony. Shaded regions indicate temporal overlap of successive neural responses.

Methods

Observers, stimulus and recording parameters were identical to those employed in Experiment 1 with the exception that the duration of the leading display was systematically increased while the ISI and duration of the trailing display were held constant at 10 msec each. The range of leading display durations was chosen so that the SOAs employed in Experiments 1 and 2 were identical.

For stimulus durations of less than about 100 msec, perceived brightness is determined by both the intensity and the duration of a stimulus. Time-intensity reciprocity holds over this range of stimulus durations for both threshold (Bloch's law) and suprathreshold levels of stimulus intensities. Since several of the experiments described below employ brief stimuli of unequal durations, the effect of the experimental manipulation would be confounded by brightness mismatches. To avoid this, brief displays were plotted at higher intensity levels so that all displays appeared as equally bright. The appropriate intensity values for each duration were determined in a separate psychophysical procedure described in detail by Di Lollo (1979). Figure 11 illustrates the configuration of stimuli employed in Experiments 1 and 2.

Control Experiment

It is well known that pattern offset responses are obtained when a stimulus pattern is presented for durations of greater than about 50 msec (Jeffreys, 1977). In light of this, the possibility exists that the response to the offset of the first stimulus may overlap with the response to the onset of the second display and confound its interpretation. To examine this possibility, 2 of the three subjects (J.S. and W.P.) participated in a separate control study in which only the first half of the display was presented, for durations corresponding to those of the leading display in the main experiment. To make this condition resemble the conditions of the main experiment as closely as possible, the single presentations were randomly intermixed with regular trials in which both a leading and trailing display were presented in a proportion of 1:4

single:standard presentations. EEG collection was triggered only by the single half-matrix presentations.

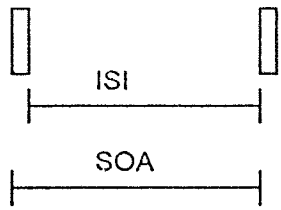

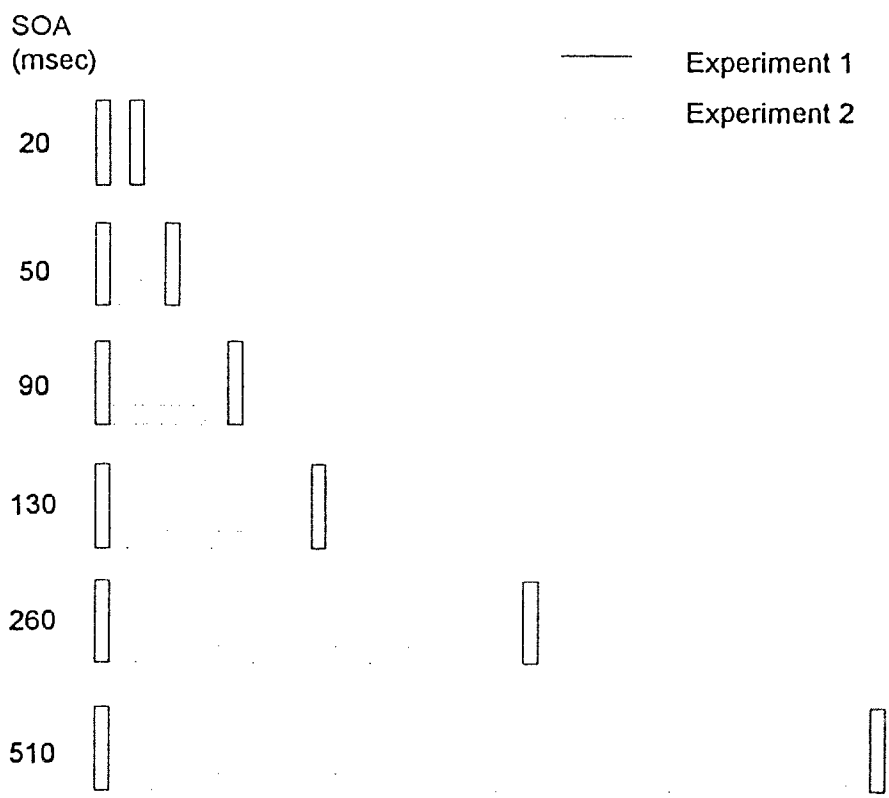

Figure 11. Temporal patterning of stimuli in Experiments 1 and 2. Inset: Measurement of interstimulus interval (ISI) and stimulus onset asynchrony (SOA).

Results and Discussion

Figure 12 (top) shows the percentage of correct responses at each duration of the leading display plotted separately for each subject. Performance was essentially errorless at leading-display durations of 40 msec and less, but declined markedly thereafter, although the slope of the performance curves is less steep past 120 msec. Subject W.P. is seen to have a higher level of performance over the entire range of leading display durations, but the overall shape of the curves is similar in all three subjects. These results closely replicate those previously reported by Di Lollo (1980), who employed a similar experimental paradigm. Di Lollo's (1980; p. 78) results are replotted in Figure 12 (bottom) for comparison with the results of the present experiment. Clearly, the overall patterning of results is very similar.

The phenomenal appearance of the display should be noted: At the brief display durations (10 and 40 msec), all dots in the display appeared as a single, integrated matrix, while at the longer durations (250 and 500 msec) the display was seen as two distinct frames of dots separated by a noticeable temporal gap.

Comparing the psychophysical results of Experiments 1 (Figure 2) and 2 (Figure 12) it is apparent that (1) the rate of decline in performance is less steep for the F1 duration manipulation than for the ISI manipulation and that (2) the final level of performance at the leading display duration of 500 msec is well above chance performance. Clearly, performance is not identical under the two conditions. This observation has not been previously reported or discussed in the visible persistence literature (Di Lollo, 1991; personal communication).

Given the observed decline in performance with increasing F1 duration, it can be concluded that, to a first approximation, the duration of visible persistence is, as predicted, related to the onset of the first flash of points, since no decline would be predicted if it were the case that persistence were solely related to the offset of the inducing stimulus. Given the differences in performance between Experiments 1 and 2, however, clearly something is left unaccounted for. Discussion of the possible explanations for this interesting discrepancy will be

dealt after considering the VEP results. For the purposes of the argument at hand, it is sufficient to note that a storage hypothesis is entirely incapable of dealing with these results.

Figures 13 to 15 show the VEP results. For each subject, two averages of 50 trials obtained with the same stimulus conditions are superimposed. As in Experiment 1, large, robust PNP waveforms were elicited in each subject. The morphology of each waveform is dominated by the broad N1 wave described in Experiment 1. The superimposed waveforms show that the individual responses are clearly reliable.

Figures 16-18 show the average of the replicated waveforms of Figures 13-15, shown with stimulus markers above each grand average waveform. Following the method used in Experiment 1, the P1 of the initial PNP complex is identified by the first vertical line, while the second vertical line indicates the time point determined by adding the SOA for that condition to the P1 latency. Referring to the 500 msec leading display condition at the bottom of Figures 16-18: two clearly identifiable PNP complex are observed in each subject. The latency of the second complex corresponds closely to that predicted by adding the SOA (510 ms) to the latency of the initial P1. By the same method, a second PNP complex can be identified in each subject for the 250 msec condition and for the 120 msec condition in all three subjects. For the 80 msec condition, a second PNP complex can be seen overlapping with the rising portion of the N1 wave of the first PNP complex. Single, integrated PNP waves are seen in the 40 msec and 10 msec conditions. The N1 peak of the 40 msec condition is delayed relative to the N1 peak of the 10 msec condition by a mean of 24 msec (averaged over the 3 subjects), corresponding well to the difference in SOA between the two conditions (20 msec).

In summary, two distinct VEP complexes were elicited by the successive stimuli at leading display durations of 500, 250 and 120 msec. The two responses are overlapping in the 80 msec condition, and completely integrated in the 10 and 40 msec conditions. To compare the results of Experiments 1 and 2, Figures 19-21 show the VEPs obtained in Experiment 1 superimposed upon the VEPs obtained at the corresponding SOAs in Experiment 2. The superimposition shows that the temporal patterning of the VEPs obtained in the two experiments

are strikingly similar: similar VEPs are elicited when either ISI or duration of the leading display are manipulated. The sole exception to this pattern of results are the VEPs of subject W.P. at an SOA of 130 msec - the similarity between the waveforms obtained in Experiments 1 and 2 for this SOA is not as close as is seen in all other conditions.

VEPs obtained in the control experiment are shown in Figures 22 and 23, superimposed on the waveforms of Figures 19 and 21. Little evidence was seen of offset responses: For subject J.S. (Figure 22) a small negative deflection in the single stimulus waveform is seen beginning at the second vertical marker. For Subject W.P. (Figure 23) a small PNP waveform is seen beginning some 30 msec after the second vertical line marker. It was concluded that offset responses were not larger than the background noise of the EEG and were unlikely to significantly affect the waveform of the response evoked by the second stimulus in the sequence.

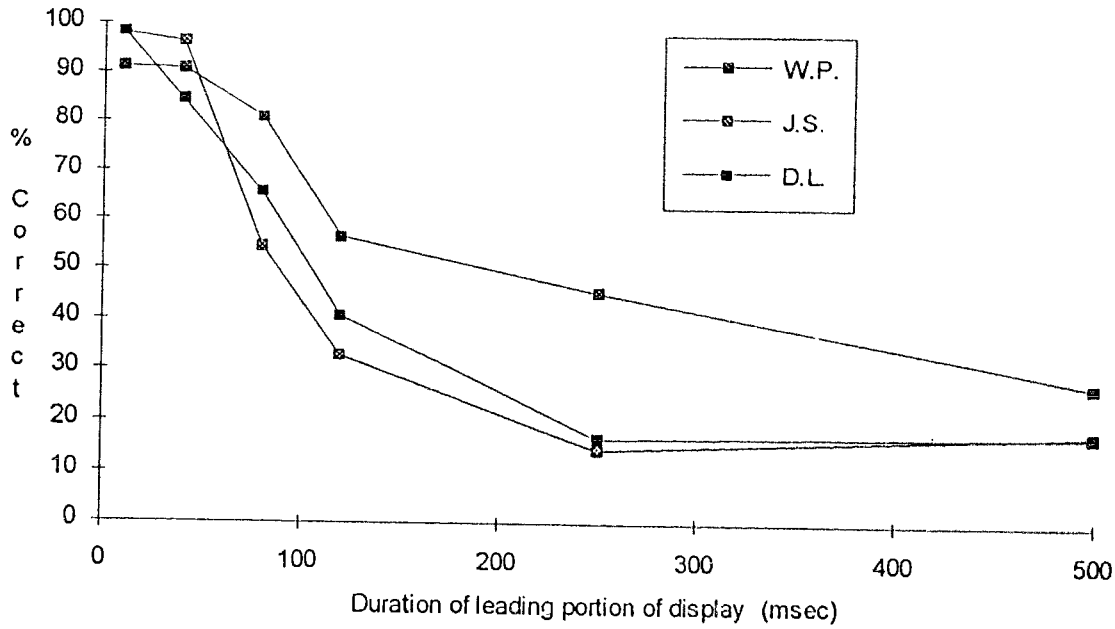

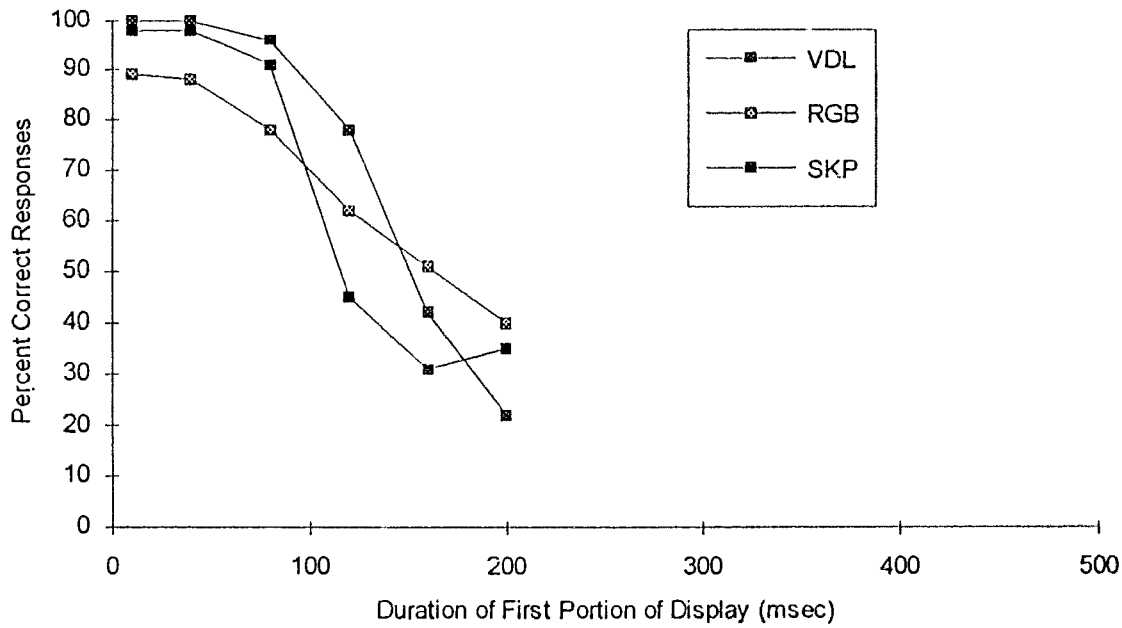

Figure 12. Top: Percentage of correct responses plotted separately for each subject at each of the six durations of the leading portion of the display. Bottom: Data of Di Lollo (1980; Figure 1), replotted for comparison.

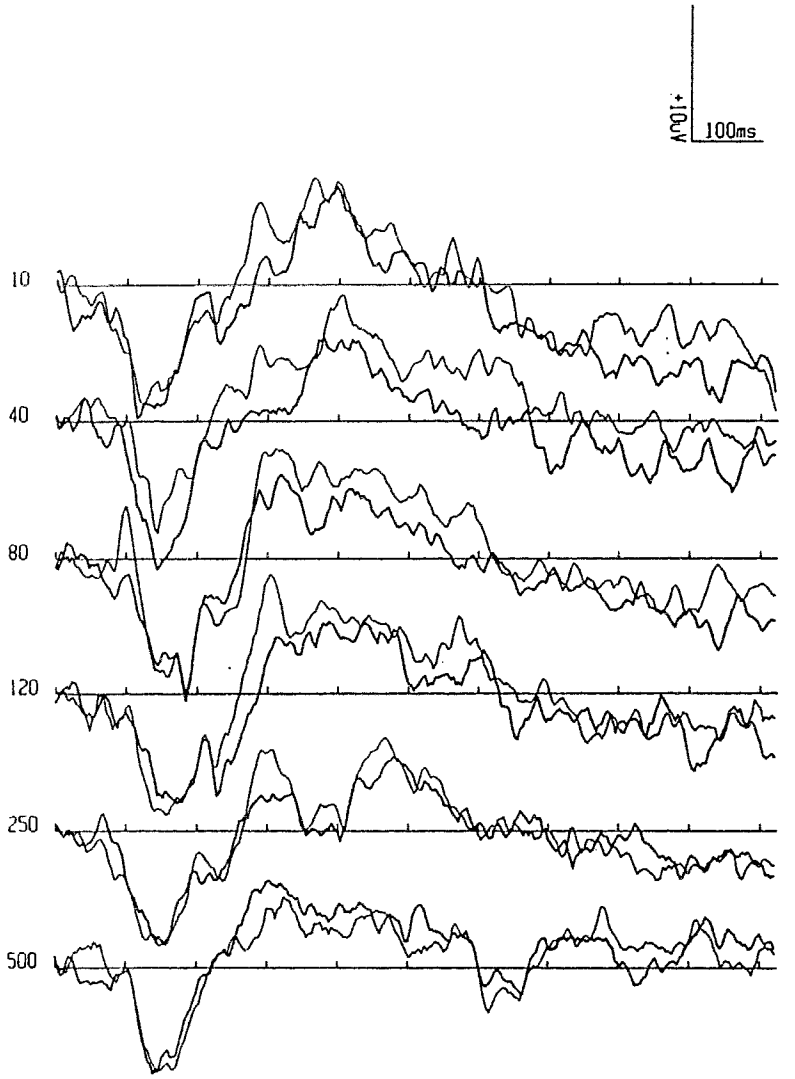

Figure 13. Visual evoked responses to sequential dot matrix stimuli plotted for each of the six durations of the leading portion of the display (Subject J.S., Replications).

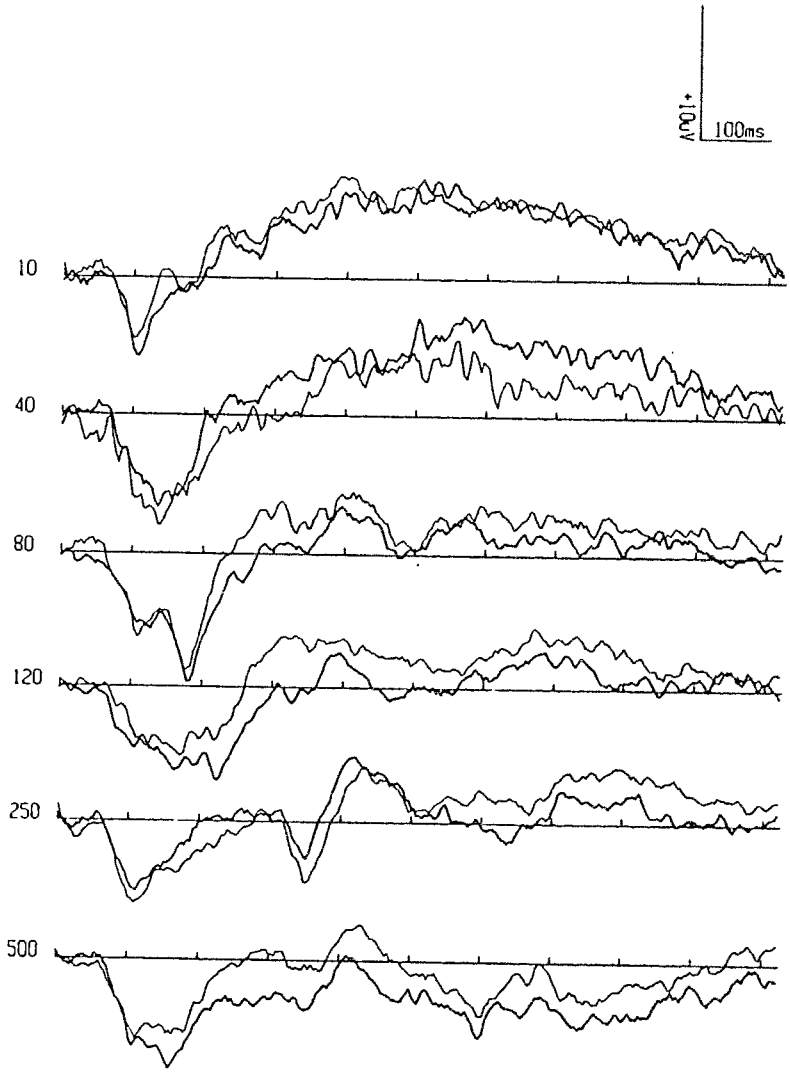

Figure 14. Visual evoked responses to sequential dot matrix stimuli piotted for each of the six durations of the leading portion of the display (Subject D.L., Replications).

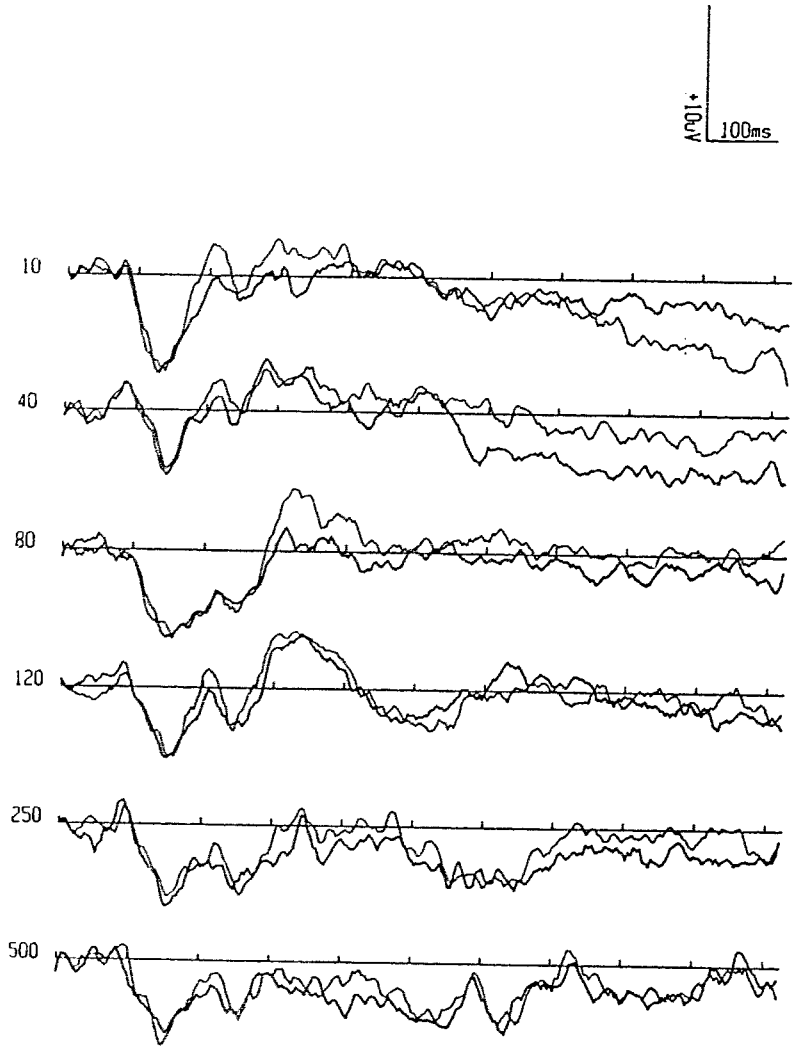

Figure 15. Visual evoked responses to sequential dot matrix stimuli plotted for each of the six durations of the leading portion of the display (Subject W.P., Replications).

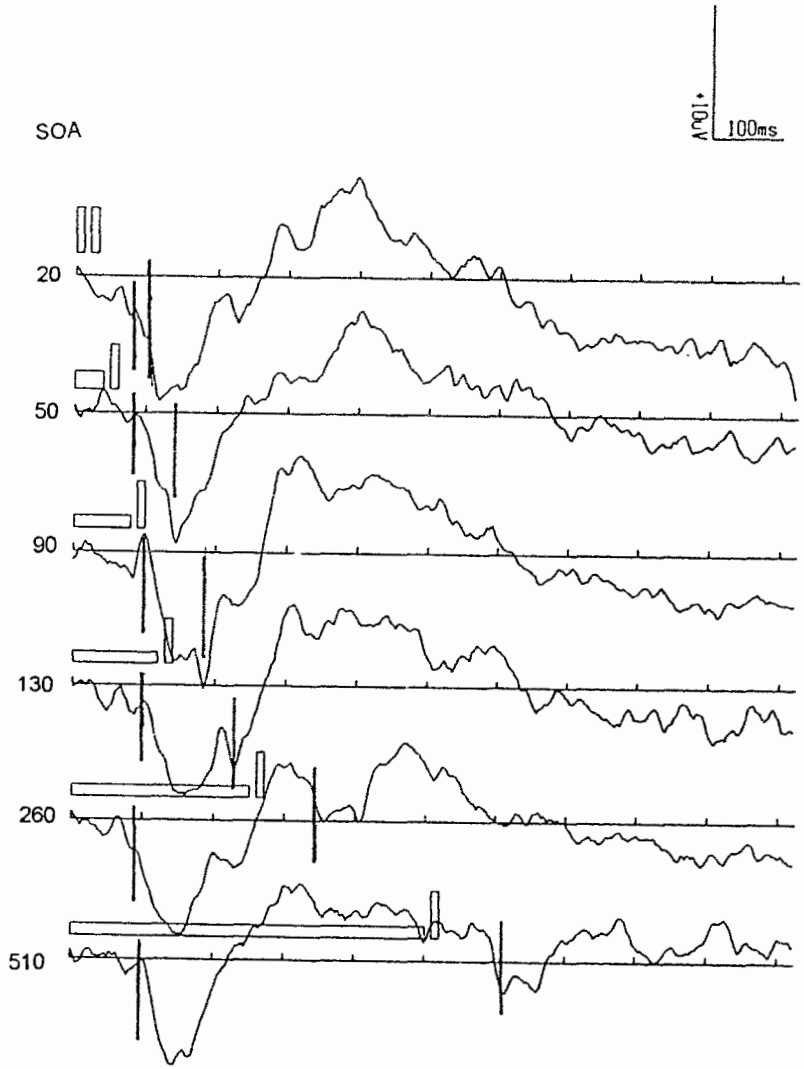

Figure 16. Grand average visual evoked responses to sequential dot matrix stimuli plotted for each of the six durations of the leading portion of the display, shown with stimulus markers (Subject J.S.).

Vertical lines: First line indicates the position of P1 or the initial point of the N1; Second line indicates the time point obtained by adding the SOA for that condition to the latency of the P1 or initial point of the N1.

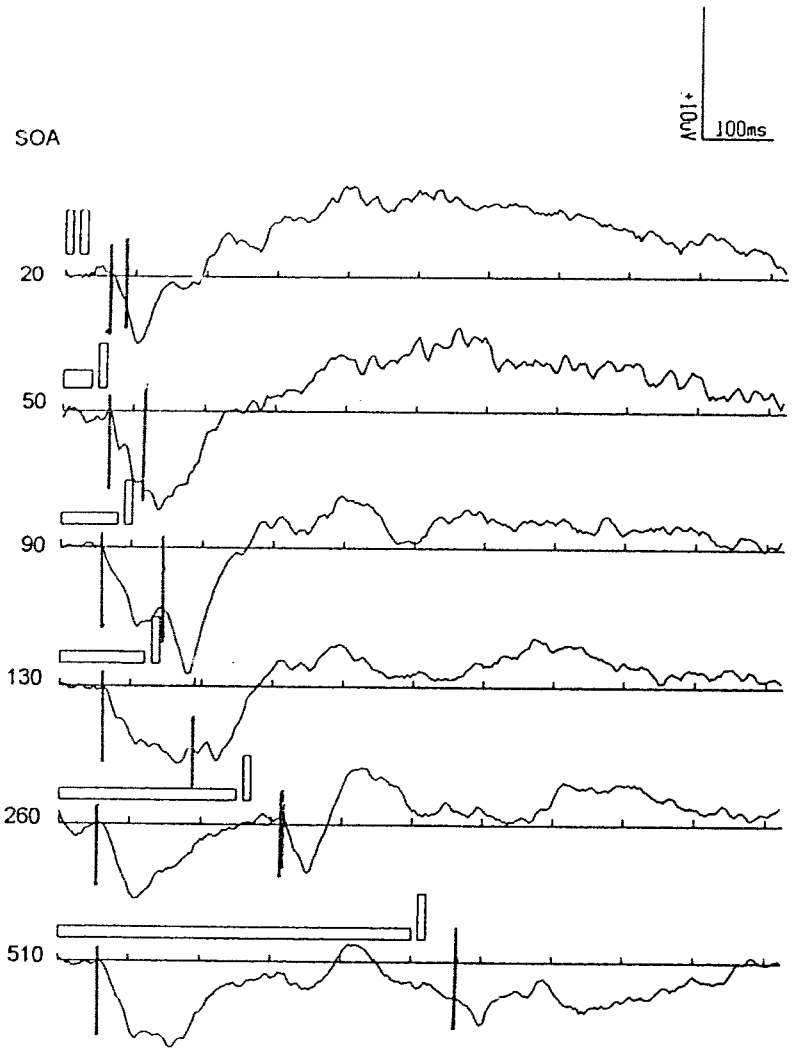

Figure 17. Grand average visual evoked responses to sequential dot matrix stimuli plotted for each of the six durations of the leading portion of the display, shown with stimulus markers (Subject D.L.).

Vertical lines: First line indicates the position of P1 or the initial point of the N1; Second line indicates the time point obtained by adding the SOA for that condition to the latency of the P1 or initial point of the N1.

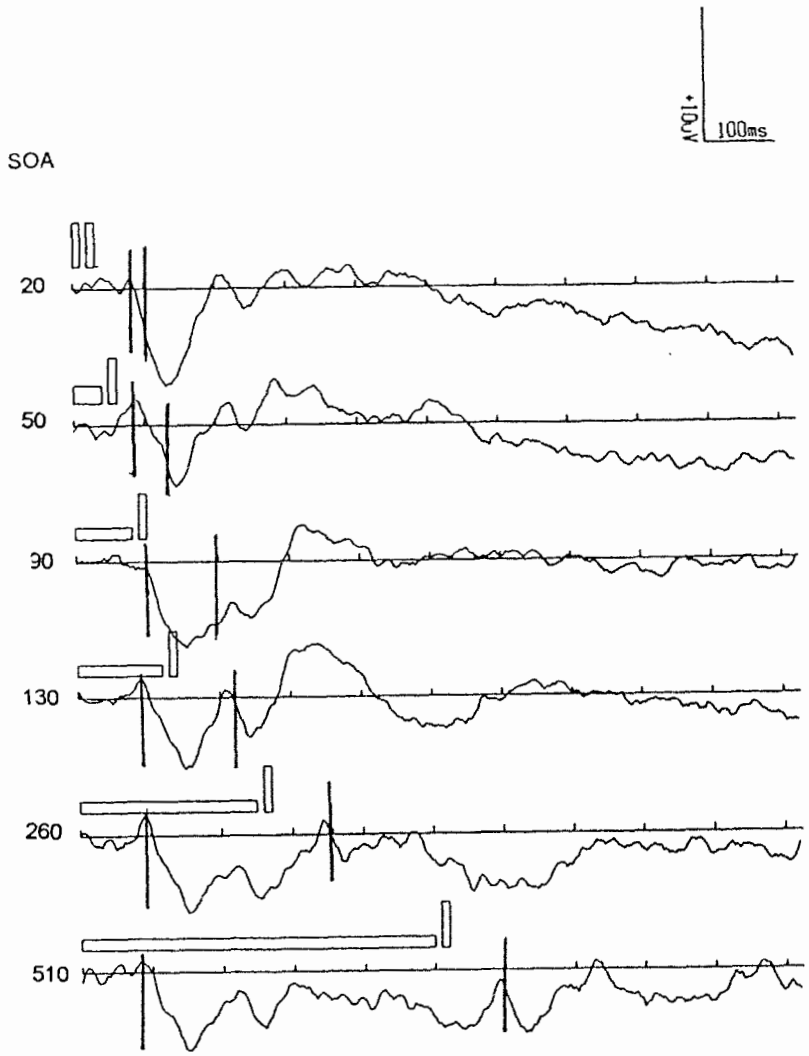

Figure 18. Grand average visual evoked responses to sequential dot matrix stimuli plotted for each of the six durations of the leading portion of the display, shown with stimulus markers. (Subject W.P.).

Vertical lines: First line indicates the position of P1 or the initial point of the N1; Second line indicates the time point obtained by adding the SOA for that condition to the latency of the P1 or initial point of the N1.

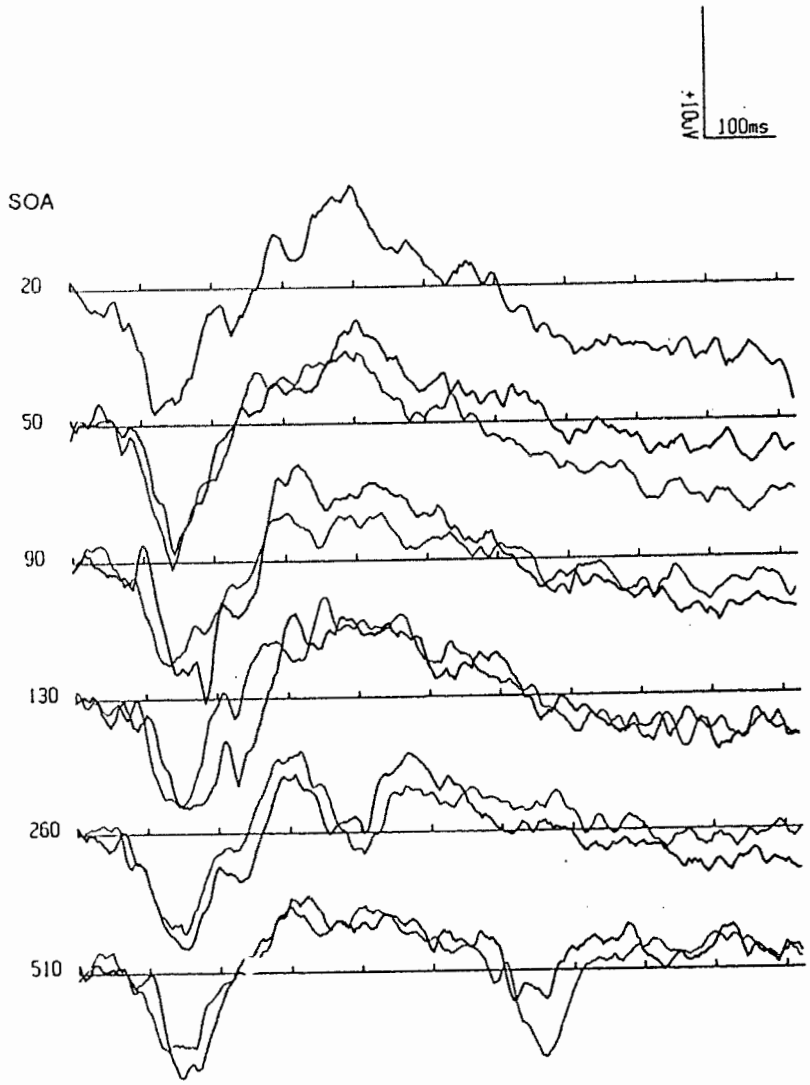

Figure 19. Visual evoked responses to sequential dot matrix stimuli plotted for each of the six durations of the leading displays, superimposed upon the responses obtained at a corresponding stimulus onset asynchrony in Experiment 1 (Subject J.S.).

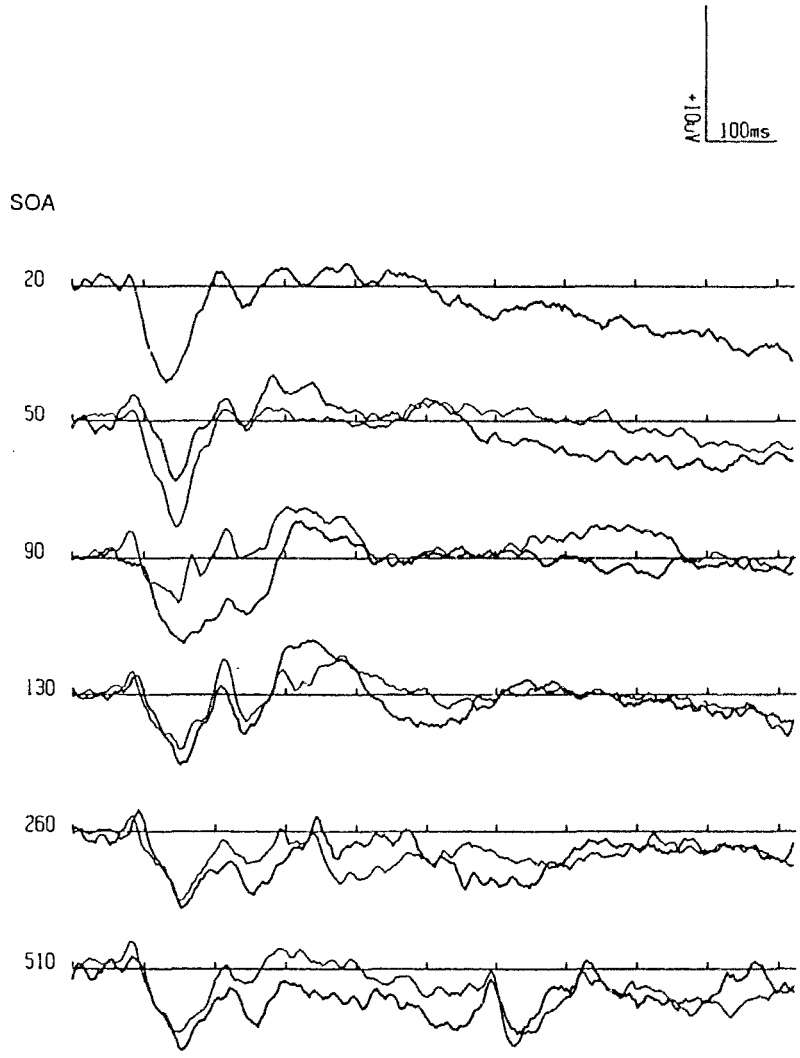

Figure 20. Visual evoked responses to sequential dot matrix stimuli plotted for each of the six durations of the leading displays, superimposed upon the responses obtained at a corresponding stimulus onset asynchrony in Experiment 1 (Subject D.L.).

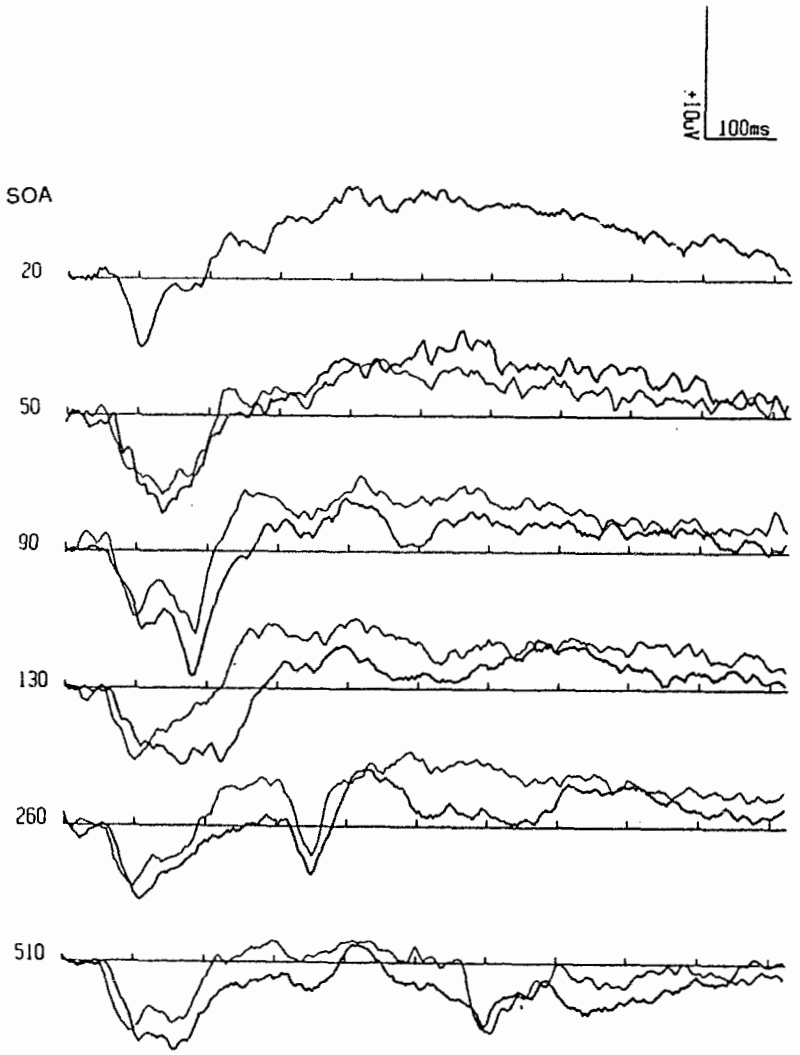

Figure 21. Visual evoked responses to sequential dot matrix stimuli plotted for each of the six durations of the leading displays, superimposed upon the responses obtained at a corresponding stimulus onset asynchrony in Experiment 1 (Subject W.P.).

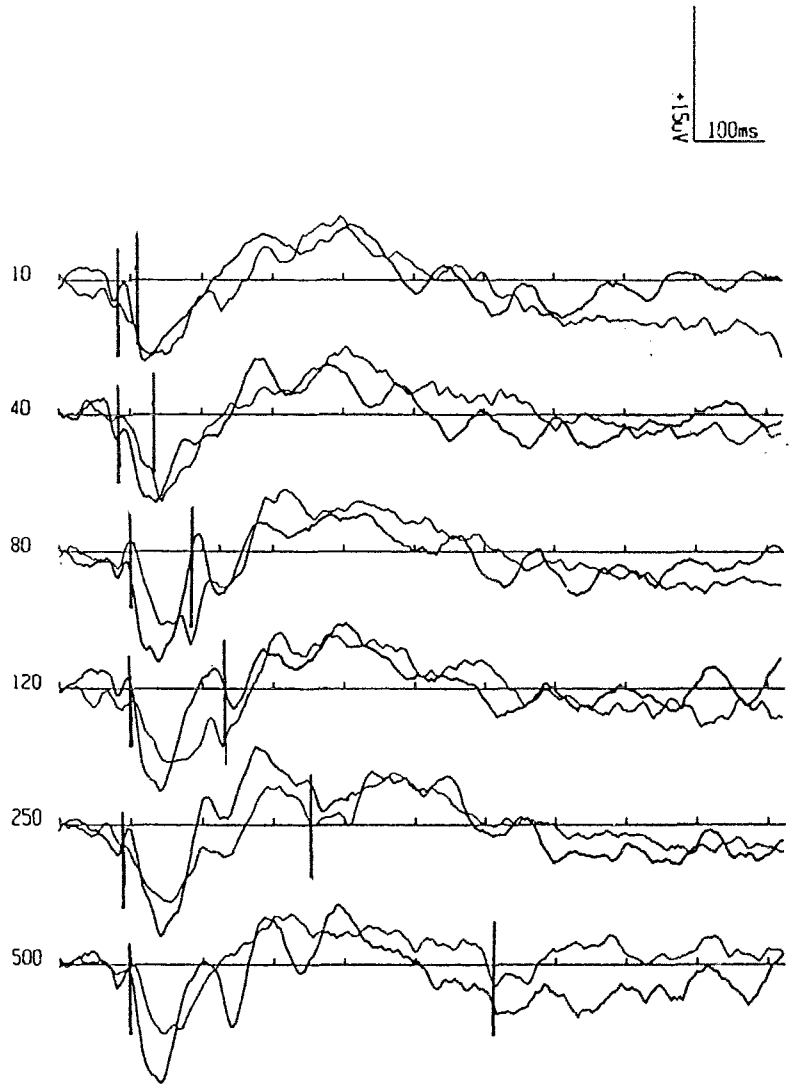

Figure 22. Visual evoked responses to a singly presented half of the dot matrix display at each of the six stimulus durations (darker waveforms), superimposed upon the VEPs obtained with a corresponding duration of the leading display in the standard two stimulus sequence (lighter waveforms). (Subject J.S.)

Vertical lines: First line indicates the position of P1 or the initial point of the N1; Second line indicates the time point obtained by adding the SOA for that condition to the latency of the P1 or initial point of the N1.

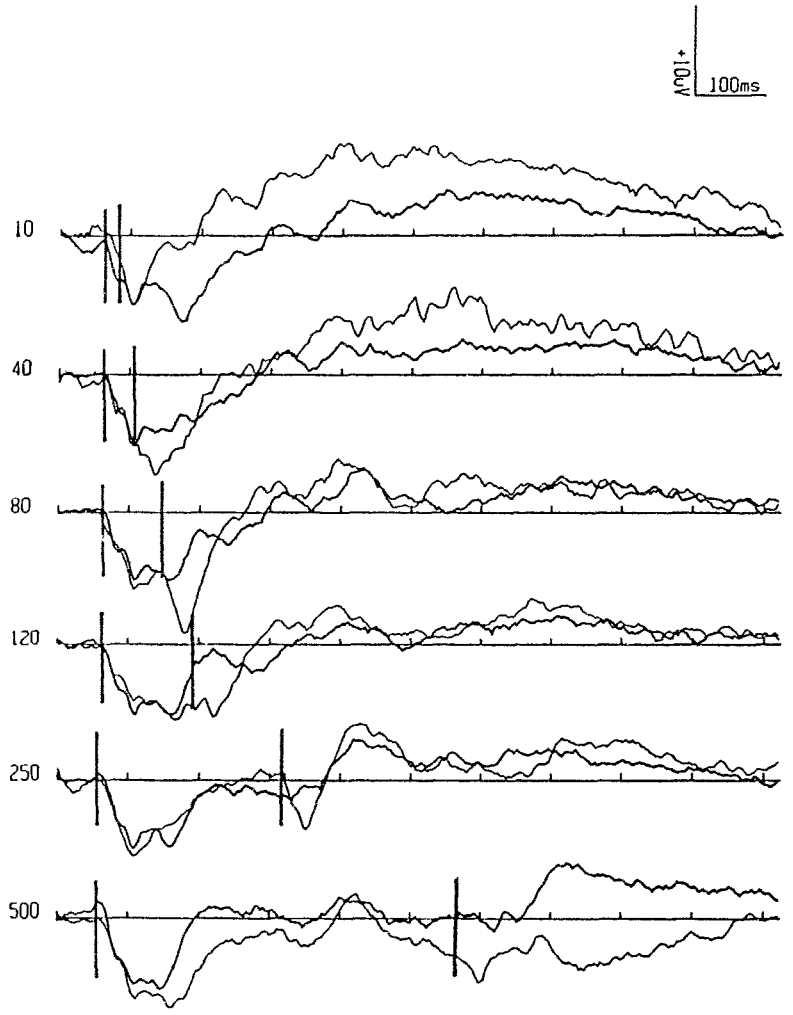

Figure 23. Visual evoked responses to a singly presented half of the dot matrix display at each of the six stimulus durations (darker waveforms), superimposed upon the VEPs obtained with a corresponding duration of the leading display in the standard two stimulus sequence (lighter waveforms). (Subject W.P.)

Vertical lines: First line indicates the position of P1 or the initial point of the N1; Second line indicates the time point obtained by adding the SOA for that condition to the latency of the P1 or initial point of the N1.

Taken together, the results of Experiments 1 and 2 show clearly that the primary determinant of the dot matrix evoked potentials is SOA, rather than ISI. For the behavioral data as well, the primary temporal correlate is SOA: the marked degradation in performance with increasing duration of the leading display while ISI is held constant cannot be accommodated by any explanation that holds that ISI is the critical variable in visible persistence. Any version of a storage account of visible persistence is therefore unambiguously contradicted by both the behavioral and physiological data.

The hypothesis of Sakitt states that "information about the icon is stored primarily in the rod photoreceptors" (1975, p. 1319). According to this account, when light is absorbed in the photoreceptors, it takes a finite amount of time for the receptor photocurrent to recover after stimulus offset. This residual photoreceptor activity is necessarily passed to higher levels of the visual system so that the visual display remains perceptually available after stimulus offset for the time it takes the photocurrent to decay to resting levels. This hypothesis thus predicts that ISI should be the critical determinant of the brain activity underlying visible persistence: This prediction is not supported by the VEP evidence. The brain activity measured in this paradigm therefore cannot be encompassed within a framework of passive sensory storage.

Sensory-perceptual events whose primary temporal determinant is SOA are often explained in terms of active processing events that occur during the SOA (e.g. Kahneman, 1967; Sperling, 1971). Di Lollo's (1980) processing hypothesis states that visible persistence is the product of the activity of sensory encoding mechanisms recruited at an early stage of visual information processing. Once recruited, the encoding activities performed by these mechanisms proceeds to completion whether or not the inducing stimulus remains on display. The neuronal mechanisms performing these encoding operations would thus be expected to become active at some finite latency from the onset of the visual stimulus and to remain active for some finite duration required for the completion of the particular sensory encoding operation being performed. Thus, the duration of visible persistence would be determined by the difference between the duration of the encoding process and the duration of the inducing stimulus. The

temporal properties of the brain activity elicited by the stimuli in the present study are wholly supportive of this prediction.

While the psychophysical and physiological data presented here are broadly consonant with a processing theory of visible persistence, it must be noted that it is unlikely that the psychophysical results of Experiment 2 were determined solely by the activity of sensory coding mechanisms at an early stage of processing. If, as predicted by the processing hypothesis, the time between stimulus onset and persistence offset is a constant, behavioral performance would be expected to fall off in an identical manner in Experiments 1 and 2, and there should be no visible persistence at the longest durations of the leading display in Experiment 2. The data do not support this prediction: the ability to integrate two successive visual stimuli falls off at a a more gradual rate when an increasing SOA is determined by increasing the duration of the leading display than when it is determined by increasing the ISI, and the final level of performance at the longer durations of the leading display is still better than chance.

Obviously, some portion of the behavioral data is left unaccounted for by the processing hypothesis. On reflection, this is not a particularly surprising conclusion, since the total duration of perceptual persistence must ultimately be determined by neuronal responses at all levels of the visual system between the photoreceptors in the retina and the level at which relevant neuronal activity is elaborated into perceptual experience. It is well-known that neurons at different levels of the visual system have widely varying temporal response properties (Uttal, 1981), and the temporal properties of perceptual persistence would be expected to be determined by some complex admixture of the temporal properties of all of the neurons involved in elaborating a perceptual experience from the patterned light on the retina. According to the processing hypothesis, only neurons active during the recruiting phase of sensory processing and involved in the obligatory sensory encoding of stimulus features would be expected to respond in precisely the same manner to the sequential visual stimuli of Experiments 1 and 2. The persistence of neurons at both lower (for example, photoreceptors) and higher (for example, hypothetical cortical areas involved in monitoring the constancy of the visual environment;

Donchin & Coles, 1988) would be expected to respond in a different manner to an SOA in which the leading stimulus is continuously available during most of the interval, versus the same SOA in which stimuli are separated by a long temporal gap.

What the present data do strongly indicate is that SOA is the principal temporal correlate of behavioral performance, consonant with the hypothesis that visible persistence is primarily determined by the activity of neural encoding mechanisms active during an early stage of visual information processing. The neuronal generators of the N1 component of the VEPs measured in the present study exhibit precisely the SOA properties predicted by the processing hypothesis, and as such, are excellent candidates as the principal neuronal determinants of visible persistence. These neuronal generators have tentatively been identified with those of the C.II component of the pattern onset response, which, according to Jeffreys and Musselwhite (1986), is generated by cortical mechanisms involved in the spatial analysis of the visual stimulus, located in the extrastriate regions of visual cortex. Part 2 of this study will attempt to further delineate the generator structures of the dot matrix VEPs.

PART 2: SPATIAL PATTERNING OF VISUAL EVOKED POTENTIALS

Introduction

The first section of the present study focused on an intensive investigation of the temporal parameters of the VEPs recorded at a single occipital location, with the goal of establishing a correspondence between physiological and psychophysical measures. The focus of investigation now changes to an multichannel investigation of the spatial parameters of these VEPs, with the goal of deriving reasonable inferences concerning their cerebral generators. This goal may alternatively be described as a reduction in the number of parameters required to adequately describe an exceeding complex spatiotemporal distribution of scalp potentials: As will be seen, the VEP sampled at 256 temporal locations at each of 20 spatial locations can be adequately explained with only 6 (Cartesian) parameters specifying the location (three parameters) and orientation (three parameters) of a single equivalent dipole source. Drawing on knowledge of the functional organization of the visual system allows the inference that the equivalent source thus obtained likely represents a distributed region of active cortex in the extrastriate region of the occipital lobe.

Two series of investigations were carried out in this phase of the present study. In the first series of studies, the goal was to obtain a description of VEP topography at 20 locations placed according to the International 10-20 System of Electrode Placement (Jasper, 1958). The topographic distribution of VEPs was recorded for several different stimulus conditions. On the basis of the topographical information thus derived, a dense occipital montage was used in the second series of studies, in combination with the presentation of visual stimuli to restricted regions of the retina. Source localization techniques were applied to this data.

1. Scalp Topography

Topographical distributions were obtained for four stimulus conditions: The dot matrix stimulus was presented at two ISIs in order to compare the spatial maps under conditions at which complete temporal integration was obtained in Part 1 (10 msec), to a condition in which temporal integration was impossible (500 msec). For comparison to a more conventional stimulus, a checkerboard stimulus was presented at corresponding ISIs. The checkerboard pattern was of the same size and interelement separation as the dot matrix display, but the displays were not comparable in several respects: unlike the matrix display, the checkerboard display appeared on a continuously present uniform field with no change in space-averaged luminance; the two displays in a sequence were identical, rather than halves of a complete display; and the onset of the display was not under the control of the subject. Strict comparability of the stimuli was not necessary for the purposes of the investigation, since the goal was simply to obtain a comparison of the matrix VEP topography and that of a more conventional stimulus used in the study of the pattern onset response (e.g. Butler et al., 1987).

Method

With the exceptions described below, stimulus generation and display, EEG recording and general procedure were the same as described in the preceding section. Two subjects participated in this preliminary investigation, one of whom had participated in the studies in Part 1 (J.S.).

20 recording electrodes were placed on the scalp according to the international 10-20 system of electrode placement (Jasper, 1958), illustrated in Figure 24. (Fpz was interpolated on-line from the surrounding electrodes) and referenced to linked ears. All other recording parameters were identical to those employed in Part 1.

The two halves of the dot matrix display, each 10 msec in duration, were presented at ISIs of 10 and 500 msec. As in the previous experiments, one side of the total display of 25 dots subtended 2 degrees of visual angle at a viewing distance of 57 cm.

A 4 x 4 checkerboard pattern of 50% contrast, subtending 2 degrees of visual angle per side at a viewing distance of 57 cm, was generated and displayed on the same equipment as the dot matrix displays. The pattern appeared for a duration of 10 msec on a continuously present uniform field with no change in space-averaged luminance (26 cd/m^2). On each trial, two patterns were displayed, separated by an ISI of 10 or 500 msec. Subjects fixated a dim crosshair in the middle of the uniform field. Each stimulus sequence was separated by an intertrial interval of 4000 ms.

Results

The results are shown in Figures 25 to 32, with waveforms plotted according to recording location on the head. Two VEPs, consisting of an average of 50 trials each, are shown superimposed to allow for the assessment of the reliability of the waveforms. The important observations are summarized as follows:

(1) Cerebral and Non-cerebral artifact: Subject J.S.'s responses are contaminated throughout with 10 Hz alpha activity. There is some jaw muscle artifact evident at the electrodes situated just above the ear (T6 and T4) in both subjects , which is very prominent in Figure 30. There is a large eyeblink artifact in the frontopolar traces (Fp) of Figure 26. There is a slow D.C. shift evident in both traces at the frontal sites in Figure 31.

(2) Comparison to results of Part 1: The prominent PNP waveform described in Part 1 is clearly distinguishable at the occipital electrodes for both subjects and all conditions. Two large responses are seen at an ISI of 500 msec.

(3) Topography: The occipital peaks are tracked by positive peaks at sites on the midline. This polarity reversal between occiput and midline is much more prominent in Subject E.R.'s

responses than in subject J..S.'s, likely because J.S.'s responses are contaminated with alpha. It is not a complete polarity reversal, however, since the polarity-reversed peaks are not precisely aligned in time.

(4) Matrix versus checkerboard VEP: The checkerboard responses are smaller in amplitude at both ISIs and the respective peaks are delayed in latency (an average of 30 msec) relative to the matrix VEP for both subjects. However, scalp topography is quite similar for both stimuli.

(5) 10 msec ISI versus 500 msec ISI matrix VEPs: Comparing the PNP complex elicited with a 10 msec ISI matrix to the first PNP complex elicited by a 500 msec ISI matrix it is evident that the scalp distributions are very nearly the same.

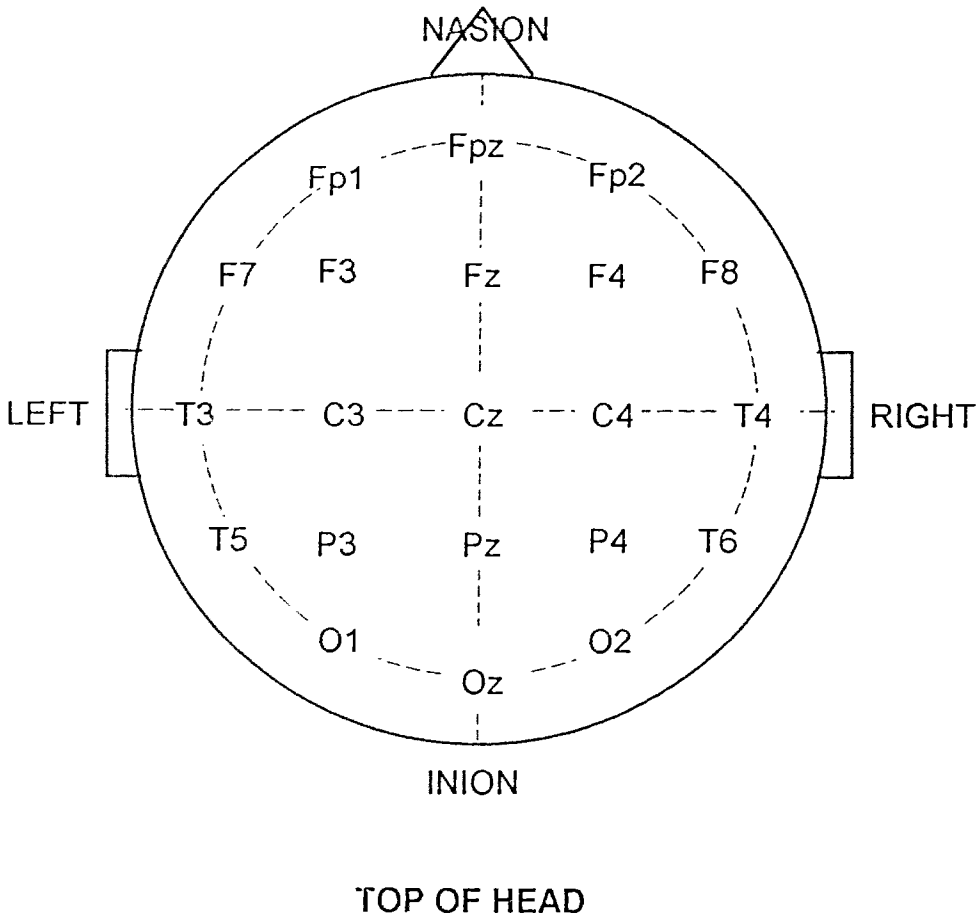

Figure 24. International 10-20 System of Electrode Placement.

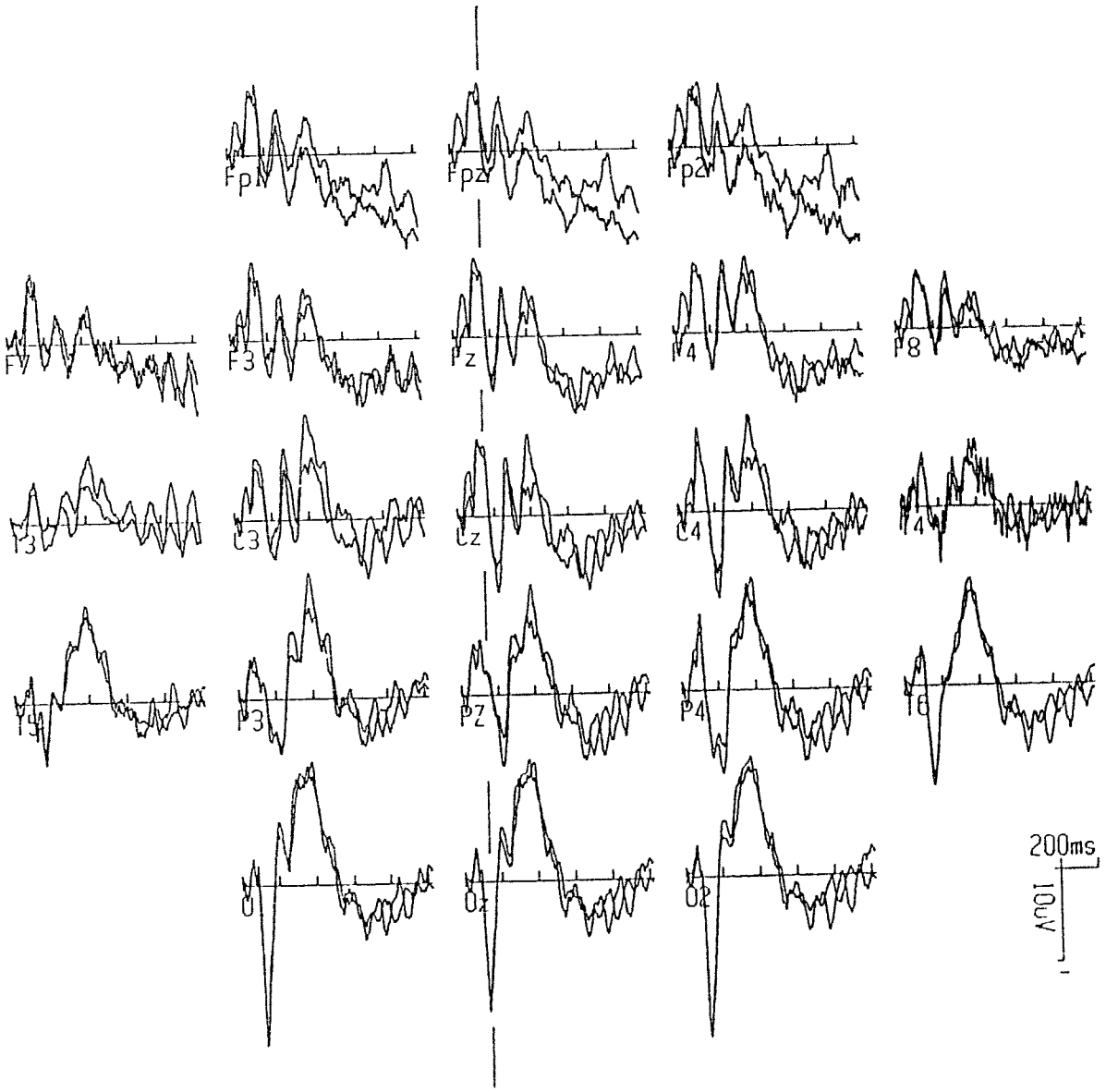

Figure 25. Visual evoked responses to 10 msec ISI dot matrix stimuli. (Subject J.S., Replication Superimposed).

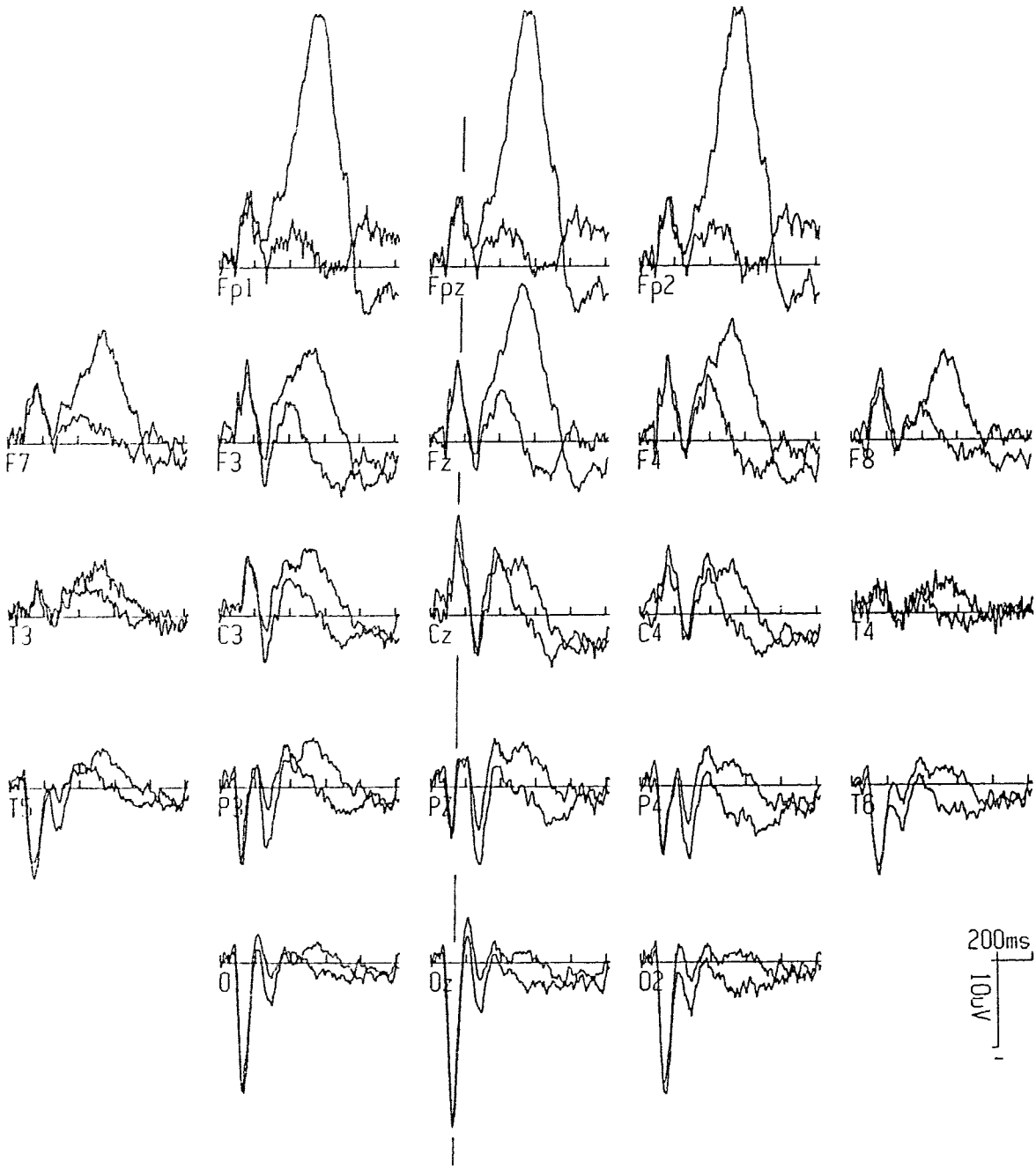

Figure 26. Visual evoked responses to 10 msec ISI dot matrix stimuli. (Subject E.R., Replication Superimposed).

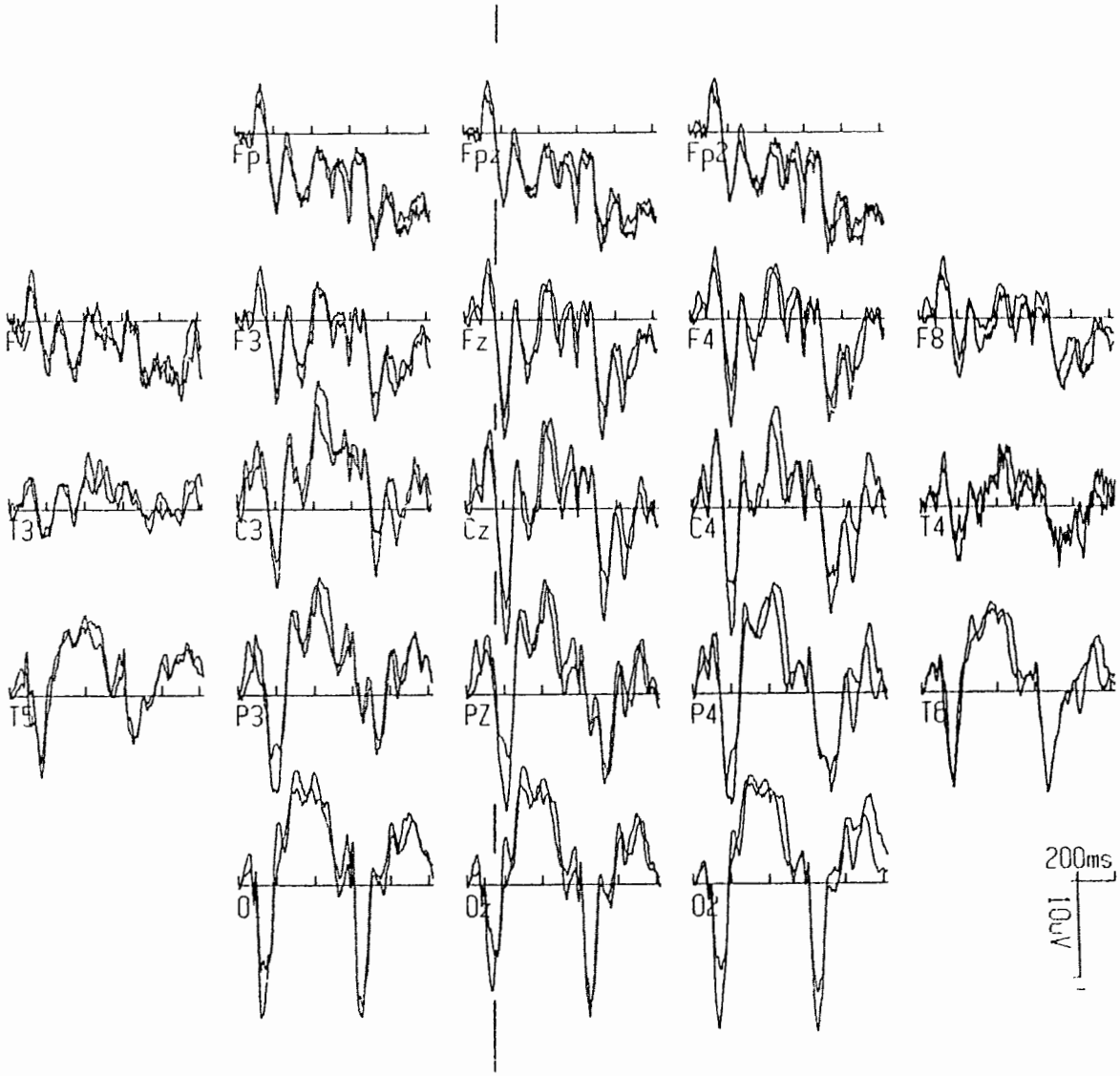

Figure 27. Visual evoked responses to 500 msec ISI dot matrix stimuli. (Subject J.S., Replication Superimposed).

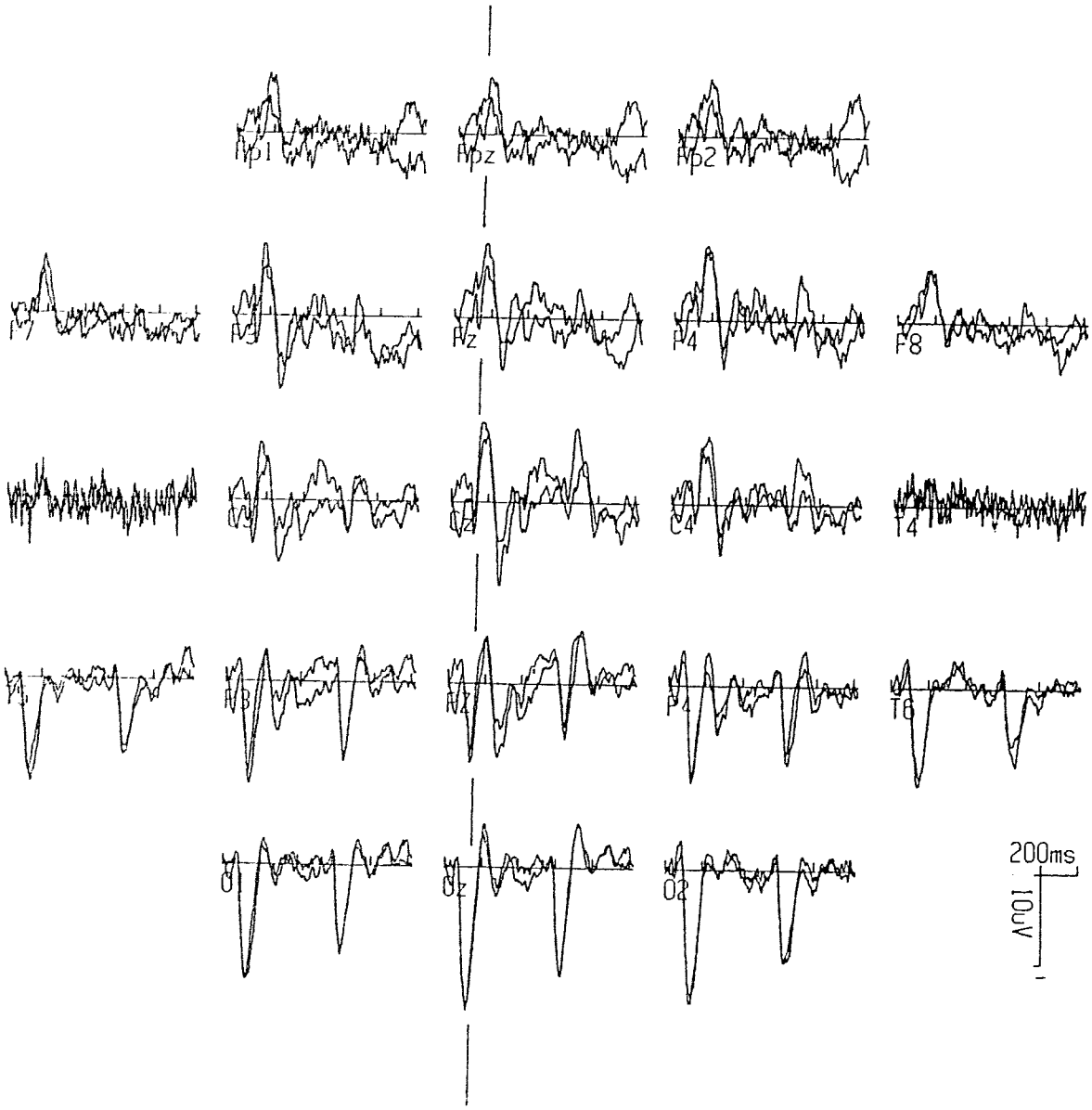

Figure 28. Visual evoked responses to 500 msec ISI dot matrix stimuli. (Subject E.R., Replication Superimposed).

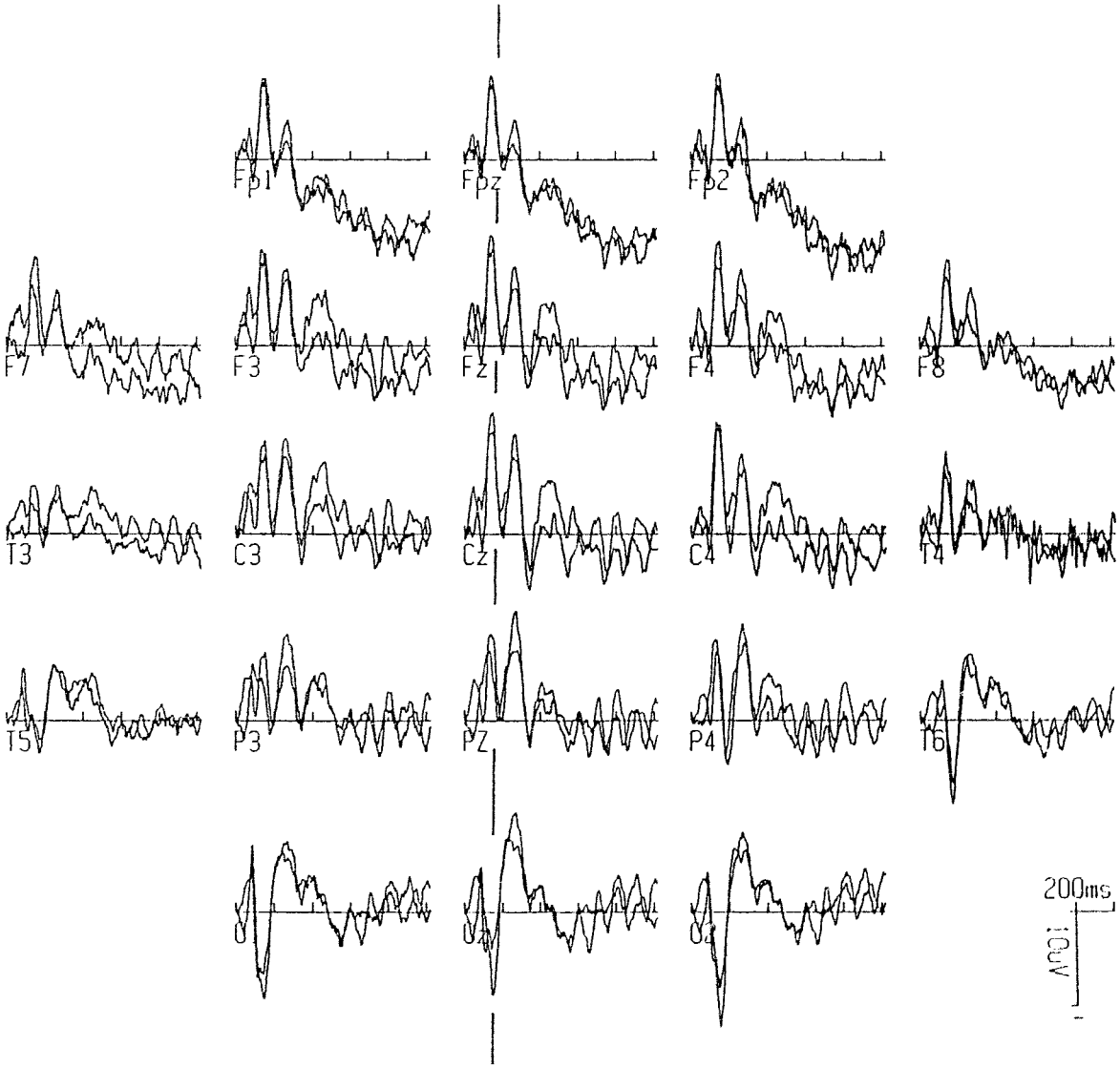

Figure 29. Visual evoked responses to 10 msec ISI checkerboard stimuli. (Subject J.S. Replication Superimposed).

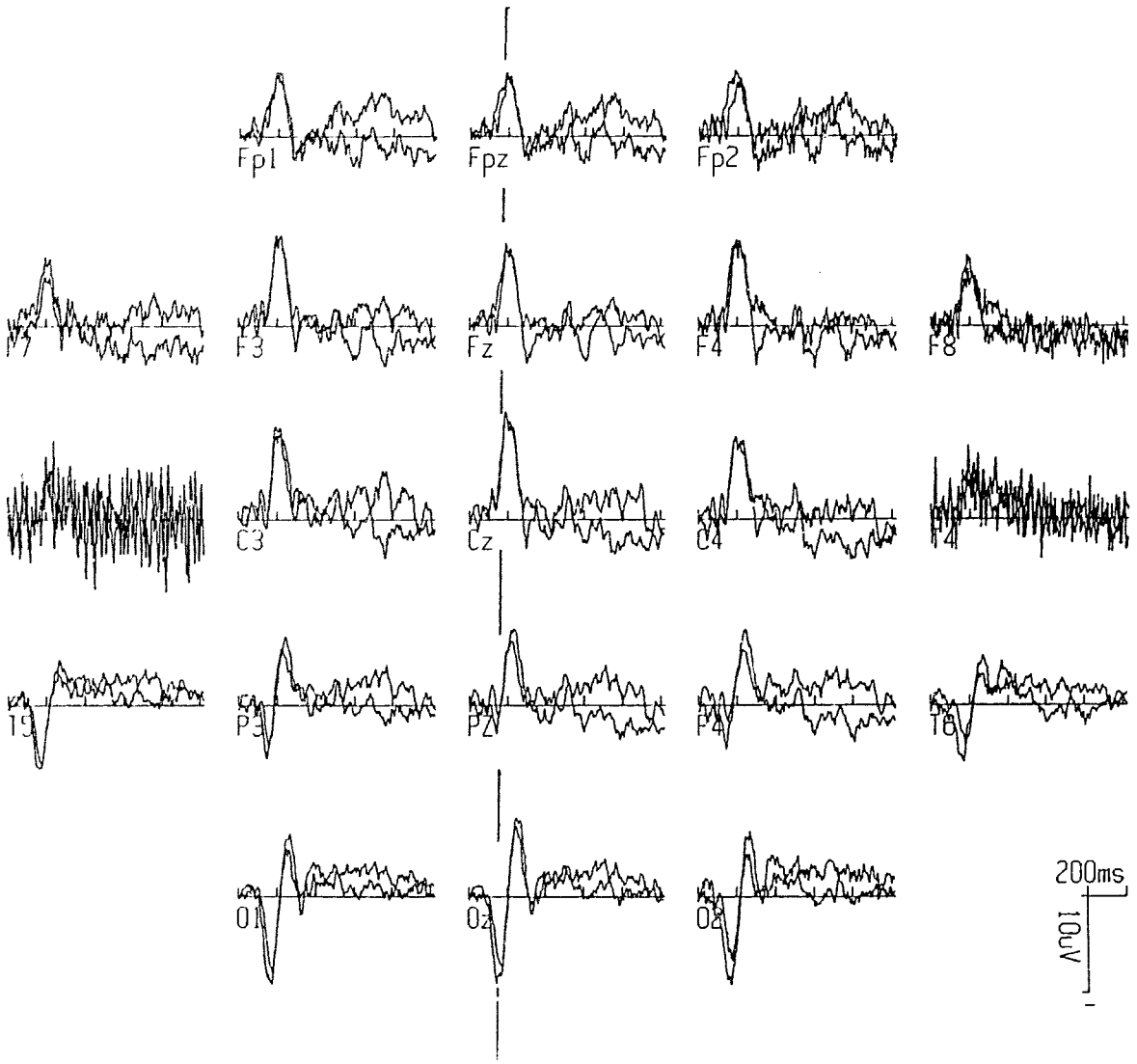

Figure 30. Visual evoked responses to 10 msec ISI checkerboard stimuli. (Subject E.R., Replication Superimposed).

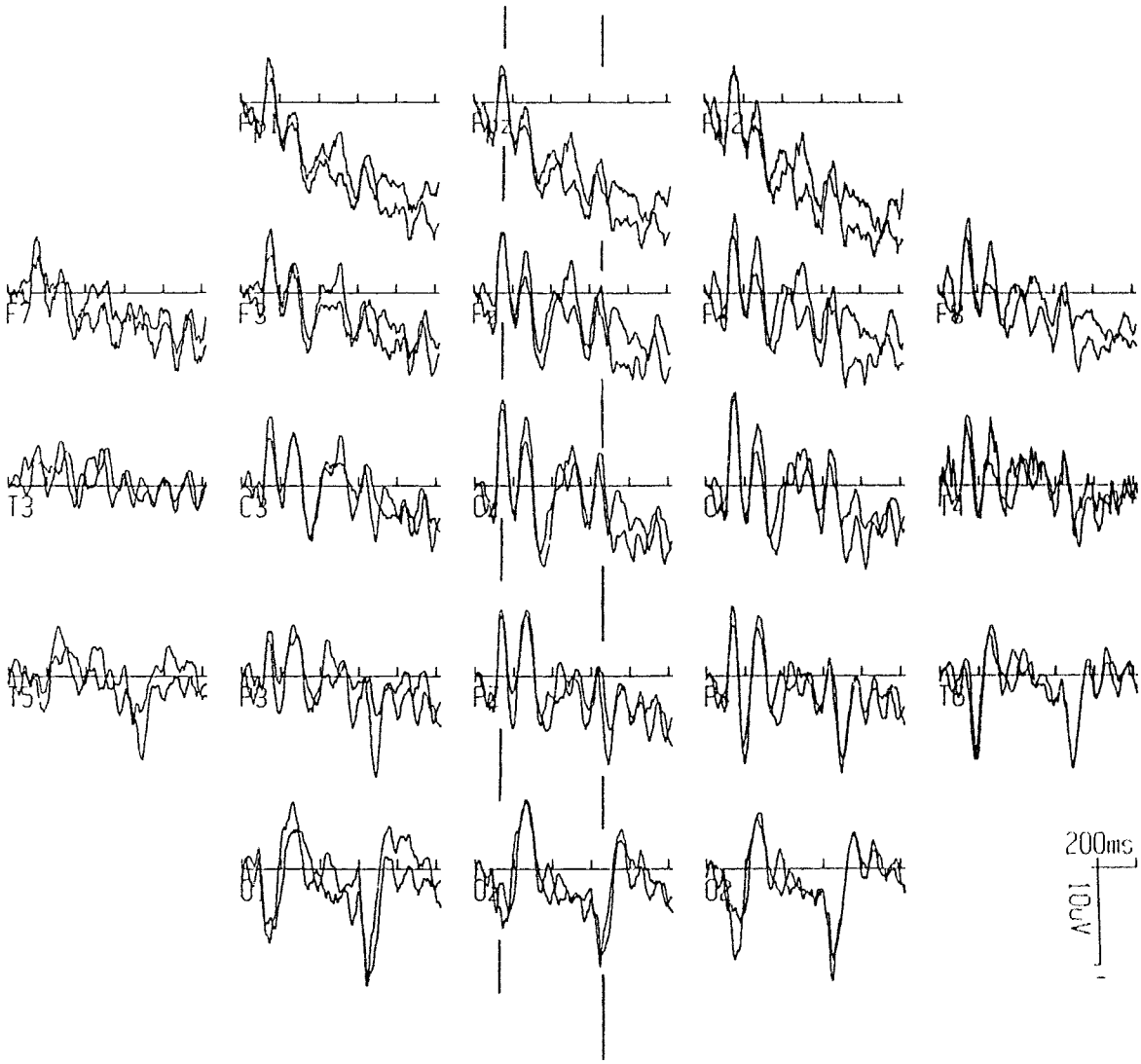

Figure 31. Visual evoked responses to 500 msec ISI checkerboard stimuli. (Subject J.S., Replication Superimposed).

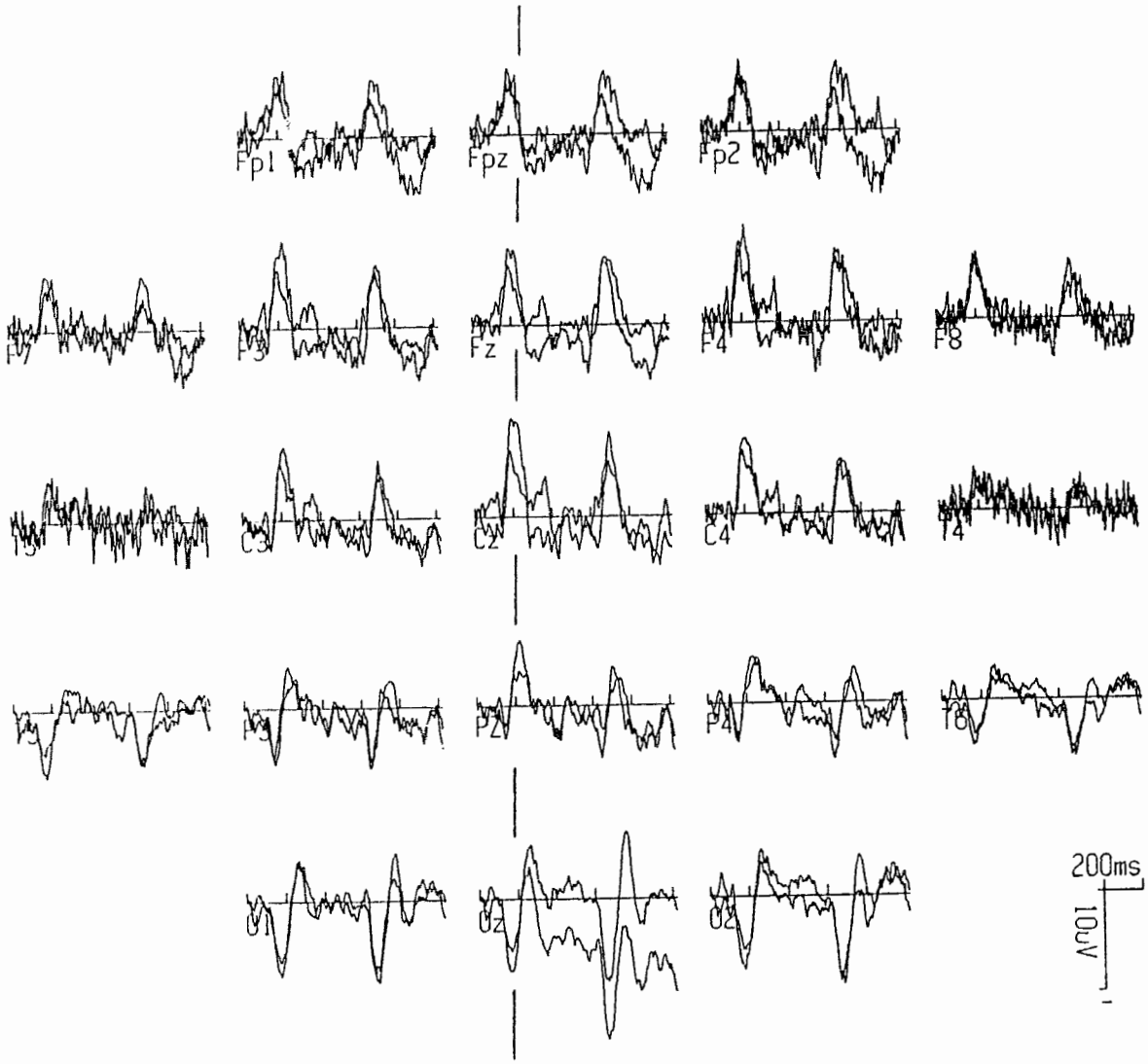

Figure 32. Visual evoked responses to 500 msec ISI checkerboard stimuli. (Subject E.R., Replication Superimposed).

The superimposed traces of Figures 25-32 were averaged and subjected to a Laplacian transformation, which suppresses the effect of current flow transverse to the scalp and enhances vertically directed current flow. The resulting plots are shown in Figures 33-40. A detailed comparison of these plots is not plausible: the plots of the edge waveforms are less reliable than those of the central waveforms because the estimate of the Laplacian at the edge sites is based on fewer neighboring electrodes. However the spatial sharpening of the scalp topography with the Laplacian transformation is immediately apparent, and it can be concluded that no current sinks or sources of importance exist in the region occupied by the eight frontal electrodes.

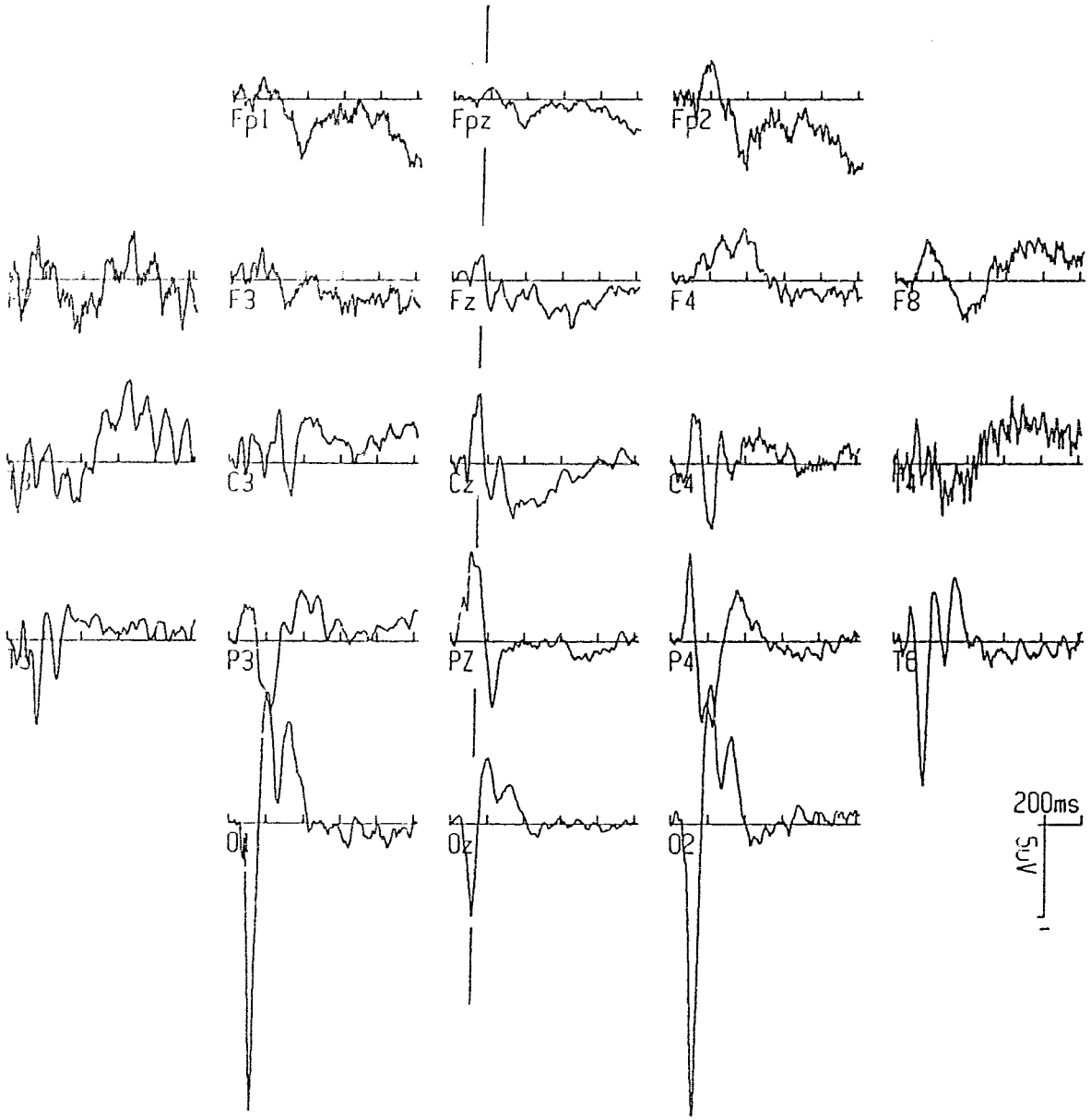

Figure 33. Visual evoked responses to 10 msec ISI dot matrix stimuli. (Subject J.S., Laplacian Transformation).

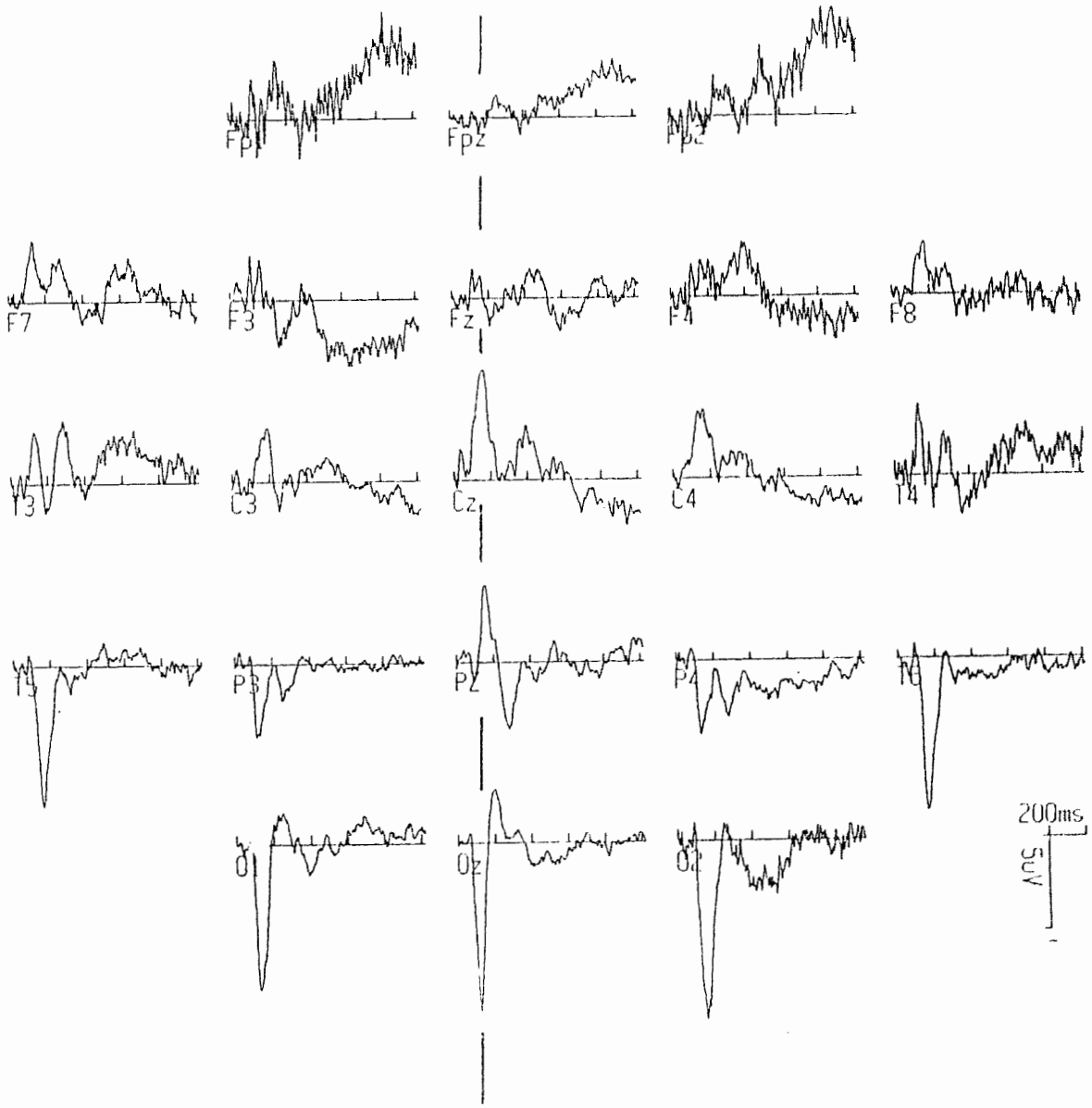

Figure 34. Visual evoked responses to 10 msec ISI dot matrix stimuli. (Subject E.R., Laplacian Transformation).

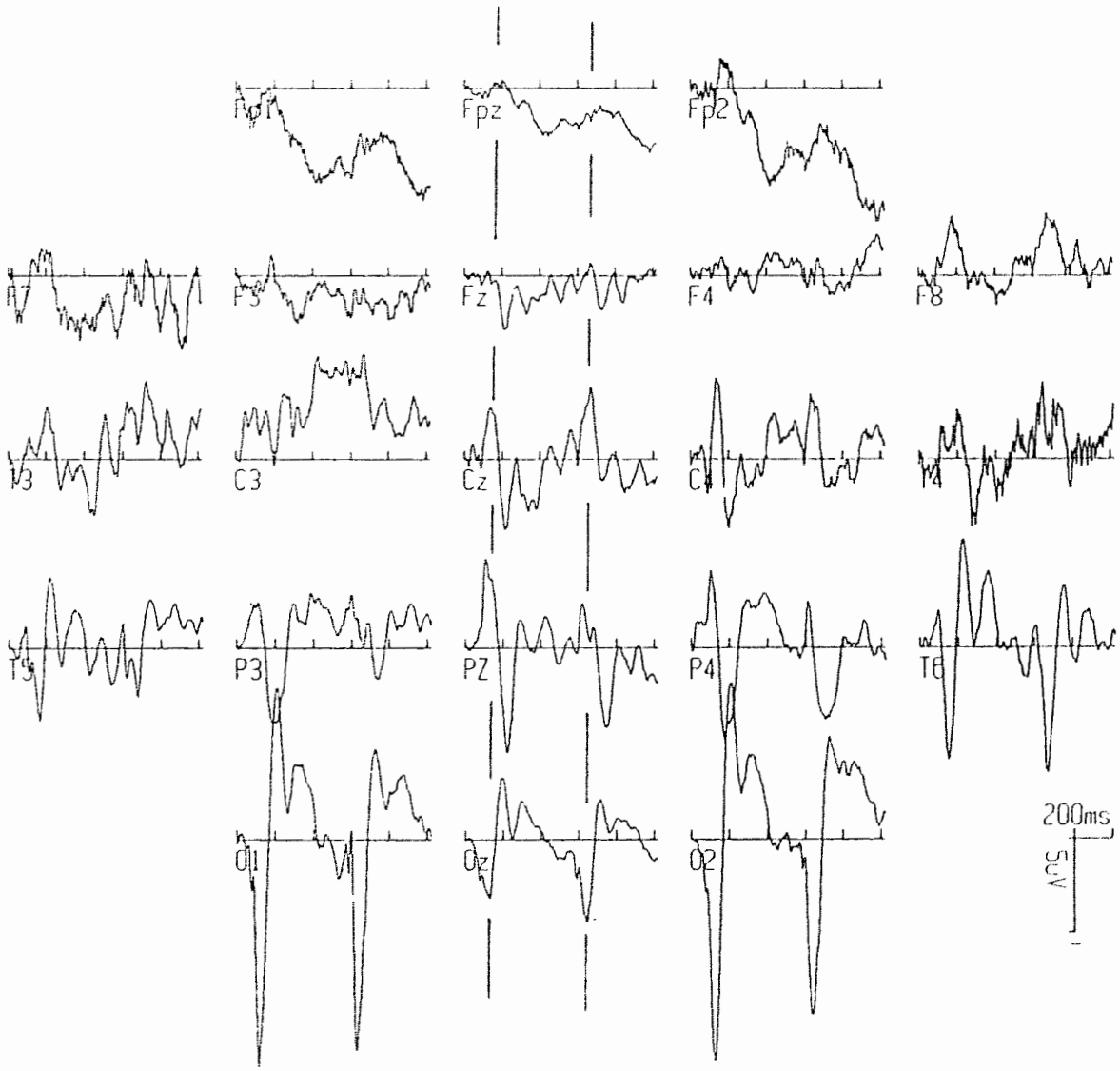

Figure 35. Visual evoked responses to 500 msec ISi dot matrix stimuli. (Subject J.S., Laplacian Transformation).

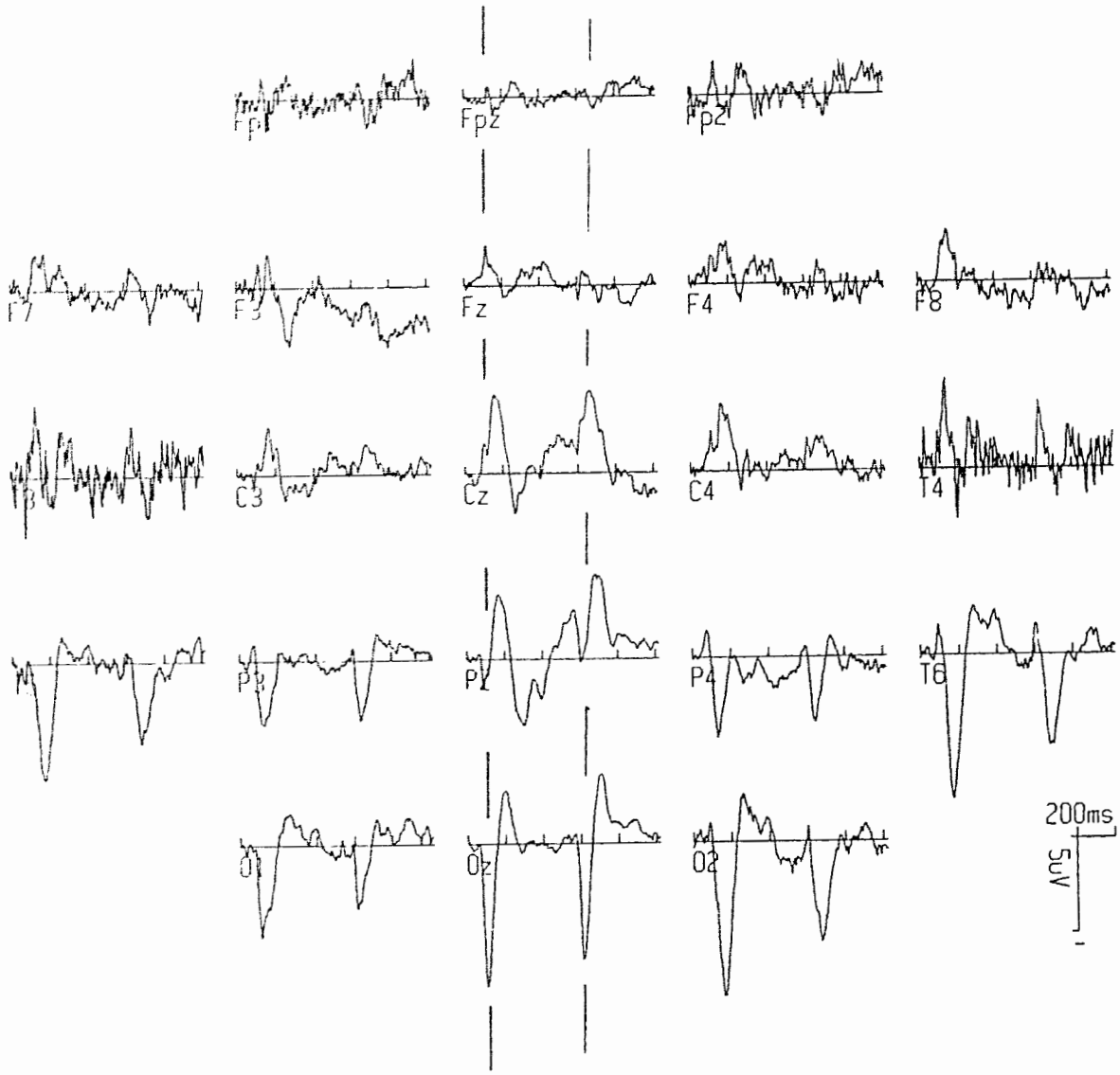

Figure 36. Visual evoked responses to 500 msec ISI dot matrix stimuli. (Subject E.R., Laplacian Transformation).

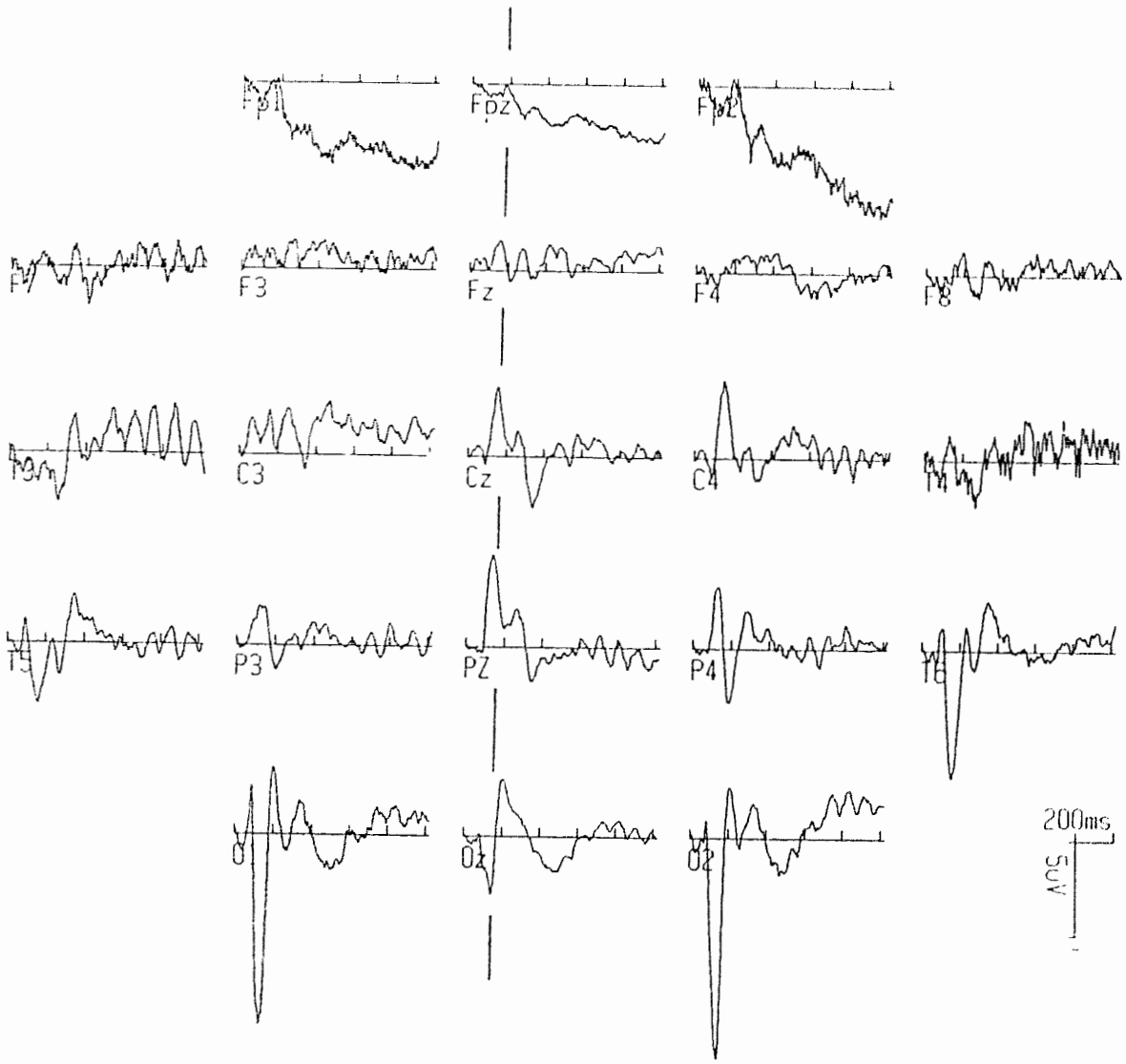

Figure 37. Visual evoked responses to 10 msec checkerboard stimuli. (Subject J.S., Laplacian Transformation).

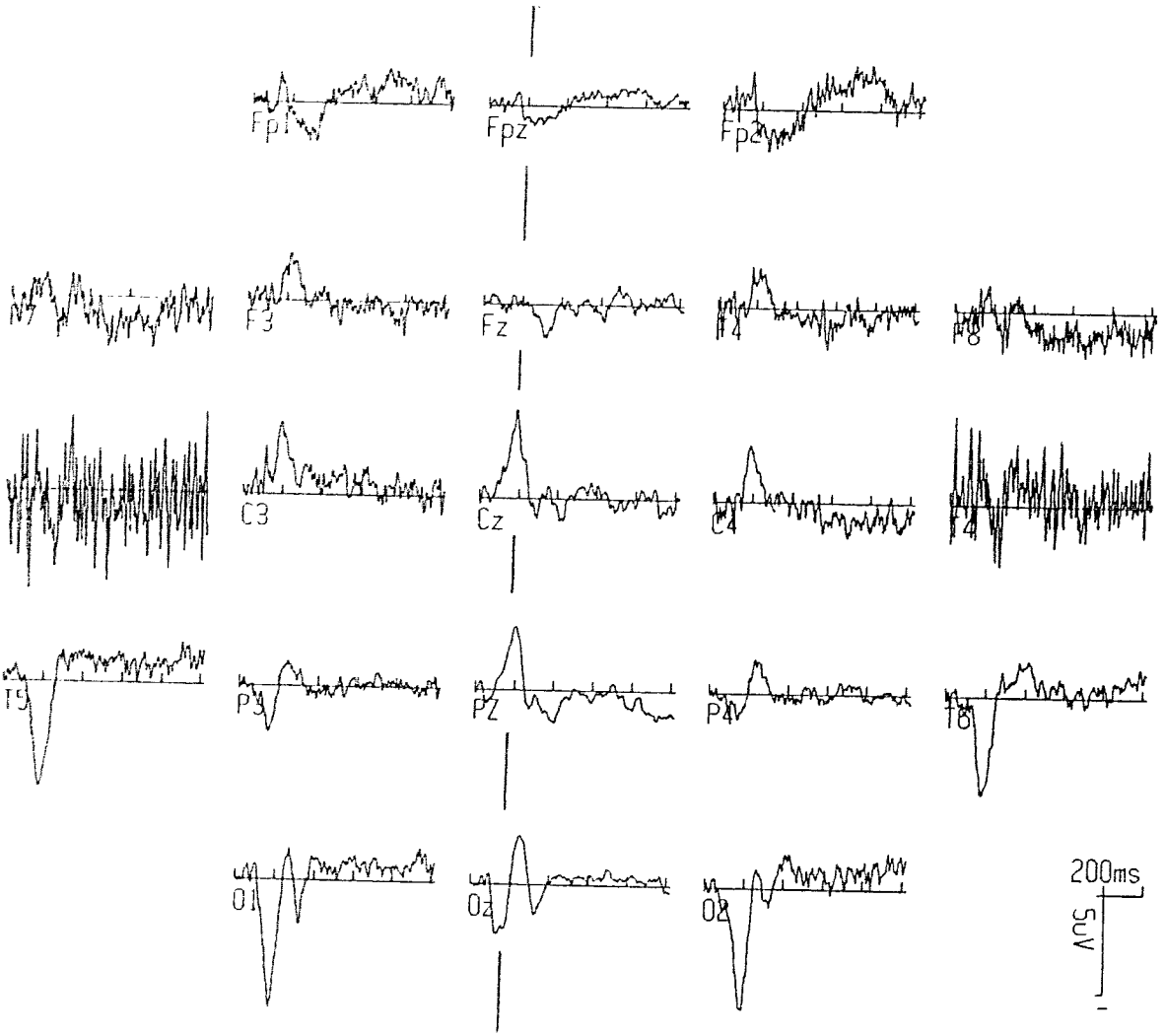

Figure 38. Visual evoked responses to 10 msec ISI checkerboard stimuli. (Subject E.R., Laplacian Transformation).

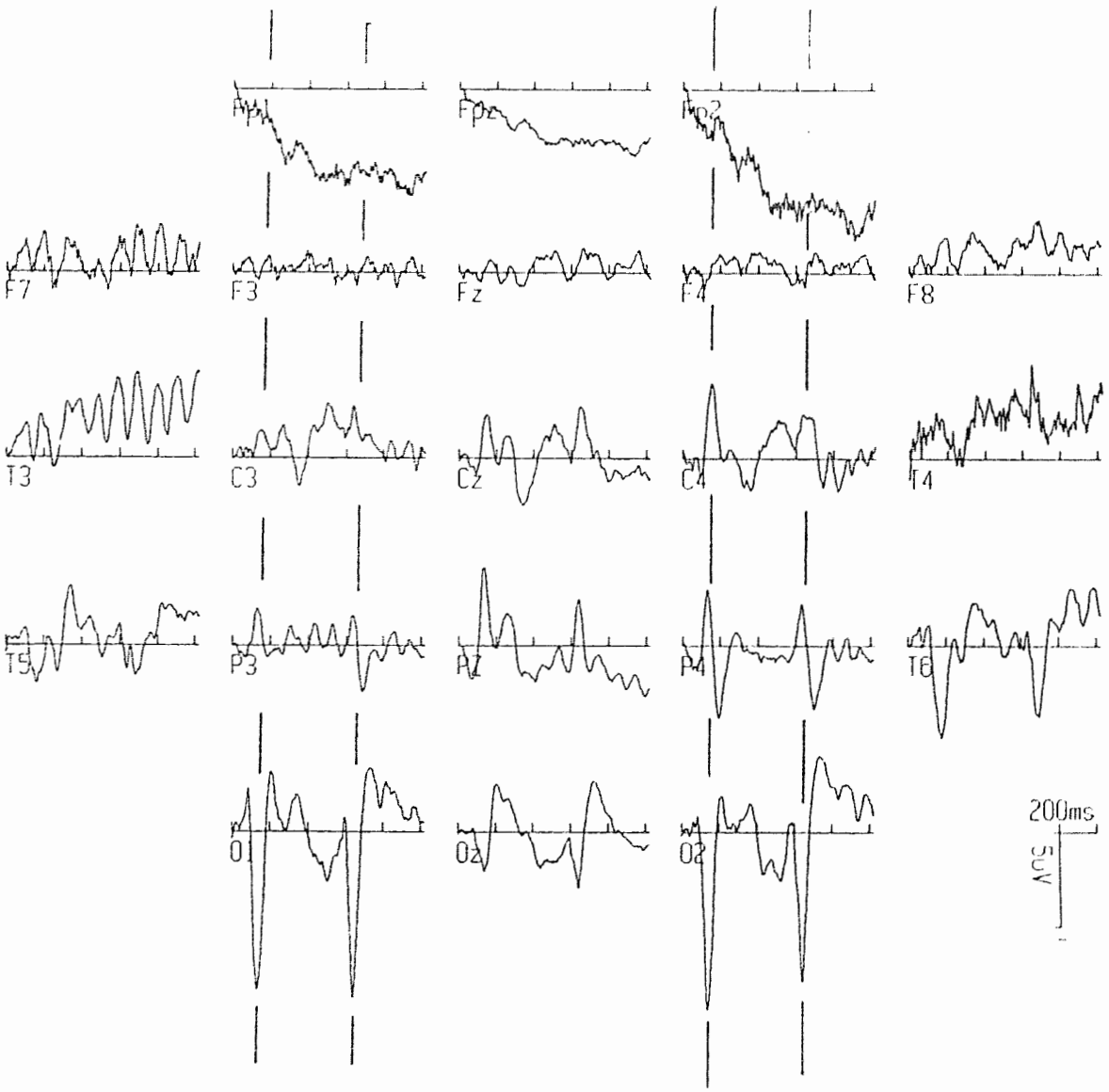

Figure 39. Visual evoked responses to 500 msec ISI checkerboard stimuli. (Subject J.S., Laplacian Transformation).

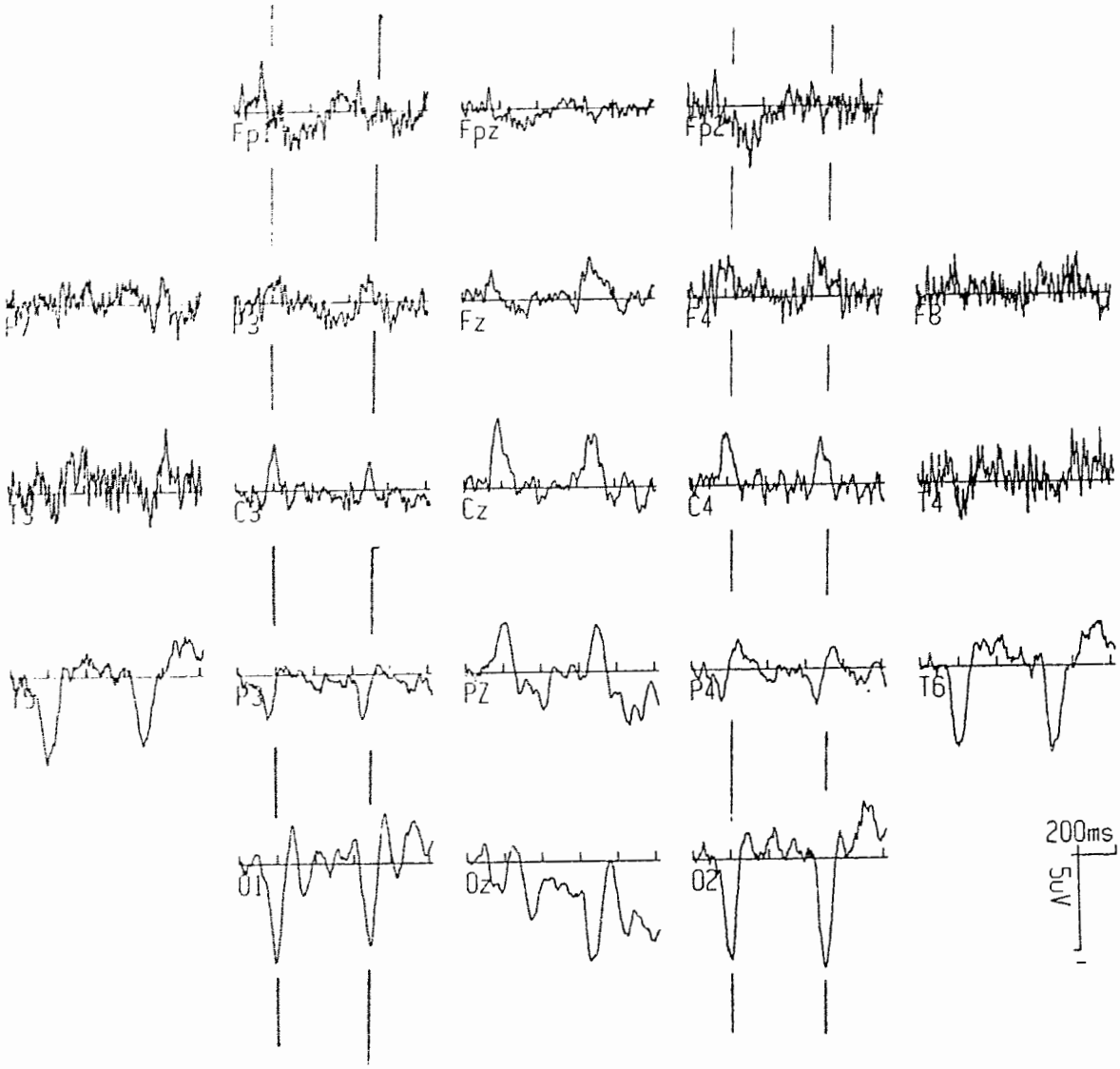

Figure 40. Visual evoked responses to 500 msec ISI checkerboard stimuli. (Subject E.R., Laplacian Transformation).

Discussion

Two general observations from the results of this investigation are of importance. First, a very similar VEP topography is obtained with the two different stimuli and with the two different ISIs, and the topography of the response to the trailing display is broadly similar to that to the leading display in both subjects. This allows the inference that the same or a very similar configuration of brain mechanisms are recruited by all of the various stimuli employed and, in addition, permits a comparison of the VEP results obtained here with those obtained by other researchers with a variety of patterned visual stimuli. Thus, the identification of the dot matrix VEPs with the pattern onset response originally described by Jeffreys & Axford (1972a; 1972b) is further bolstered. The second observation of importance is that the brain activity of interest is localized by the Laplacian transformation to the posterior region of the head. The next series of studies attempts a more specific localization of the dot matrix VEPs.

2. Source Localization

Previous VEP Source Localization Studies

Jeffreys and Axford (1972a; 1972b) were among the first to attempt to solve the inverse problem for pattern-onset VEPs, using as a stimulus a brief (25 msec) patterned visual stimulus of isolated squares. They found that the scalp distributions of the C.I and C.II components of the pattern-onset VEP were dramatically influenced by the region of the retina to which the stimulus was presented, suggesting that the cortical neurons which generate both components are retinotopically organized. On the basis of the known retinotopic organization of visual cortex, they concluded that the generators of the two components could be modeled as simple equivalent dipoles, originating in striate cortex (C.I) and extrastriate cortex (C.II).

Other investigators have reached different conclusions. Lesevre and Joseph (1979) proposed that C.I and C.II are generated in areas 18 and 19 respectively, and that the activity of the two generators overlaps in time. They also identified an early (60 msec) negative peak which they considered to originate in area 17. Halliday and Michael (1970) concluded that all of the peaks of the pattern onset response originate in extrastriate cortex.

Darcey, Ary and Fender (1980) studied the pattern onset response with a montage of more than 40 electrodes. They concluded that the C.I and C.II peaks are generated either by one source that reverses its polarity or by two very closely spaced sources of opposite polarity. They also reported that the dense spatial sampling of the potential field allowed the observation of important data that a less densely spaced montage would miss.

Early source localization studies neglected to account for the conductive inhomogeneities of the brain and its coverings, which have important consequences for the electrotonic spread of voltage to the scalp. More recent studies have employed a physical model of the head to account for these distorting effects. Butler et al. (1987) combined a physical model with a dipole localization method (DLM) in a study of the C.I component evoked by patterns presented to foveal octants. While the location of their fitted dipoles were consistent with a striate origin, the obtained orientations were not consistent with current conceptualizations of the retinotopic organization of the foveal projections regions of striate cortex, and they concluded that their data did not allow them to distinguish reliably between a striate or an extrastriate origin.

Maier et al. (1987) used a physical model of the head in combination with principal components analysis (PCA) to define the dimensionality of the data space, making the assumption that PCA would allow them to dissect out the overlapping activities of simultaneously active sources. They concluded that the C.I-C.II interval of the pattern onset response has its origins in two different cortical regions: a fast positive-negative component arising from area 18 or 19, and a slower negative component corresponding to the initial part of C.II which arises from area 17. Stok (1986) reached similar conclusions in a study comparing in a study comparing EEG and MEG (magnetoencephalographic) measures of the pattern onset response.

Most of the studies cited above make the claim of being able to distinguish between striate and extrastriate origins for the various components of the pattern onset responses. In spite of this, there is substantial disagreement between studies regarding the generator sites of the various components. At least three locations have been posited for the generator of the C.II component: area 18 (Jeffreys & Axford, 1972b); area 19 (Lesevre & Joseph, 1979); and area 17 (Maier, 1987; Stok, 1986). In addition, several authors have suggested that the C.I and C.II components are generated by two temporally overlapping sources (Lesevre & Joseph, 1979; Maier, 1987).

Source Localization in the Present Study

Method

The visual stimulus consisted of the sequential dot matrix stimuli presented at a 10 msec ISI. Left, right, lower and upper hemifield stimulation was achieved by having the subjects fixate a small, dim fixation box immediately to the right, left, upper or lower side of the region of stimulus presentation on the oscilloscope. Appropriate fixation in this study was assured by monitoring behavioral performance: For stimuli as brief as were used here, eye movements result in a blurred perception of the stimulus which makes performance impossible. Stimulus size was maintained at two degrees of visual angle as in the previous investigations: this size of stimulus is still maintained within the foveal portion of the retinal receptive field (some 4 to 6 degrees of visual angle). Since the previous investigation had determined that current sources and sinks were confined to the posterior region of the scalp, it was possible to improve the spatial sampling rate in this study by placing all 20 electrodes between vertex and inion. This nonstandard electrode placement is illustrated in Figure 41.

Analysis

Forward solutions were calculated using a modification of an algorithm provided by Stok (1986) for the calculation of electric potential on the surface of a spherical volume conductor due to a dipolar current source. To correct for conductive inhomogeneities, the head was modeled as four concentric spheres, with radii corresponding to the surface of the brain, the inner surface of the skull, the outer surface of the skull, and the surface of the scalp. In this implementation, the radii of the four concentric spheres were taken as .875, 0.90, 0.9625 and 1.0 relative to an outer sphere radius of 1.0. Relative values adopted for the volume conductivities of the brain and scalp (0.33 Ωm^{-1}), CSF (1.00.Ωm^{-1}) and the ratio of conductivity of brain to bone (80:1) were those published by Geddes & Baker (1967).

Radius of the outer sphere, the coordinates of the center of the sphere, and electrode position on the surface of the sphere were determined individually for each subject employing the method of De Munck, Vign and Spekreijse (1991), involving the definition of a coordinate system with respect to the head (Figure 42). The origin of the coordinate system was defined as the middle of a line segment connecting the preauricular points of the ears. The positive Y axis runs from the origin to the left preauricular point (ear indentations) and the negative X axis runs from the origin to the inion. The positive z axis begins at the origin and is oriented normally to the x-y plane. In practice, the z axis thus defined emerges from the top of the head at a position approximately 3 cm posterior to the vertex (Position Cz of the international 10-20 System of Electrode Placement: Jasper, 1958). According to Cheyne (1986), the origin of the head coordinate system thus defined is approximately at the level of the pons in the brainstem.

Electrode positions were measured with respect to the three reference points of the inion and left and right preauricular points. Cartesian coordinates of each electrode were determined by solving a series of algebraic relations (De Munck et al. 1991). The best-fitting sphere (defined as the sphere which minimizes the sum of the squared distances from all electrode positions to the surface of the sphere) was found by a Simplex minimization algorithm (Caceci & Chacheris, 1984). Employing this method, the best fitting spheres for each subject were found to have radii

of 8.48 (J.S.), 8.66 (E.R.) and 8.72 (W.P.) cm. These values were used as the outer radii of the volume conductor in forward calculations.

Estimation of equivalent dipoles from potential field maps in the present study employed a modeling procedure developed by Cheyne (1991a), allowing the least-squares fitting of theoretical fields from one or more dipole sources to observed data for (a) a selected time point (time-slice mode); or (b) a selected time window (spatio-temporal mode). In the former mode, dipole strength, location and orientation was adjusted using a non-linear, iterative fitting algorithm (downhill simplex; Caceci & Chacheris, 1984). In the latter mode, temporal weighting functions (varying dipole strengths over time) were computed for each dipole source over the duration of the chosen epoch using a direct linear least squares solution based on the method published by Baumgartner, Sutherling & Barth (1989).

The fitting of a dipole model to an observed potential field requires a simultaneous adjustment of the initial parameters for each dipole (three for location, three for orientation) which minimizes an error function defined as the sum of squared differences (SSD) between theoretical and observed data. Because the potential field decreases quadratically with distance between the dipole and the measurement source, the parameter estimation problem for an equivalent dipole is essentially nonlinear in nature and requires an iterative fitting procedure. Dipole strength is determined as a seventh parameter representing the net dipole moment of the source flowing in the direction of the orientation vector. With this approach, dipole strength can be represented as a positive or negative weighting of a stationary dipole, and is determined directly by linear least-squares fitting of a single coefficient for each dipole, for each time point in the analysis window. Thus, in the spatio-temporal mode, dipole strength is represented as a positive or negative weighting (w) in units of current density for each dipole which can vary over time in order to best account for the total SSD over space and time.

In more formal terms, the fitting procedure (in either mode) minimized the difference between an observed potential field and a "theoretical" field due to a dipole of given location, orientation and strength:

Time-Slice Mode:

$$SSD = \sum_{i=1}^{m} [(\sum_{j=1}^{k} V'_{ik}) - V_{ik}]^2, \text{ where}$$

m = number of recording locations;

k = number of dipoles in model;

V = observed value;

V' = theoretical value.

Spatio-temporal mode:

$$SSD_T = \sum_{i=1}^{n} [\sum_{j}^{m} ((\sum_{k=1}^{p} w_{ik} \cdot P_{jk}) - V_j)^2], \text{ where}$$

m = number of recording locations;

n = number of time points;

p = number of dipoles in model;

w = dipole strength in units of current density;

P = pattern of activity for a fixed dipole of unit strength;

V = observed pattern

Estimates of goodness of fit

Adequacy of fit of the model can be expressed in terms of the proportion of the observed data that is not accounted for by the dipole model (residual variance). This can be simply expressed as the sum of squared differences (SS) between theoretical and observed fields, normalized by the total observed field (V), so that the residual variance measure is independent of absolute field values (unit-less). Thus

$$R.V. = \frac{SSD}{\sum_{i=1}^{n}(V^2)} \times 100\ \%, \text{ where}$$

n = number of recording locations.

Results

Scalp Topography

VEP topography for each stimulus condition is shown in Figures 43 to 54. Important aspects of the VEP fields are the following:

(1) Left and right half-field stimulation.

(a) Lateralization of response. For left hemifield stimulation, there is an apparent, though small, lateralization of the N1 peak on the side expected on the basis of the projections of the visual field to visual cortex (the left visual field projects to the right side of the brain and vice versa for the right visual field). This is best seen by comparing peak amplitude at electrodes 15 and 17 on either side of the midline: there is a small but reliable increase in amplitude of this peak for all three subjects. For right hemifield stimulation, there is little evidence of appropriate lateralization, except for a small increase in N1 peak amplitude at electrode 19 compared to electrode 15 in Subject J.S.

(b) Polarity-reversed peaks at anterior versus posterior electrode locations. As was the case with full-field stimulation, a large positive peak at anterior electrodes tracks the latency of the negative peak at the posterior electrodes (with the exception of subject E.R. for left hemifield stimulation- the anterior positive peak is not as apparent). The anterior and posterior peaks are not in phase for subjects J.S. and W.P.: the anterior peak has a latency some 30-50 msec earlier than that of the corresponding posterior peak. This latency difference varies with the exact electrode locations being compared, however. However, for subject E.R., right hemifield stimulation, the anterior and posterior peaks are closely matched in phase.

In conclusion, VEP topography is quite similar for right and left hemifield stimulation, closely resembling the main features of the topography obtained with full-field stimulation in the previous series of experiments. It may be concluded that hemifield stimulation does not result in

a strongly lateralized response. This result is in agreement with the results of Jeffreys and Axford (1972a).

(2) Lower and upper hemifield stimulation. Comparing the midline electrode locations for lower hemifield stimulation, the prominent positive peak at the anterior electrodes is noticeably lacking in all three subjects. For subjects J.S. and W.P., the anterior electrodes exhibit a series of small positive deflections that do not resemble the large amplitude peaks evident in the other conditions (for both of these subjects, the anterior electrodes show an artifactual baseline offset which was corrected in the subsequent analyses by rebaselining the waveforms). For subject E.R., there is no polarity reversal from anterior to posterior electrodes: the same PNP sequence of waves is seen from anterior to posterior with no change in phase of the various components. With upper hemifield stimulation, the anterior positive peak returns to prominence in all three subjects.

From these results, it may be concluded that the topography of the lower half-field VEP is substantially different from that of the other three conditions and from that of full-field stimulation.

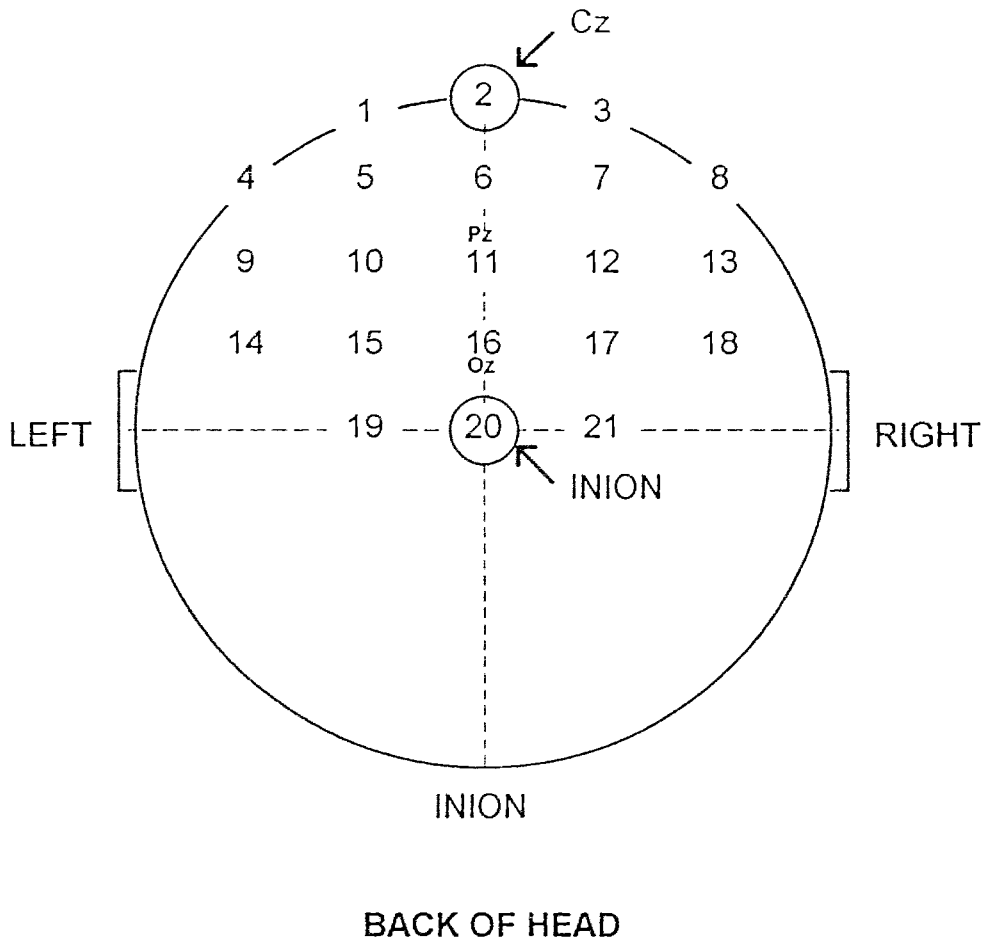

Figure 4. Dense electrode montage.

Figure 41. 20 channel electrode montage, confined to posterior region of the head.

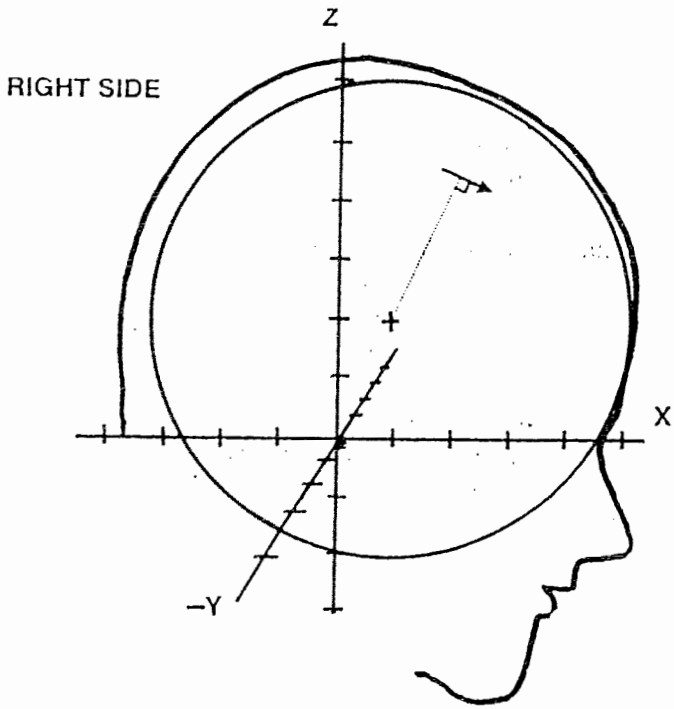

Figure 42. Definition of the head coordinate system. The negative x axis passes through the inion, the y axis through both pre-auricular points, and the z axis passes through the top of the head, approximately 3 cm posterior to Cz (From Cheyne, 1991b).

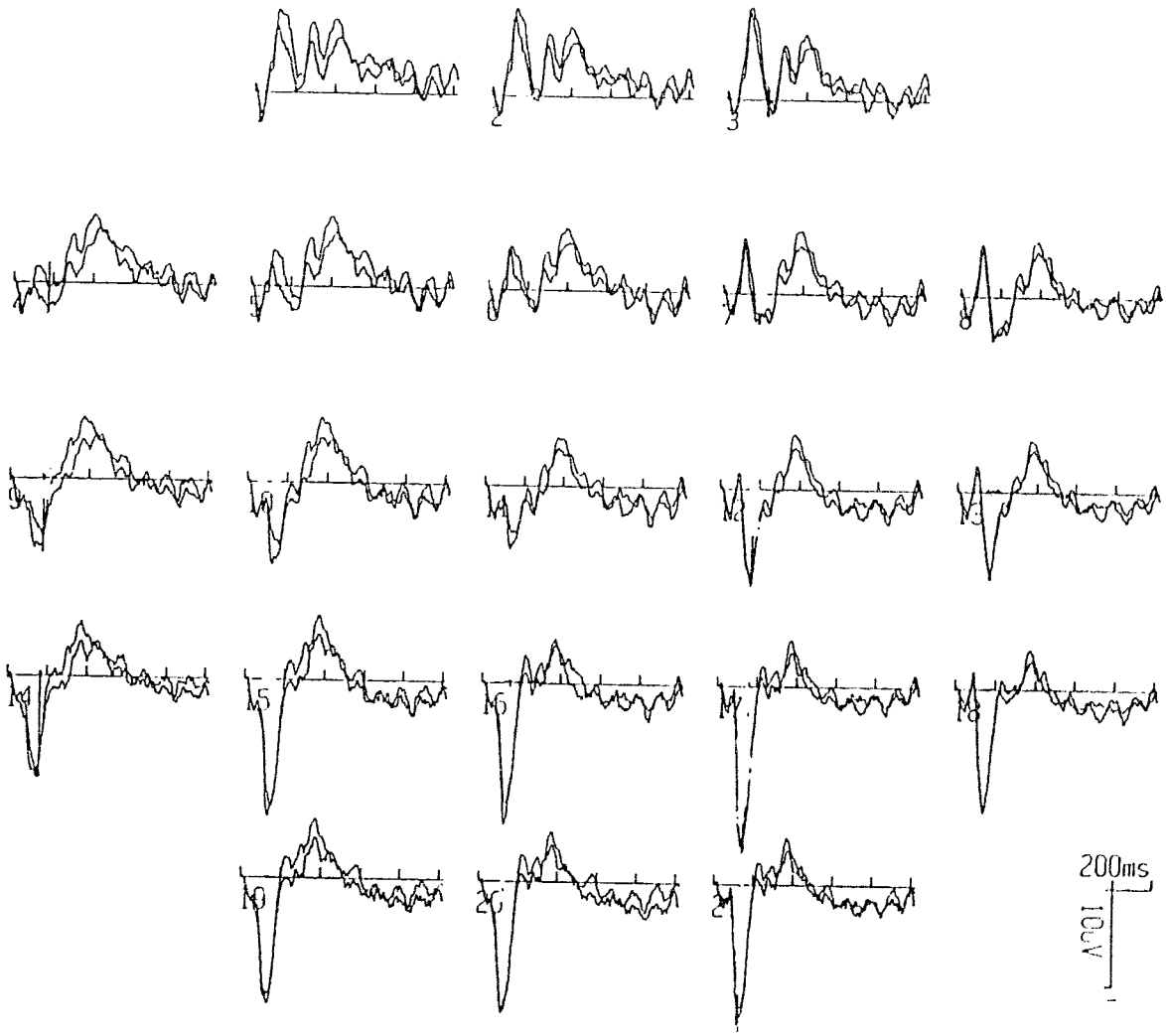

Figure 43. Visual evoked responses to left hemifield presentation of dot matrix stimuli (Subject J.S.)

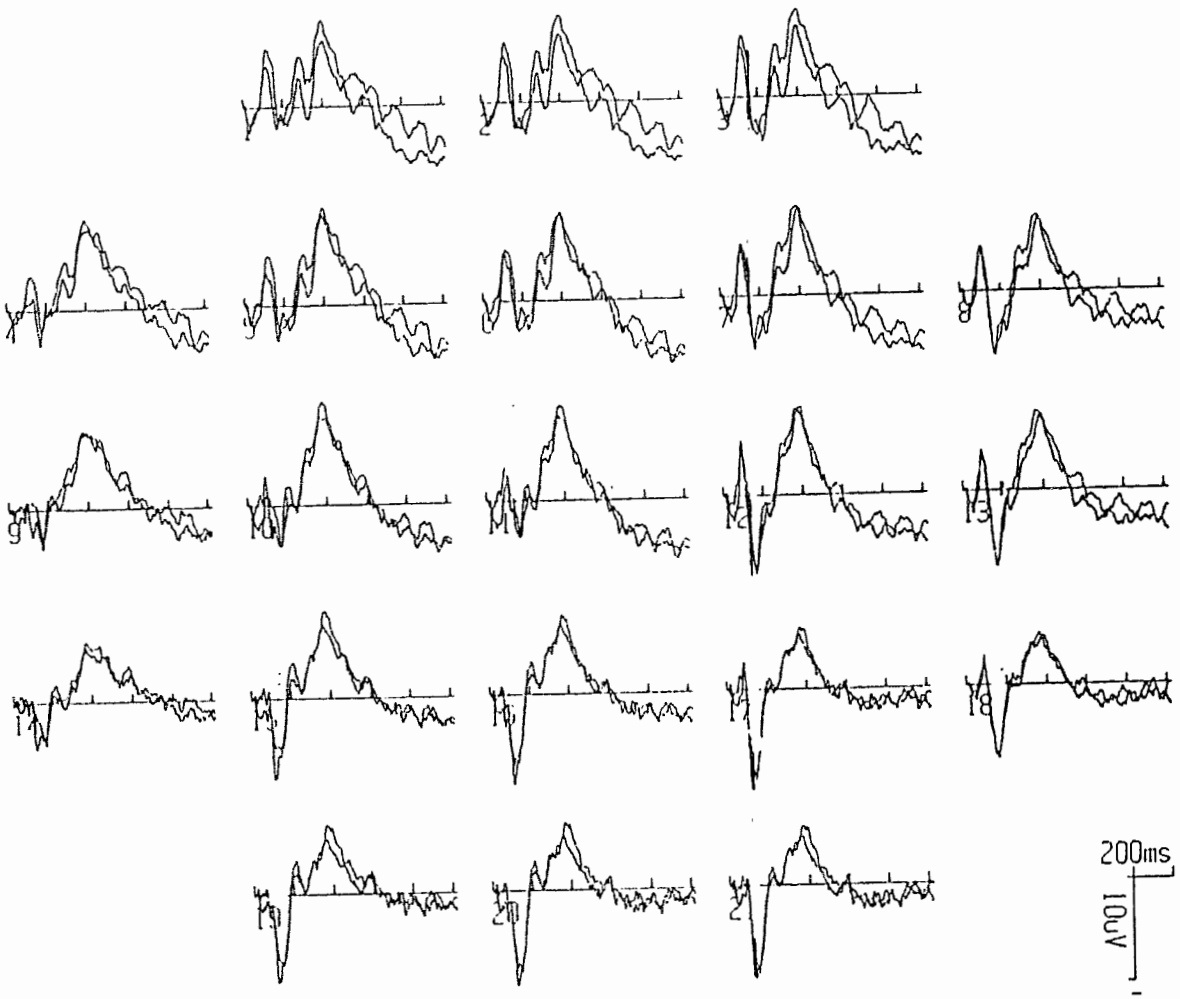

Figure 44. Visual evoked responses to left hemifield presentation of dot matrix stimuli (Subject W.P.)

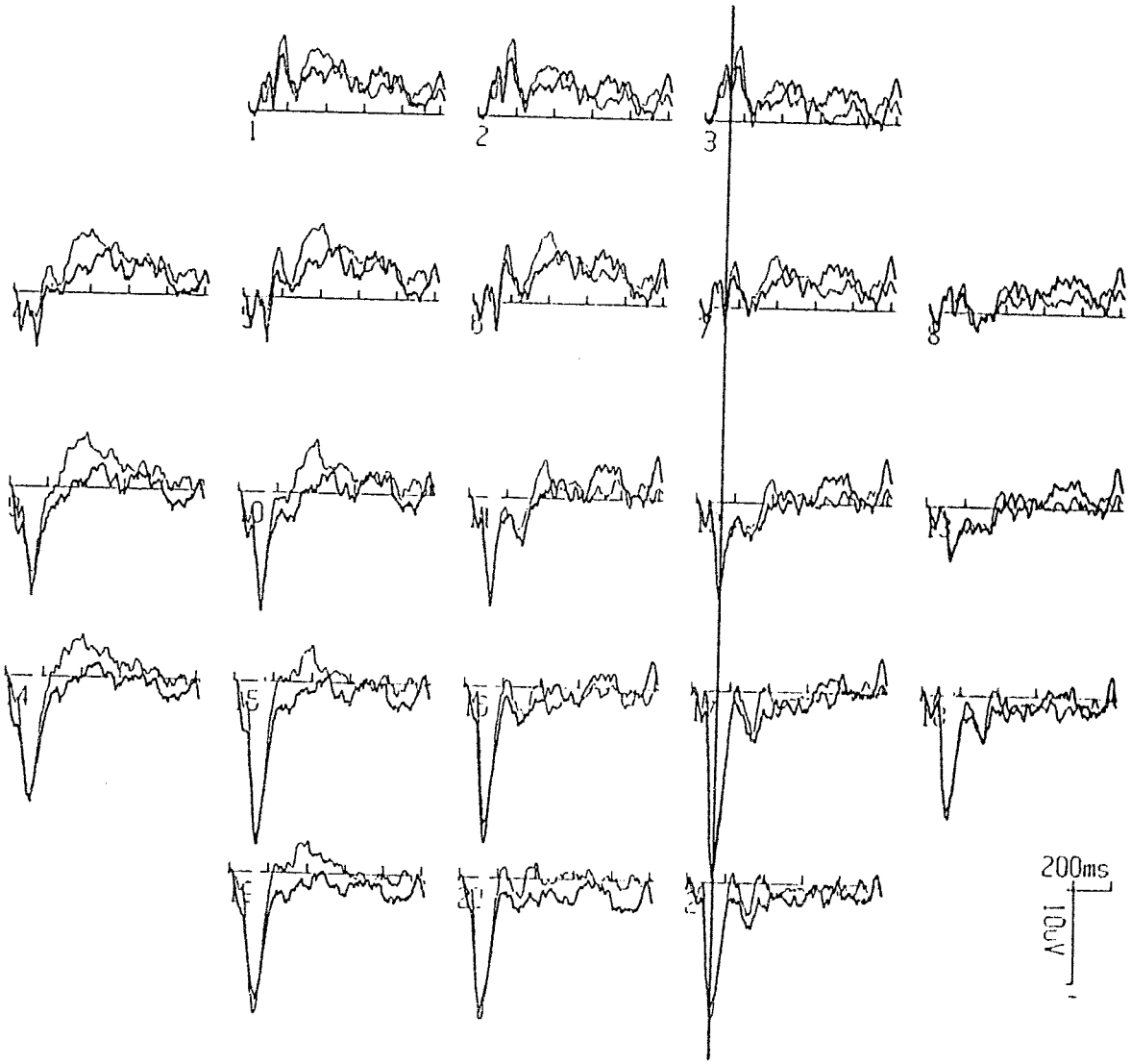

Figure 45. Visual evoked responses to left hemifield presentation of dot matrix stimuli (Subject E.R.)

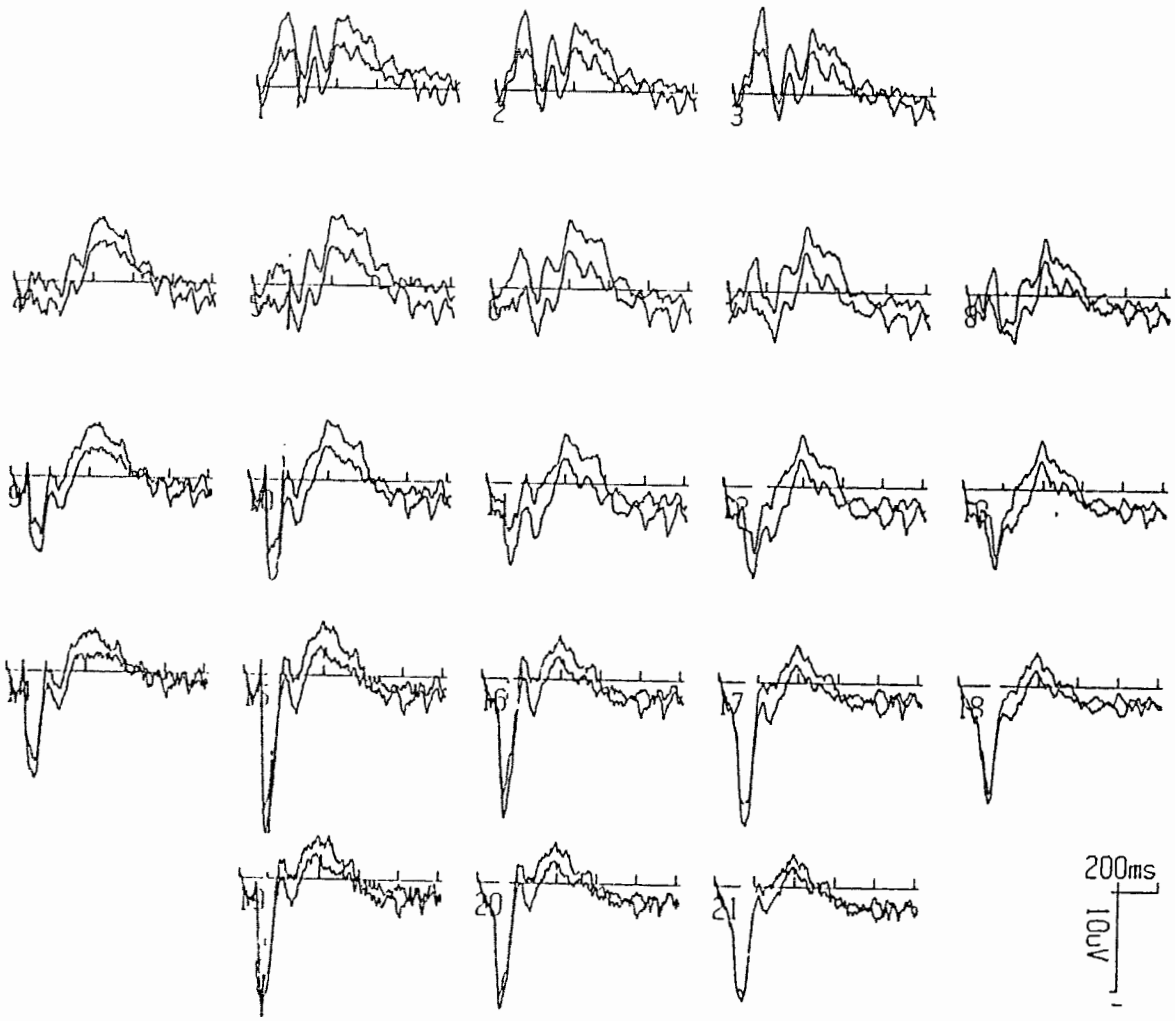

Figure 46. Visual evoked responses to right hemifield presentation of dot matrix stimuli (Subject J.S.)

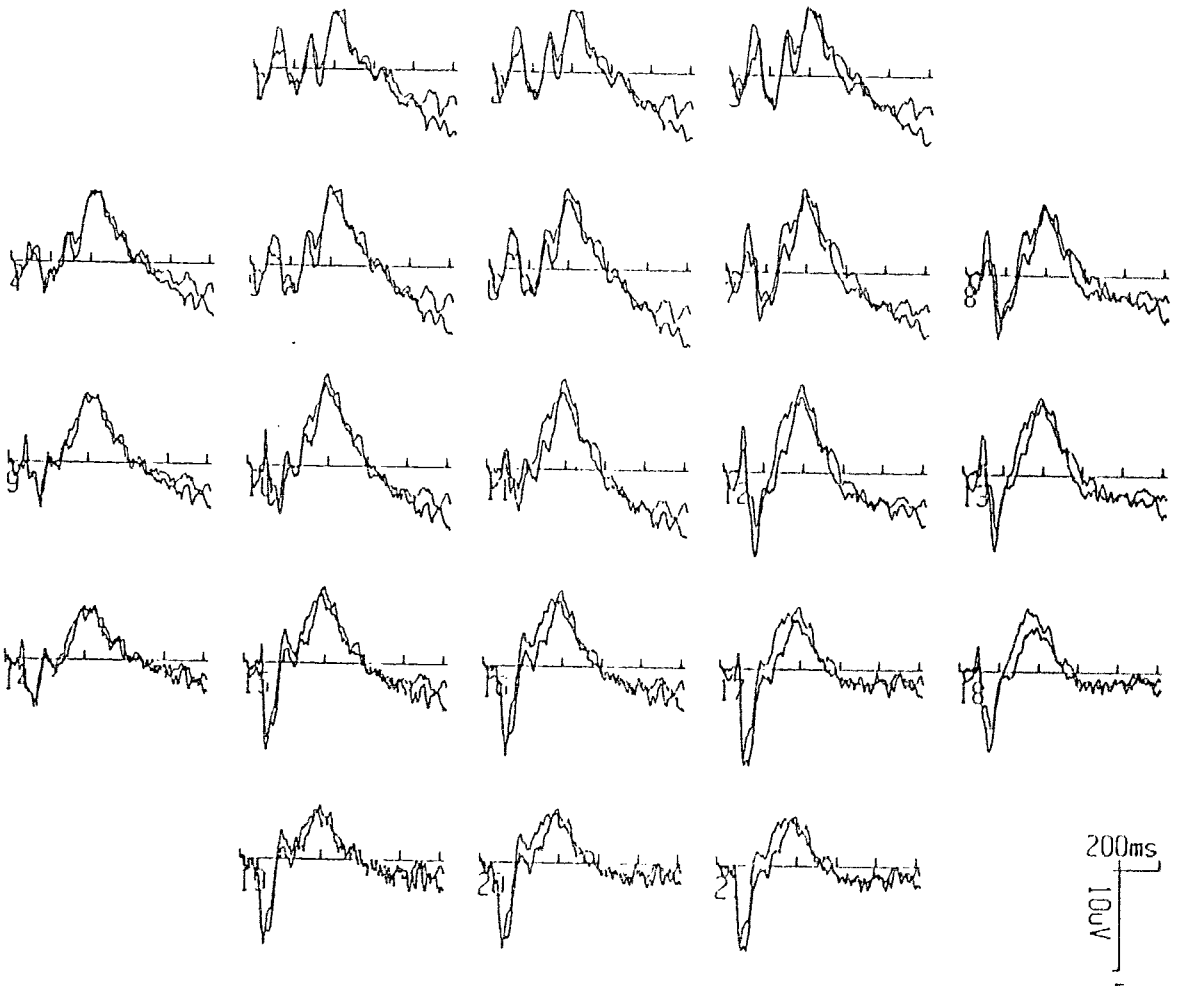

Figure 47. Visual evoked responses to right hemifield presentation of dot matrix stimuli (Subject W.P.)

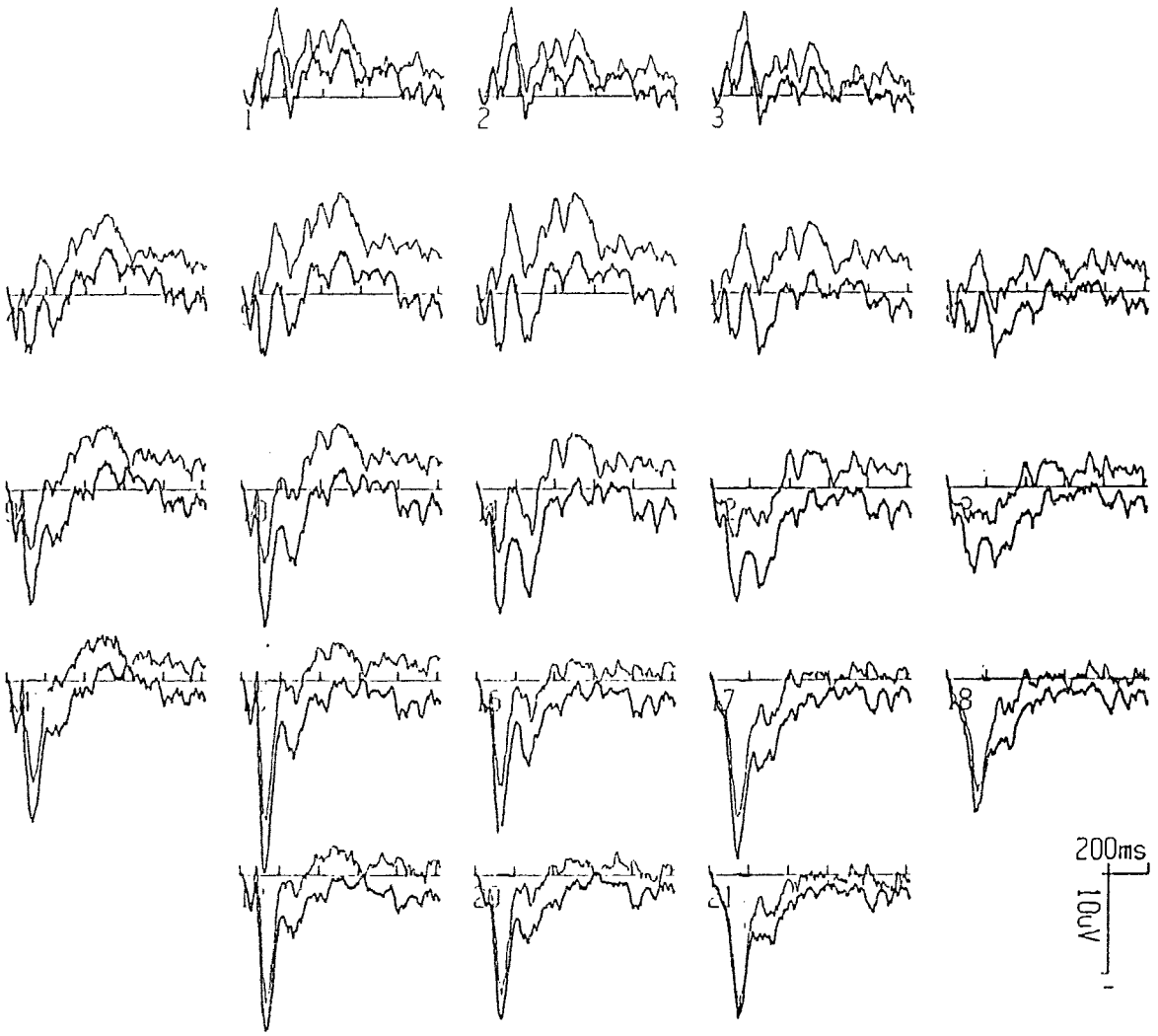

Figure 48. Visual evoked responses to right hemifield presentation of dot matrix stimuli (Subject E.R.)

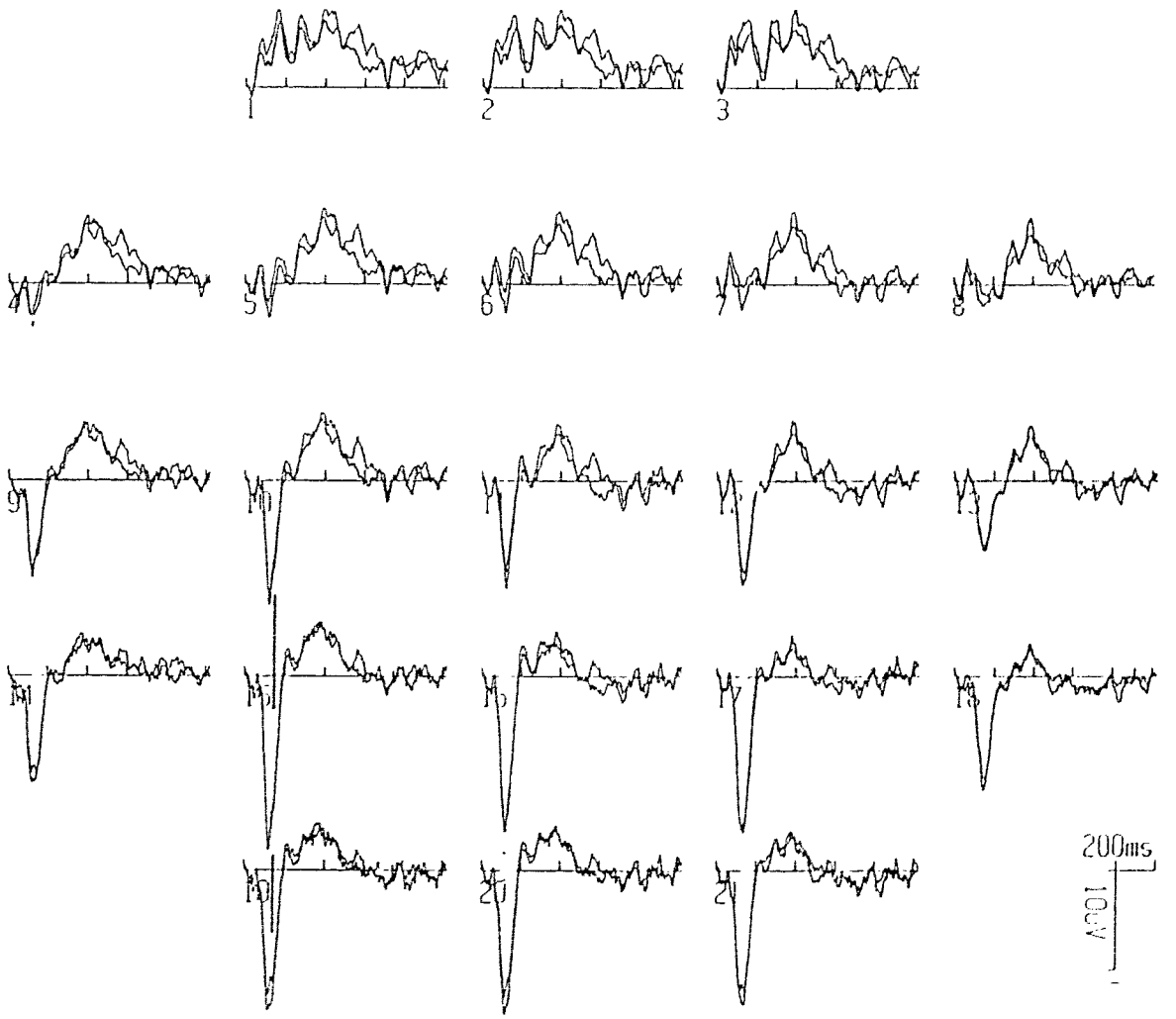

Figure 49. Visual evoked responses to lower hemifield presentation of dot matrix stimuli (Subject J.S.)

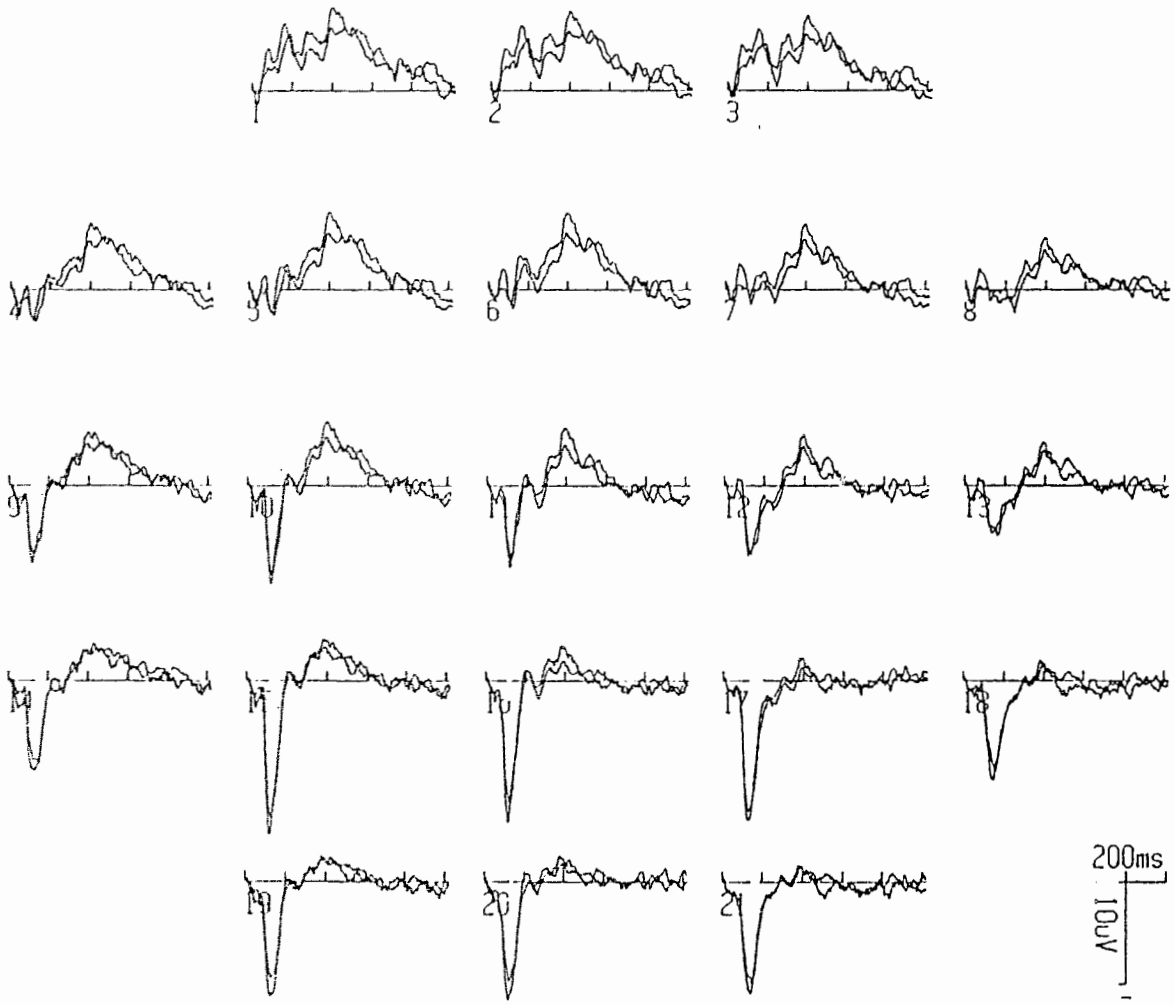

Figure 50. Visual evoked responses to lower hemifield presentation of dot matrix stimuli (Subject W.P..)

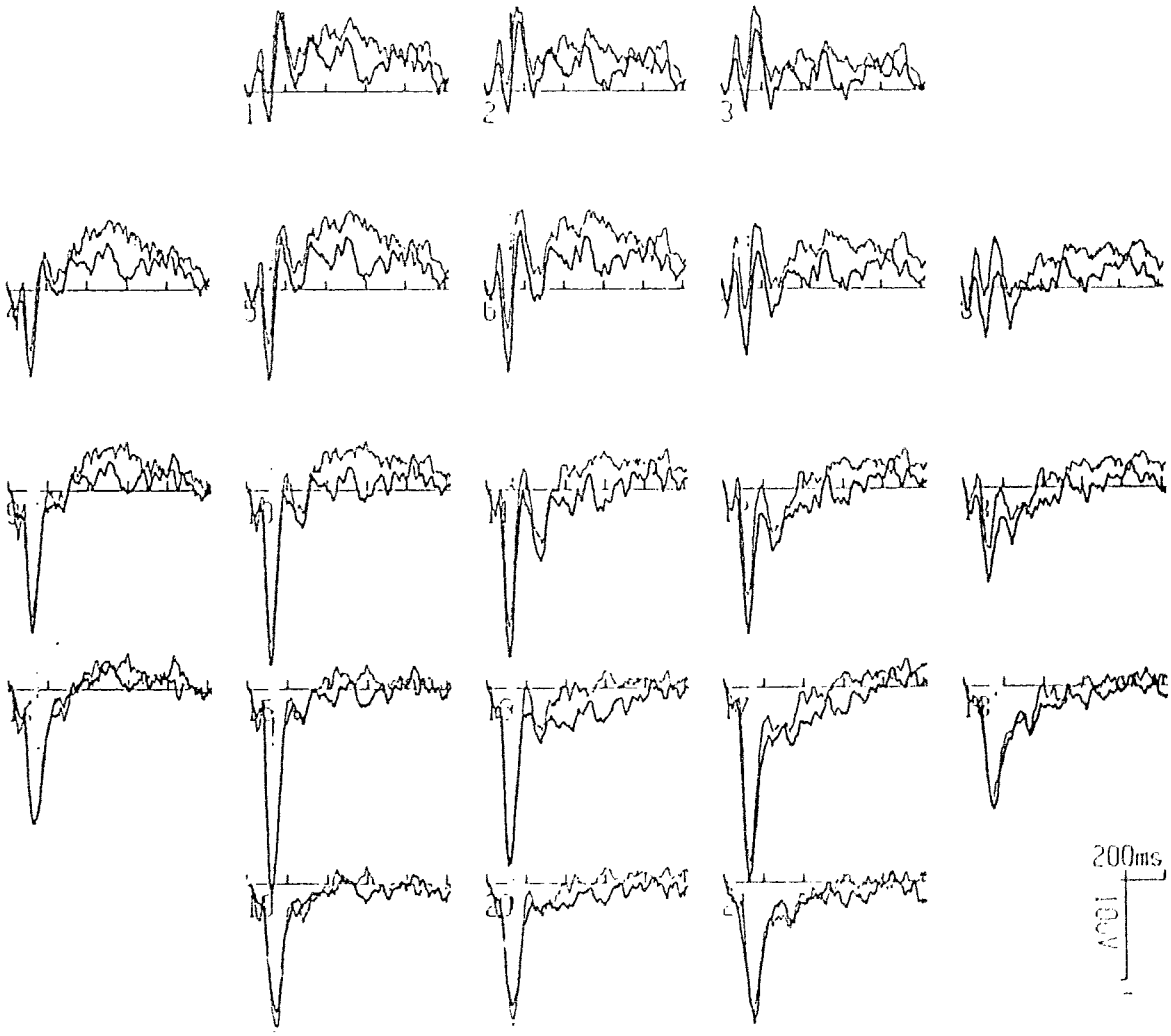

Figure 51. Visual evoked responses to lower hemifield presentation of dot matrix stimuli (Subject E.R.)

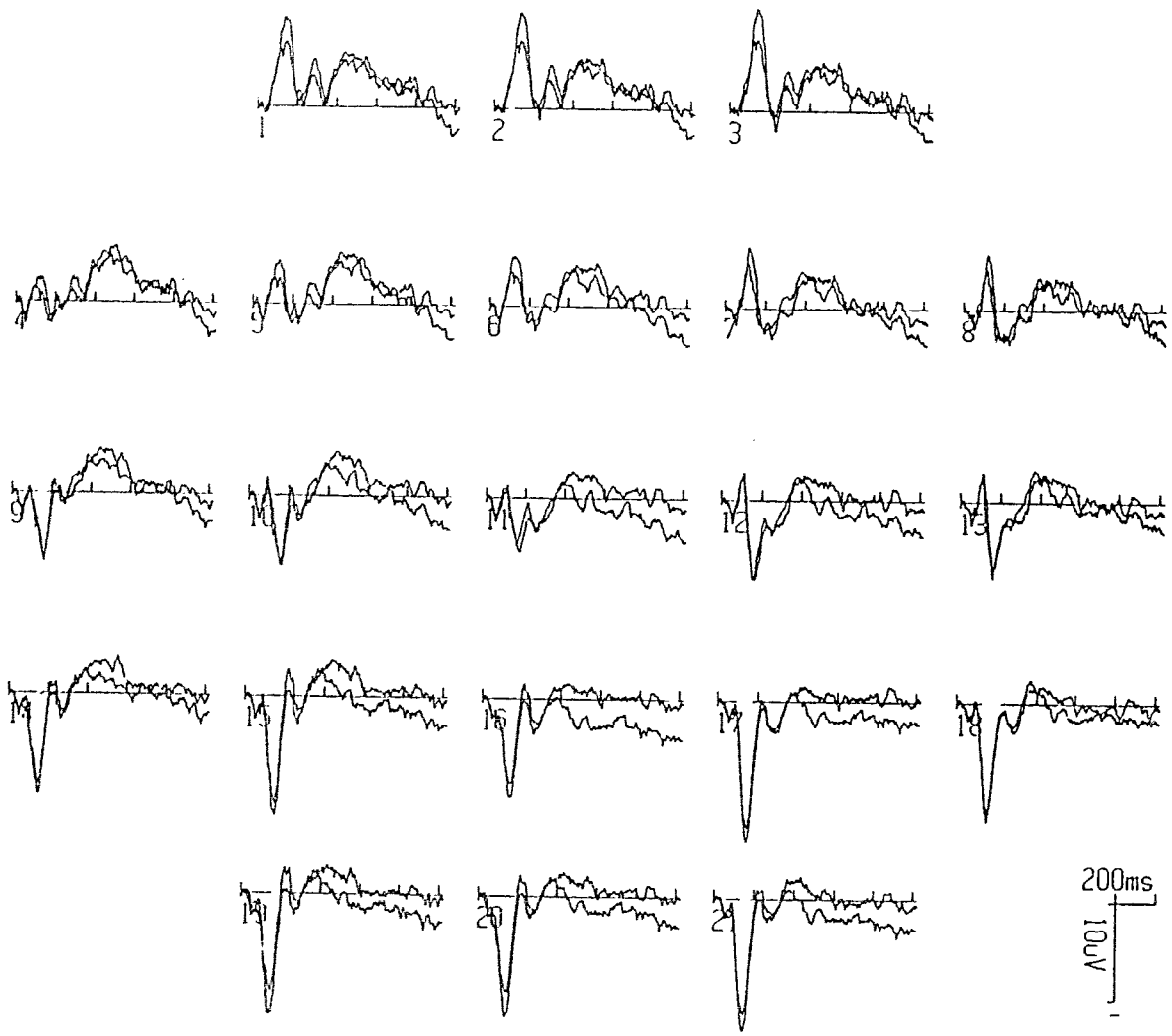

Figure 52. Visual evoked responses to upper hemifield presentation of dot matrix stimuli (Subject J.S.)

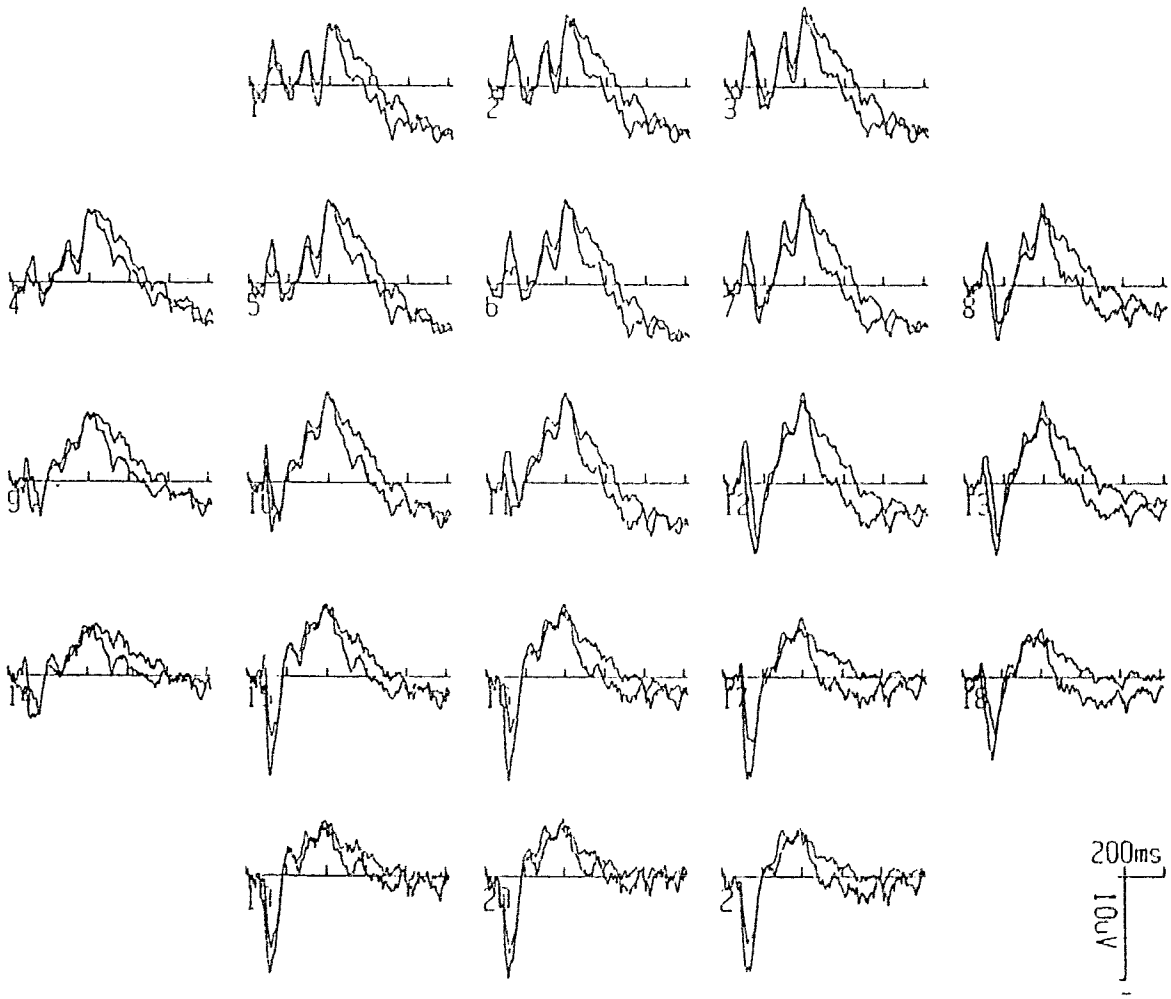

Figure 53. Visual evoked responses to upper hemifield presentation of dot matrix stimuli (Subject W.P.)

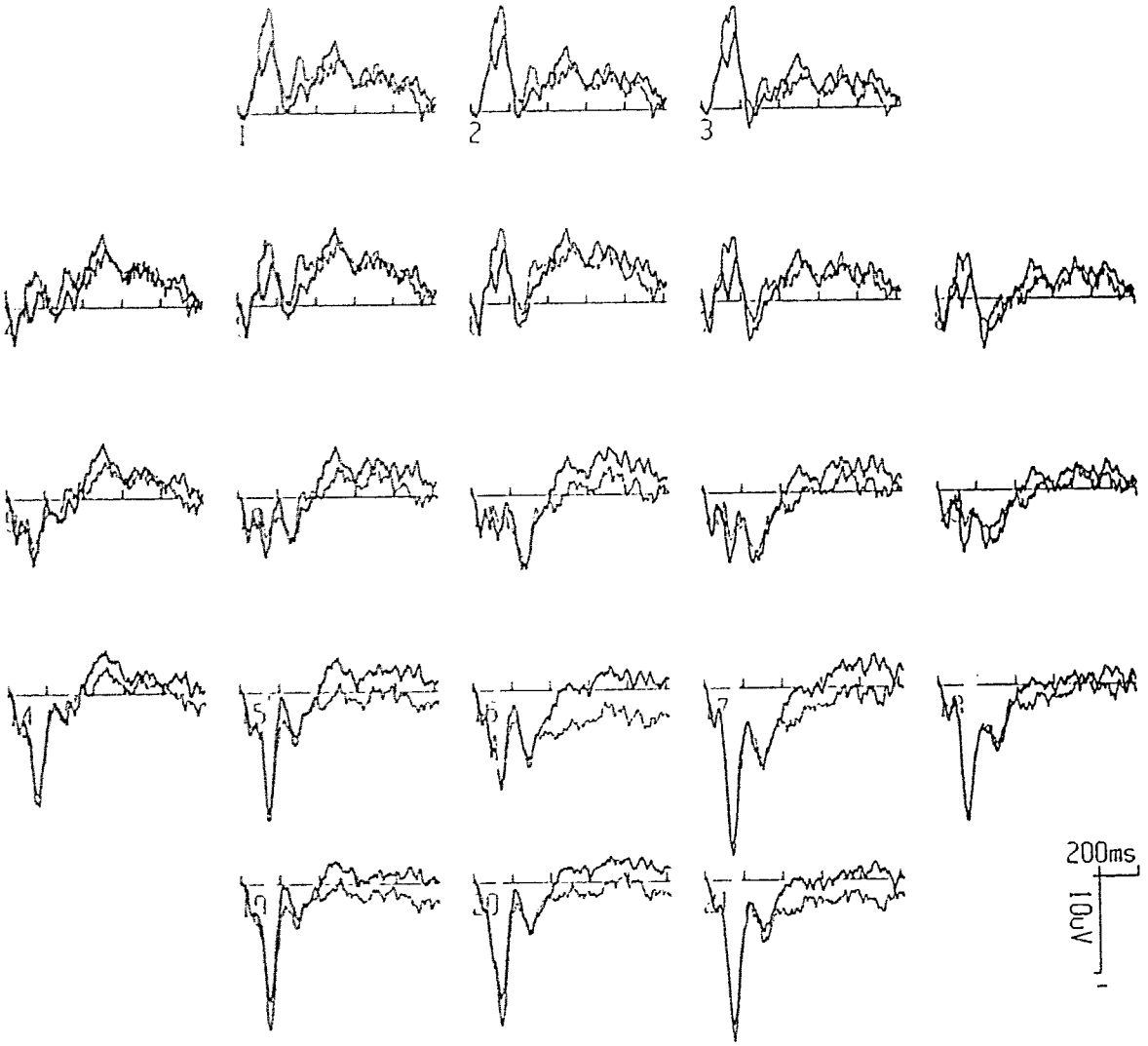

Figure 54. Visual evoked responses to upper hemifield presentation of dot matrix stimuli (Subject E.R.)

These results suggest that the cortical generators of the VEP waveform can be interpreted in terms of the retinotopic organization of visual cortex. The large change in the scalp potential field with lower hemifield stimulation suggests a corresponding change in the underlying generators, an observation of obvious localizing value if it can be related to what is known of the retinotopic organization of visual cortex.

Figure 55 (top) shows a schematic representation of the visual areas in man derived by Drasdo (1980) from neuroanatomical studies in man and macaque. The stippled regions show the projection of the central two degrees of the visual field on Brodmann's areas 17, 18 and 19 (the projections for areas 18 and 19 are derived from comparative data and remain hypothetical in man). The upper half of the visual field projects to cortex below the calcarine sulcus, while the lower half projects to cortex above this sulcus. It can be seen that the upper and lower half-fields representations become progressively more separated in space as one moves from area 17 to area 19. In addition, the orientation of cortical cells of areas 18 and 19 is different in the upper and lower half-field projections: with respect to the plane defined by the base of the brain in Figure 55, cortical cells of area 18 and 19 are oriented perpendicularly in the upper half field representation the under-surface of the occipital lobe, but approximately parallel to this plane for the lower half-field representation in the superior aspect of the occipital lobe. For area 17, projecting to the occipital pole, there is not such a a radical change in orientation between the regions representing the upper and lower and upper half-fields.

Jeffreys and Axford (1972b) invoked this anatomical scheme to support their hypothesis that component C.II component of the pattern onset VEP was generated in the extrastriate regions of cortex (specifically, area 18) on the upper and lower surfaces of the occipital lobes. According to their hypothesis, the C.II generators could be modeled in this manner as two simple equivalent dipoles representing the upper and lower half-field projections of the retina. Their model is shown in Figure 55 (bottom).

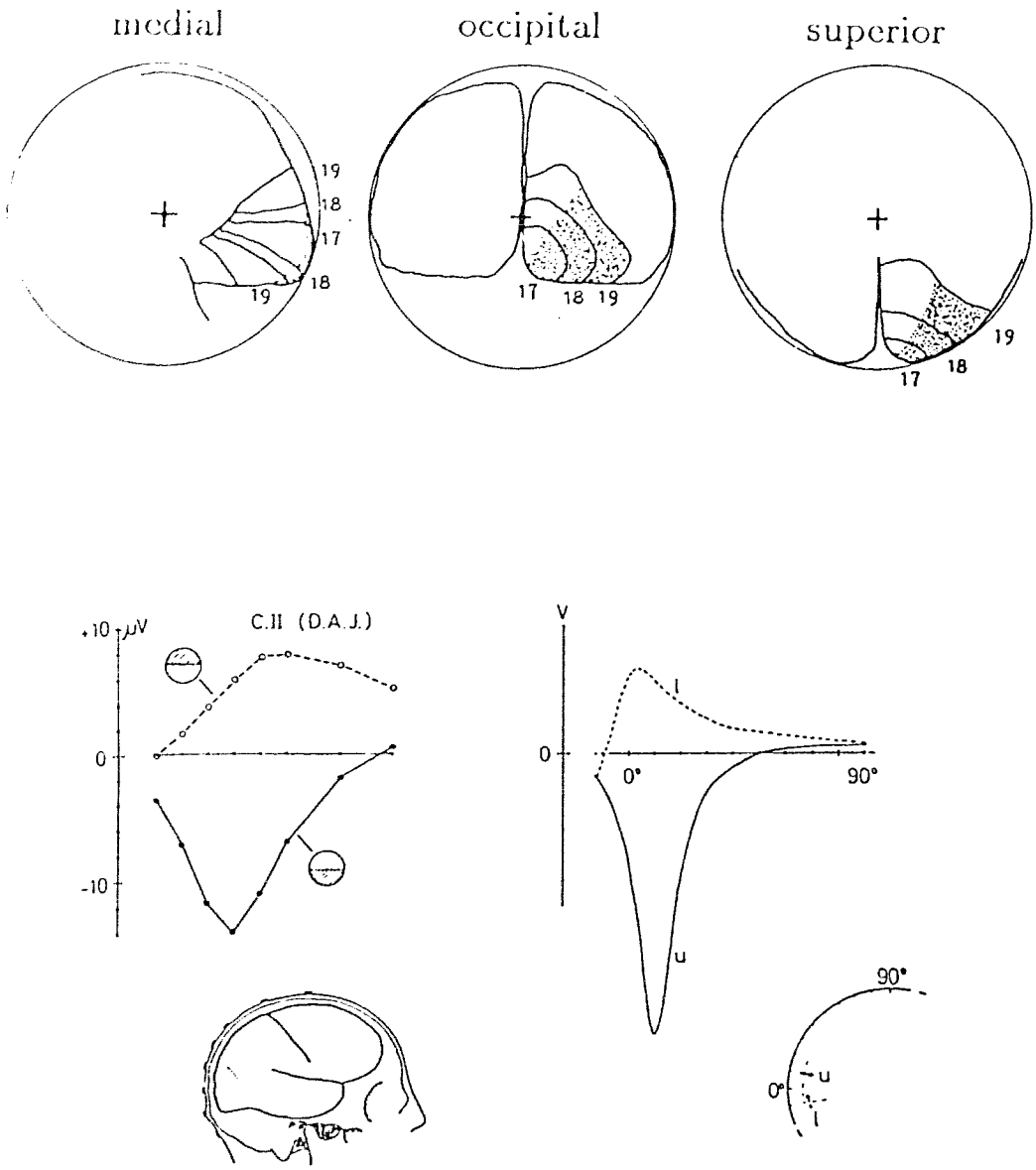

Figure 55. Top: Schematic representation of the extent of the central visual fields on Brodmann's areas 17, 18 and 19. Circle indicates the approximate fit of occipital cortex to the inner surface of the sphere (From Stok, 1986, p. 74).

Bottom: Jeffrey's and Axford's (1972) model of C. II generators. Top left: C.II amplitude plotted against longitudinal recording location for upper and lower hemifield stimulation. Top right: Calculated amplitude distributions for dipoles in a spherical volume conductor (From Jeffreys and Axford, 1972b, p. 33).

A comparison to the data of Jeffreys and Axford (1972a; b) shows that the VEPs obtained in the present study are very similar in form (PNP), amplitude (5-15 uV for the N1 peak), topography, effect of hemifield stimulation, and interindividual variability in those descriptors. The only major difference with the VEPs in the present study is in latency: (110-130 msec N1 peak latency compared to 90-110 msec reported by Jeffreys and Axford; this difference can be fully accounted for by the difference in adapting luminance (10 cd/m^2 in the present study, compared to 36 cd/m^2 used by Jeffreys and Axford): Van der Tweel, Estevez and Cavonius (1979) have reported that, if contrast is held constant, the form of the pattern onset response varies little or not at all with adapting luminance, but that latency increases approximately 30 msec for each 10-fold decrease in adapting luminance. The invariance of the form of the pattern onset response with adapting luminance is such that Van der Tweel et al. suggested that "..it behaves as a mechanism that once triggered gives the same response, regardless of the signal that triggered it (1979; p. 1286). Indeed, very similar responses to pattern onset have been described by a large number of investigators,

Equivalent dipoles were fitted to the present data to test Jeffreys and Axford's model of the generators of the C.II component. One, two and three dipole fits were performed to assess the adequacy of fit of this dipole model. Spatiotemporal analyses were performed to assess the likely time course of activity of estimated generator sources.

Results:

(1) Single Dipole Fits (Time slice: fitted to N1 peak).

Parameters for single dipoles fitted to instantaneous fields at the peak of the N1 wave at electrode 16 are given in Tables 1-4. Dipole parameters are summarized in Figure 56, which shows dipoles for all three subjects projected on the head-centered coordinate system, for lower, upper and left hemifield stimulation. In this figure, dipole location is represented as a small dot and orientation is represented as a straight line projecting from the dot along the negative axis of the dipole.

With reference to Figure 56, dipole estimates for lower hemifield stimulation cluster closely together at the midline at an average distance of -5.23 cm from the center of the sphere along the X axis (61% of the average outer sphere radius) and an average of 2.48 cm from the center of the sphere along the Z axis (29% of sphere radius). Comparison with textbook magnetic resonance imaging (MRI) scans places these dipoles deep in the occipital lobes, several cm below the cortical surface. With regard to these depth estimates, it should be noted that fitted dipoles represent the centroid of an extended region of active cortex on the lateral surfaces of the occipital lobes. The location of this centroid is well below the cortical surface. In addition, these depth estimates correspond to those obtained for electrical dipoles by Maier (1987) and Stok (1986). Dipole orientation for all three subjects is radial to the occipital region of the sphere, corresponding to the expected orientation of cortical pyramidal cells on the superior surface of the occipital lobe.

Fitted dipoles for upper hemifield stimulation (Figure 56; middle) cluster less closely: average X distance is -4.45 cm (52% of average outer radius) and average Z distance is 1.03 cm (12% of average outer radius). Average orientation of the fitted dipoles is vertical with negative pole downward, in accordance with the expected orientation of cortical cells on the inferior surface of the occipital lobe.

Fitted dipoles for left hemifield stimulation are shown in Figure 56 (bottom). Dipole orientation is roughly 30 degrees with respect to the X-Y plane. These dipoles account well for the observed fields (negative at the occiput, positive at the vertex), but do not correspond to the expected orientation cortical pyramidal cells on any surface of the occipital lobes (except for sulcul cells, but oppositely oriented dipole fields on either side of a sulcus would likely cancel each other). The fact that these equivalent dipoles all account for more than 90% of the variance in observed fields serves as a reminder that a dipole is a statistical abstraction, with no necessary physiological meaningfulness unless constrained by other information.

From this analysis it can be concluded that the potential field observed with upper hemifield stimulation is well-described by a vertically-oriented equivalent dipole in the center of the occipital lobes, while that observed with lower hemifield stimulation is well-fitted with a horizontally-oriented equivalent dipole. The upper hemifield dipole is situated, on average, less than one cm lower and 1.5 cm more anterior (although the individual differences swamp this mean difference in location). This analysis is in complete agreement with Jeffreys and Axford's (1972b) model.

Table 1

Single Moving Dipole Source Estimates (Left Hemifield Stimulation)

S	Time Point (msec)	Q (nA·m)	Position (cm) x	Position (cm) y	Position (cm) z	*Orientation (cm) x	*Orientation (cm) y	*Orientation (cm) z	Residual variance (%)
J.S.	125	343.17	-5.4179	0.3682	4.9802	-0.4429	-0.1394	-0.8857	8.37
W.P.	125	611.0	-5.5539	-0.3986	4.5053	-0.5112	-0.3359	-0.7911	7.07
E.R.	129	323.23	-3.9713	-0.0001	2.2308	-0.6817	0.0838	-0.7268	3.40

Note. *Vector is directed toward negative pole.

Q = Dipole moment.

Table 2

Single Moving Dipole Source Estimates (Right Hemifield Stimulation)

S	Time Point (msec)	Q (nA·m)	Position (cm) x	Position (cm) y	Position (cm) z	*Orientation (cm) x	*Orientation (cm) y	*Orientation (cm) z	Residual variance (%)
J.S.	125	301.10	-5.9658	0.5544	4.7962	-0.6019	0.0277	-0.7981	5.70
W.P.	125	368.33	-2.2977	0.0588	4.2771	-0.5994	-0.2429	-0.7627	7.11
E.R.	129	594.52	-1.9723	0.0003	4.2318	-0.6541	0.0434	-0.7551	2.72

Note. *Vector is directed toward negative pole.

Q = Dipole moment.

Table 3

Single Moving Dipole Source Estimates (Lower Hemifield Stimulation)

S	Time Point (msec)	Q (nA·m)	Position (cm) x	Position (cm) y	Position (cm) z	*Orientation (cm) x	*Orientation (cm) y	*Orientation (cm) z	Residual variance (%)
J.S.	121	496.26	-5.332	0.116	2.9633	-0.9534	0.0271	0.1005	2.67
W.P.	121	137.48	-5.401	0.0301	2.2683	-0.9759	-0.0289	0.1163	16.8
E.R.	121	620.20	-4.9777	0.0003	2.2247	-0.8603	0.076	0.2041	6.54

Note. *Vector is directed toward negative pole.

Q = Dipole moment.

Table 4

Single Moving Dipole Source Estimates (Upper Hemifield Stimulation)

S	Time Point (msec)	Q (nA·m)	Position (cm) x	Position (cm) y	Position (cm) z	*Orientation (cm) x	*Orientation (cm) y	*Orientation (cm) z	Residual variance (%)
J.S.	136	341.63	-3.4235	0.1268	0.8638	-0.2667	-0.0352	-0.8232.	6.08
W.P.	125	76.79	-6.988	-0.3963	1.0093	-0.236	0.0209	-0.9715	12.09
E.R.	140	687.86	-2.9722	-0.0002	1.2318	-0.4091	-0.0837	-0.9086	4.71

Note. *Vector is directed toward negative pole.

Q = Dipole moment.

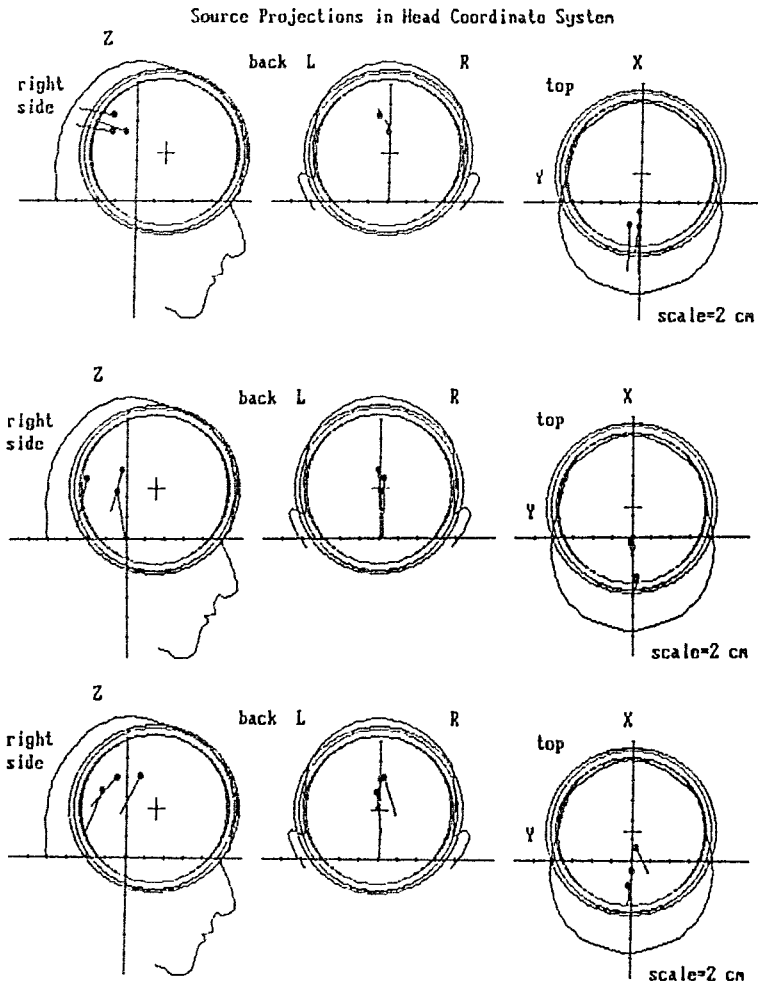

Figure 56. Single dipole parameter estimates for all three subjects. Top: Lower hemifield stimulus. Middle: Upper hemifield stimulus. Bottom: Left hemifield stimulus.

2. Two-dipole, spatio-temporal dipole fits.

Since right and left hemifield stimulation will simultaneously activate cortex devoted to both upper and lower hemifields, it was predicted that these fields would be well-fitted with a combination of the two dipoles. To test this prediction, two equivalent dipoles were fitted to the fields evoked by right and left hemifield stimuli. Spatiotemporal dipole analysis was applied to the observed fields initially for a time window of 50 msec, centered at the N1 peak at electrode 16. Once a stable solution was derived, the window was extended to 250 msec, starting at time zero (stimulus onset), in order to examine source activity level over an extended epoch including the time before and after maximum source activity. In nearly all cases, dipole parameters remained remarkably stable after extending the analysis window, and total residual variance over the time window increased only marginally.

Spatio-temporal dipole parameter estimates are given in Tables 5 and 6. These parameters are represented graphically in Figures 57-62 for each subject and condition. Four types of analysis are given in these figures: (1) Dipole parameter estimates shown in the head coordinate system; (2) Residual variance for each time point plotted over the analysis window (0 to 250 msec); (3) Calculated source activity level (in units of nanoAmpere·meters) for each time point in the analysis window; and (4) topographic contour plots of the observed, predicted and residual fields for a selected time point (indicated by the vertical line in the source activity level and residual variance plots).

Dipole Parameter Estimates:

The dipole locations obtained in this analysis correspond only approximately to those obtained in the previous (time-slice) analysis. Two factors are pertinent to this result: First, if extended sources vary in time in their centroid of maximal activity (as suggested by the analysis of Stok, 1986), this type of analysis will result in spatial averaging of the location estimates; second, the right and left hemifield stimuli will result in the activation cortical projections for only the upper and lower quadrants of the visual field. Full-field stimulation would be a better comparison; however, accuracy in estimation of dipole parameters is critically dependent on the source being as spatially restricted as possible. On balance, the half-field comparisons represent the best compromise of these opposing considerations.

The prediction that the best fitting sources would have an orientation approximately orthogonal to each other is borne out at least approximately for all subjects and conditions. Orthogonality of the two sources is particularly striking in four of the six cases (Figures 58, 59, 60 and 62).

Residual Variance and Source Activity Plots

In all cases, source activity is high for a discrete epoch of time corresponding to the duration of the PNP complex in the observed fields. Little activity is seen in the periods preceding and following this epoch. Pointwise residual variance is minimal during a correspondingly discrete epoch. It can be concluded that the model has an excellent temporal fit to the observed data. Interestingly, in each case there is a local maximum of residual variance corresponding to the P1 and P2 peaks of the PNP complex. If the P1 peak of the present data corresponds to the C.I component described by Jeffreys and Axford (1972a), this result is not surprising: The C.I component likely is generated by a separate cortical source, and the fit of the present model would not be expected to be good during the times C.I source is active.

Table 5

Two Dipole Spatio-Temporal Source Estimates (Left Hemifield Stimulation)

			Position (cm)			*Orientation (cm)			Residual variance (%)
S	Window (msec)	Dipole	x	y	z	x	y	z	
J.S.	1-250	1	-3.1560	-6.8658	2.7640	-0.8137	0.5802	-0.0361	
		2	-3.7331	0.0699	0.4540	-0.6537	0.1850	-0.7338	8.15
W.P.	1-250	1	-2.7187	1.7164	1.2671	-0.9973	-0.0727	0.0094	
		2	-2.2762	-0.2894	0.5573	-0.1353	-0.5003	-0.8552	8.6
E.R.	1-250	1	-4.9281	0.8788	2.3415	-0.9954	0.0438	-0.0846	
		2	-5.5281	-0.0595	0.6449	-0.0592	-0.2207	-0.9736	9.84

Note. *Vector is directed toward negative pole.

Table 6

Two Dipole Spatio-Temporal Source Estimates (Right Hemifield Stimulation)

			Position (cm)			*Orientation (cm)			Residual variance (%)
S	Window (msec)	Dipole	x	y	z	x	y	z	
J.S.	1-250	1	-4.0366	-0.1101	1.2280	-0.9888	-0.0071	0.1490	
		2	-2.1303	-0.0149	0.0808	-0.1954	0.0418	-0.9798	22.58
W.P.	1-250	1	-4.2509	-0.6361	3.6120	-0.9893	0.1183	-0.0854	
		2	-2.3039	-0.0287	0.5074	-0.4659	-0.0189	-0.8847	15.38
E.R.	1-250	1	-3.9240	0.9700	1.0274	-0.9839	-0.1433	-0.1071	
		2	-3.2080	-0.4786	0.3063	0.1703	-0.6675	-0.7249	7.62

Note. *Vector is directed toward negative pole.

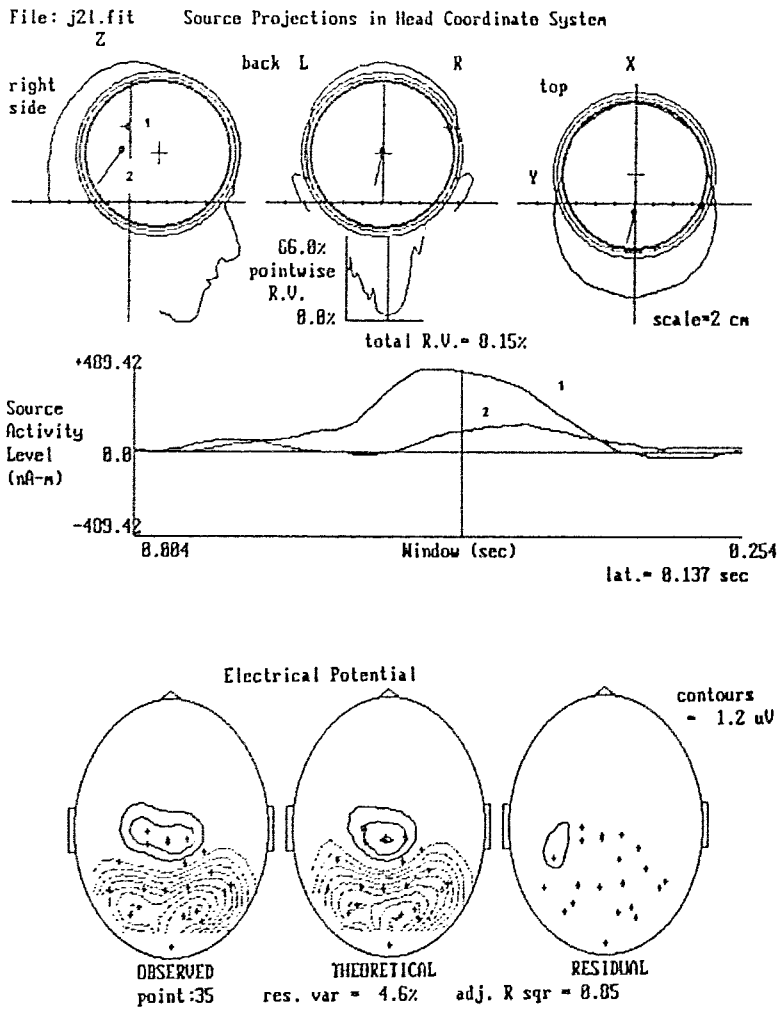

Figure 57. Two dipole spatio-temporal source estimates: Left Hemifield Stimulation (Subject J.S.).

Top: Right, posterior and top views of estimated dipoles. Middle: Source activity level over analysis window. Bottom: Observed, predicted and residual (observed minus predicted) fields.

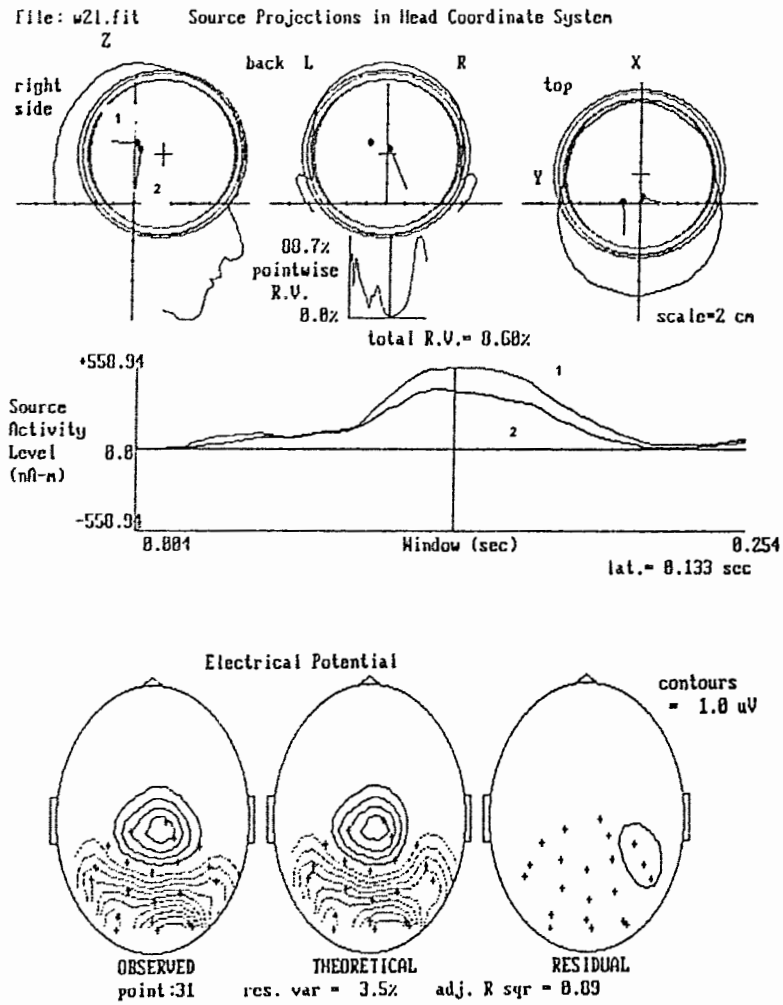

Figure 58. Two dipole spatio-temporal source estimates: Left Hemifield Stimulation (Subject W.P.).

Top: Right, posterior and top views of estimated dipoles. Middle: Source activity level over analysis window. Bottom: Observed, predicted and residual (observed minus predicted) fields.

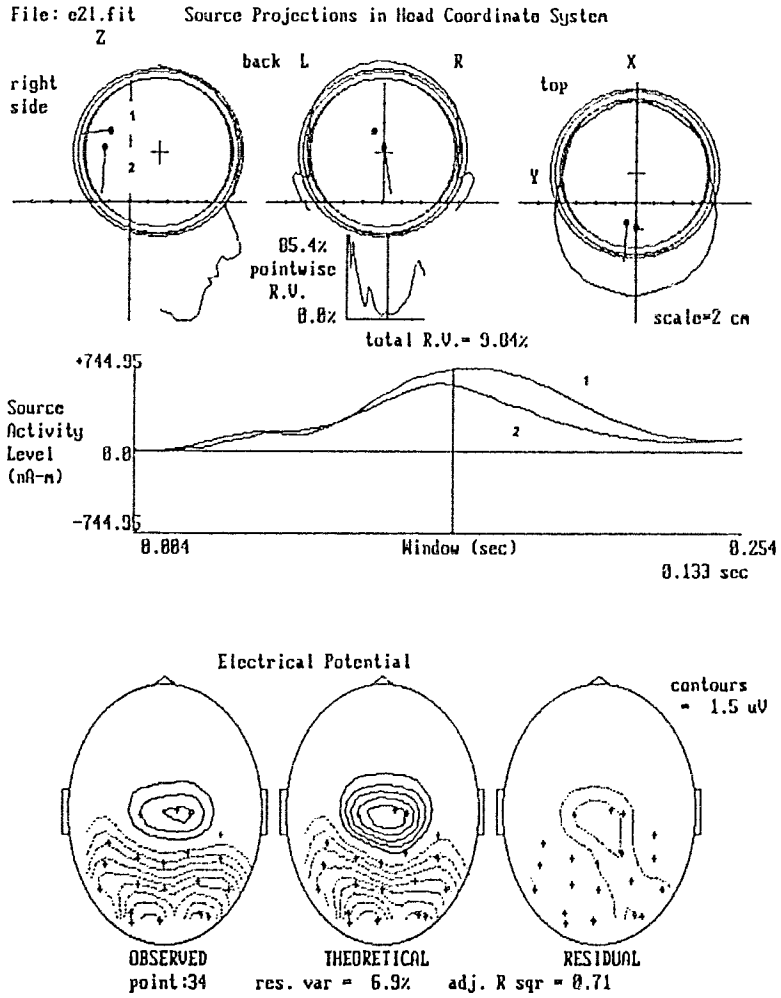

Figure 59. Two dipole spatio-temporal source estimates: Left Hemifield Stimulation (Subject E.R.).

Top: Right, posterior and top views of estimated dipoles. Middle: Source activity level over analysis window. Bottom: Observed, predicted and residual (observed minus predicted) fields.

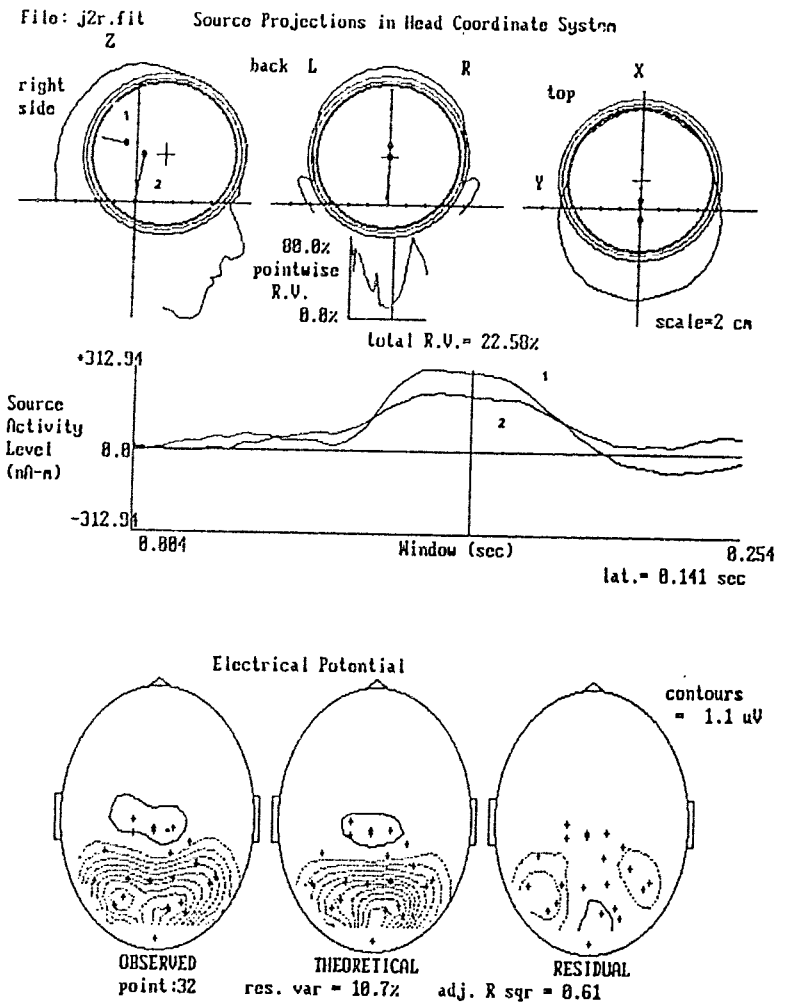

Figure 60. Two dipole spatio-temporal source estimates: Right Hemifield Stimulation (Subject J.S.).

Top: Right, posterior and top views of estimated dipoles. Middle: Source activity level over analysis window. Bottom: Observed, predicted and residual (observed minus predicted) fields.

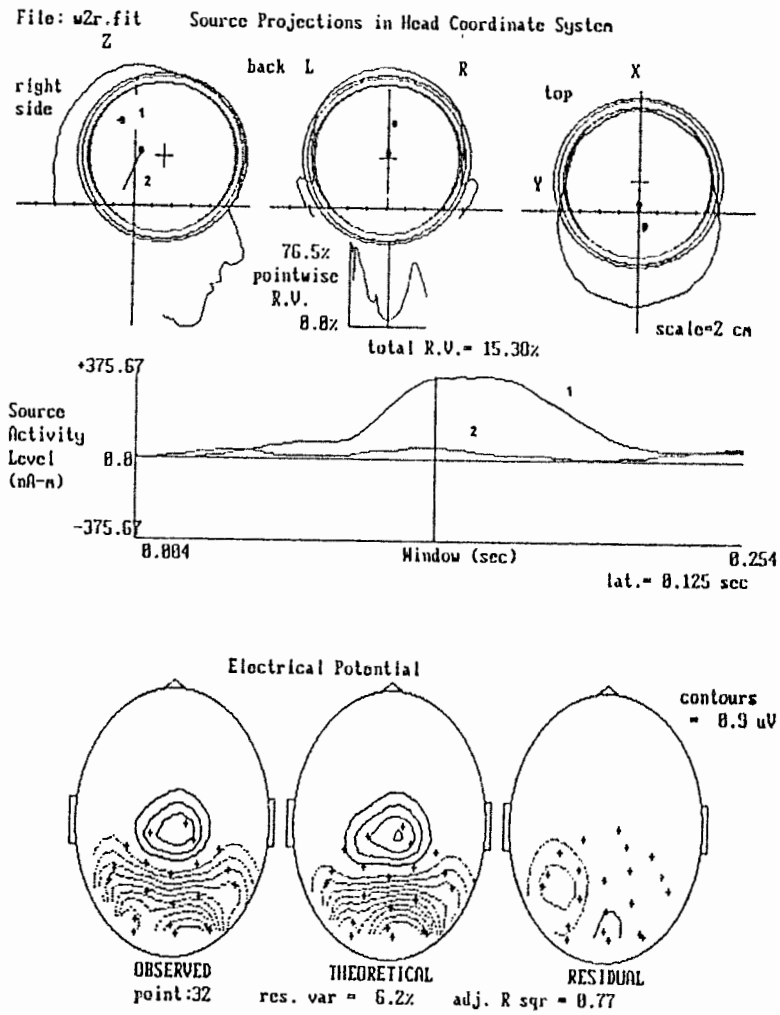

Figure 61. Two dipole spatio-temporal source estimates: Right Hemifield Stimulation (Subject W.P.).

Top: Right, posterior and top views of estimated dipoles. Middle: Source activity level over analysis window. Bottom: Observed, predicted and residual (observed minus predicted) fields.

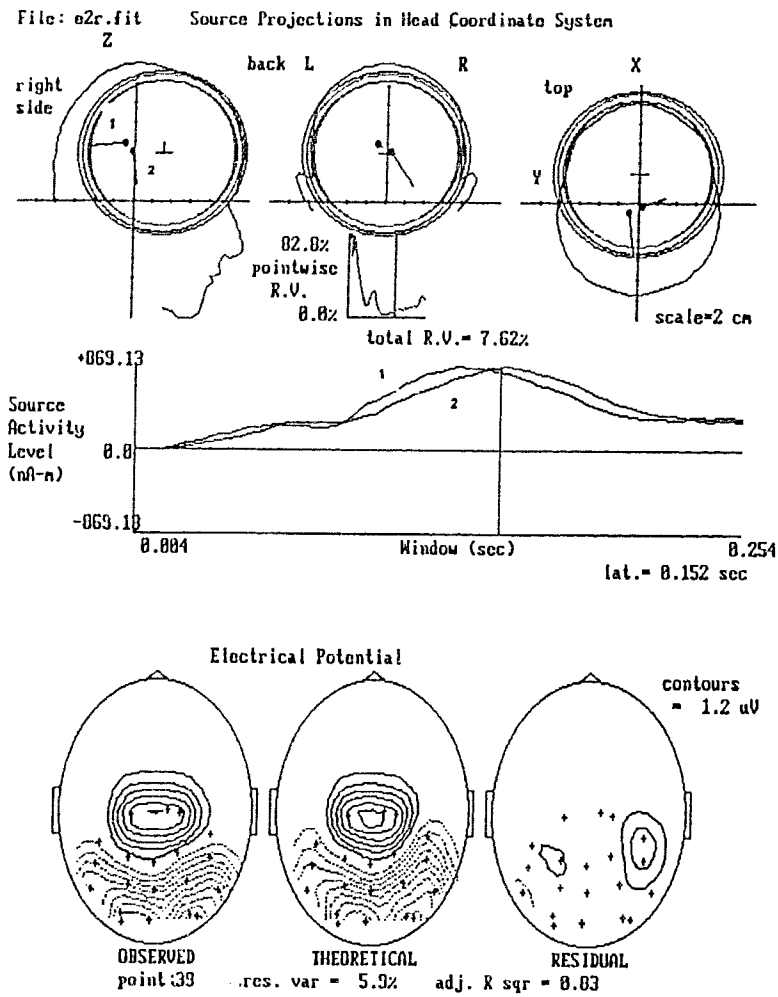

Figure 62. Two dipole spatio-temporal source estimates: Right Hemifield Stimulation (Subject E.R.).

Top: Right, posterior and top views of estimated dipoles. Middle: Source activity level over analysis window. Bottom: Observed, predicted and residual (observed minus predicted) fields.

Discussion

The results of the preceding analysis converge to support the hypothesis that the N1 component of the VEP elicited by the dot matrix stimuli in a temporal integration of form parts paradigm is generated in extrastriate regions of the occipital lobe. This inference is drawn from the finding that the best-fitting equivalent sources of the observed fields for upper and lower half-field stimulation respectively are oriented nearly orthogonally to each other. Further, the best fitting equivalent source for the right and left hemifield stimulation consists of two orthogonal dipoles, one oriented with negative pole posterior, the other with negative pole vertical down. This model does not correspond to the known neuroanatomical projections of the fovea to area 17: the regions representing the upper and lower half fields are oriented in a similar direction (with respect to the surface of a fitted sphere) above and below the calcarine sulcus. The model does correspond well to the hypothesized cortical representations of these visual half-fields in areas 18 or 19: orientation of cortical pyramidal cells is expected to be nearly orthogonal for the regions containing the projections of the upper and lower half-fields. The spatial localization achieved here is not fine-grained enough to be able to distinguish between areas 18 or 19 or both as the most likely candidate sources.

SUMMARY AND CONCLUSIONS

This thesis has examined the temporal and spatial patterning of VEPs elicited by stimuli in a psychophysical paradigm used to study visible persistence.

In part 1, it was shown that these VEPs exhibit a strong correspondence to the behavioral measures of perceptual integration. Specifically, it was found that behavioral measures of perceptual integration corresponded well to the degree of overlap of the successive VEPs elicited by the consecutive presentations of the two parts of the display. Further, it was shown that the primary temporal correlate of both behavioral and psychophysical measures was SOA, rather than ISI. It was concluded that both the psychophysical and neurophysiological data are supportive of a processing interpretation of visible persistence: visible persistence is primarily determined by the activity of neuronal encoding mechanisms at an early stage of visual information processing.

The data of part 1 of the present study cannot be explained within the framework of Sakitt's storage model, which states that visible persistence is primarily due to the persistence of photoreceptor activity after stimulus offset. It was noted that photoreceptor persistence can in principle account for the residual persistence not accounted for by the processing model, and that the total duration of visible persistence must necessarily reflect some complex admixture of neural persistences at all levels of the visual system. Within this more comprehensive framework, it is argued that the primary neuronal contributors to visible persistence are those neuronal ensembles involved in obligatory encoding processes and whose primary temporal correlate is SOA.

Having established a correspondence between behavioral and neurophysiological data, Part 2 of this thesis attempted to localize the likely cortical generators of the VEPs elicited by the visual stimuli employed in this paradigm. In the first series of investigations, it was found that the topography of the potential fields elicited by the sequential pattern parts was very similar, whether elicited by two stimuli at an ISI where perceptual integration is complete (10 ms) or at an

ISI at which perceptual integration of the two stimuli is impossible (500 msec). This strengthens the argument that perceptual integration is dependent upon temporal overlap of neuronal activity involved in relatively low-level encoding processes, and precludes any "top-down" interpretation that a different neuronal configuration may be recruited when the stimulus is "meaningful" (perceptually integrated) versus when it is "meaningless" (impossible to integrate perceptually). Further along these lines, a broadly similar VEP topography was obtained at the same ISIs with a checkerboard stimulus whose interelement separation was the same as the complete dot matrix. Applying a Laplacian transformation to these data provided a reference-free interpretation of the scalp potential fields, and localized current sources and sinks to the occipital region of the head.

In the second series of investigations, it was found that VEP topography exhibited a dipolar potential field distribution with upper half-field stimulation and a monopolar field distribution with lower half-field stimulation. Dipole localization techniques were used to test the hypothesis that the VEP was generated in extrastriate cortex.

The VEPs elicited in a psychophysical temporal integration of form parts paradigm are similar in latency, morphology and topography to the pattern onset VEP originally described in detail by Jeffreys and Axford (1972a; 1972b). A large body of literature has since accumulated concerning the physiological response properties of the pattern onset response. To the extent that this VEP can be considered to reflect the activity of the principal neuronal encoding mechanisms underlying visible persistence, this literature can be brought to bear upon the interpretation of the functional significance of these encoding operations. For example, C.II of the pattern onset response is known to be predominantly and specifically sensitive to the appearance of discrete and sharply defined stationary contours in the central few degrees of the visual field (Jeffreys, 1977; Jeffreys & Musselwhite, 1986; Spekreijse et al., 1973). C.II is significantly degraded by pattern defocusing, and by pattern preadaptation with contours at the same or at spatially adjacent locations of the visual field (Jeffreys, 1977).

Jeffreys and Musselwhite concluded that C.II reflects the activity of "contour-specific cortical processes involved in the spatial analysis of the visual stimulus" (1986; p. 640). This

description fits well with the assertion that the VEPs elicited by the stimuli in a temporal integration of form parts paradigm reflect the activity of neuronal mechanisms that are involved in the encoding of "as yet meaningless features such as dots, bars, edges and discontinuities" (Di Lollo, 1980, p. 74) and can account for the persisting visibility of the spatial locations of the dot stimuli that makes possible the perceptual integration of temporally discrete form parts. The retinotopic organization of the probable generators of the dot matrix VEPs strongly supports the inference that spatial location is encoded at this level of visual information processing.

The stated aim of the present thesis was to gather neurophysiological evidence bearing on the major theoretical accounts of visible persistence. It has accomplished this goal to the extent that the persistence manifest in perception can be plausibly related to the persistence manifest in visual evoked potentials. It must be noted at this point that the relation demonstrated here is that of a compelling covariation between the temporal properties of the neurophysiological and psychophysical measures, and as is well-known, correlation does not imply causation.

The disciplines of perceptual psychophysics, on the one hand, and visual neurophysiology, on the other, have quite different historical origins and deal with different levels of phenomena (mental versus physical events). Brindley (1960) originally proposed that special kinds of linking, or bridging hypotheses are required to bring psychophysical and physiological statements into a single realm of discourse. More recently, Teller (1984) has systematized the general classes of linking propositions that are commonly employed, implicitly or explicitly, by visual scientists. Her goal was to sensitize visual scientists to the logical structure and ancillary assumptions of their bridging arguments. She cautions that implicit linking hypotheses should be stated explicitly, in order to avoid the introduction of "unacknowledged, non-rigorous" steps into bridging arguments.

In the context of the present thesis, the implicit linking proposition resembles in logical structure what Teller has labeled an "analogy": The proposition that ".. if psychophysical and physiological data can be manipulated in such a way that they can be plotted on meaningfully

similar axes, such that the two graphs have similar shape, then that physiological phenomenon is a major causal factor in producing that psychophysical phenomenon" (1984, p. 1240). This thesis has demonstrated that a psychophysical measure of visible persistence (accuracy in the temporal integration of form parts), and a physiological measure of visual cortical activity (proportion of temporal overlap of VEPs elicited by the sequential form parts), are plotted against either ISI or duration of the leading display, the two graphs have a similar shape. The shape of the graphs thus plotted is consistent with a processing account of the neuronal activity underlying the perceptual phenomenon, but not with a storage account of this neuronal activity.

It is therefore proposed that the physiological phenomenon is a major causal factor in producing the psychophysical phenomenon. However, the finding that two curves look alike does not constitute an explanation for the phenomenon. The valid use of analogy requires considerable supporting evidence. A first step in this direction was taken by characterizing, insofar as was possible, the cerebral generators of the VEP. It is now possible to further strengthen the linking proposition, (or to falsify it) in future studies relating the known properties of these cerebral generators and those of visible persistence.

APPENDIX 1: SOURCES AND SOURCE LOCALIZATION

Sources In the Brain

The genesis of cerebral fields is a complex and interdisciplinary topic, requiring an understanding of both the physical and biological underpinnings of field generation. This appendix provides a summary of relevant concepts from electromagnetism (static fields) and from neurophysiology (neuronal current sources[5]). Having established the physical and physiological bases for the generation of cerebral fields, this appendix goes on to consider two issues relevant to the interpretation of EEG. First, the morphology of individual neurons and groups of neurons is an important determinant of extracerebral fields. The open-field model of EEG generation proposes that only one class of cortical cells, pyramidal neurons, are morphologically suited to make a significant contribution to extracerebral fields. Supporting and contrary evidence for the open-field model is considered. Second, not all types of neuronal electrical events are likely to contribute to extracerebral fields. Most researchers concur that postsynaptic potentials, rather than action potentials, are the primary contributors to extracellular fields. Evidence for this position is reviewed.

Static Fields

[5] The term "source" has somewhat different meanings in different contexts in the following discussion. In the context of the extracellular space surrounding an active neuron, a source refers to a site of outward current flow, where positive charge is injected into the extracellular space from the neuron; a site of inward current flow, where positive charge flows into the neuron from the extracellular space, is referred to as a "sink". In the context of the EEG and MEG, a source refers to a configuration of current flow in a restricted region of active brain tissue. It is the aggregate flow of currents in this region of active neural tissue which generates the electric and magnetic fields which are detected at the scalp and over the surface of the head.

Electric and magnetic fields are generated by electrical currents, the movement of charged particles through space. There are several types of electrical currents caused by the motion of free charges. Conduction currents in conductors and semiconductors are caused by the drift motion of conduction electrons and/or holes; convection currents result from motion of electrons and/or ions in a vacuum; and electrolytic currents are the result of movement of positive and negative ions in solution. In electrophysiological situations, of course, charge is carried by electrolytic current.

The laws of electromagnetism form the link between electrolytic currents in the brain and the electromagnetic fields measured outside of the head. In physics, electromagnetic fields are considered in two separate situations: static and time-varying fields. The simplest situation is that in which currents and fields are static - i.e. all charges are fixed in space, or if they do move, they move as steady flow in a circuit. In this case, the electric and magnetic fields can be treated and calculated as distinct, independent phenomena. A more complicated situation arises when there are rapid changes in current flow (for example, when a capacitor is charged), since the electric and magnetic fields become coupled and must be calculated as interdependent phenomena. Biological currents are obviously time-varying, but within the low frequency range of interest in electrophysiology, the time-derivative can reasonably be approximated as zero and the currents and fields considered as if static at any given instant of time (Plonsey & Heppner, 1967). This "quasi-static" approximation represents an enormous simplification over the time-varying case, since the relatively simple equations of electrostatics can be employed.

Electrostatic Fields

The French scientist Charles Augustin de Coulomb (1736-1806) formulated a mathematical description of the forces between charged particles. Coulomb's law states that the force acting on a point charge at a distance from another point charge varies in proportion to the product of the charges and inversely as the square of their distance apart. The forces between

charged particles are discussed, as a matter of convenience, in terms of an electric field, a vector force with direction and magnitude. Electric lines of force, illustrated in Figure A-1, originate on and come out of positive charges, whereas they are directed toward and end on negative charges. The magnitude of the electric field is taken to be the electric force on a positive test charge divided by the magnitude of the test charge, with units of newtons per coulomb (or volts per meter).

Figure A-2 provides a pictorial representation of the electric field as the force on a unit positive test charge in two simple charge distributions. In the case of the charged particle A at a distance from two oppositely and equally charged particles (Figure A-2A) , A will experience a force that is the vector sum of two oppositely directed forces. Figure A-2B shows the lines of force about two positively charged particles. In these representations, it can be seen that where the lines of force are closest together the field is strongest.

When there are more than two charges to consider, the force on any single charge is the vector sum of the Coulomb forces from each of the other charges (the principle of superposition).

Electric Potential Energy

Since the electric field is defined as the force acting on a unit positive test charge, work must be done in moving a positive charge against the electric field. The work done in moving a test charge from point A to point B in an electric field is defined as the potential difference between points A and B, and is computed by multiplying the force of the electric field by the distance moved by the test charge. The units of electric potential are newton-meters per coulomb, or equivalently, volts. A close analogy exists between the potential energy of a body falling under the influence of a gravitational field and the falling of a charge across a potential difference under the influence of an electric field.

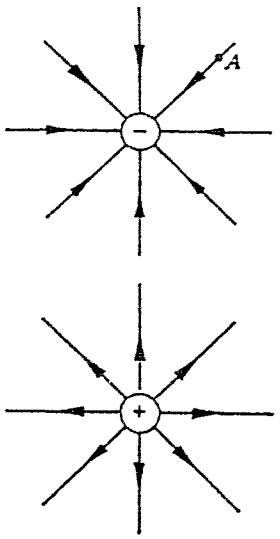

Figure A-1. The electric field is directed radially inward toward a small negative charge and radially outward from a small positive charge. (Figures 1-4 are from Bueche, 1977).

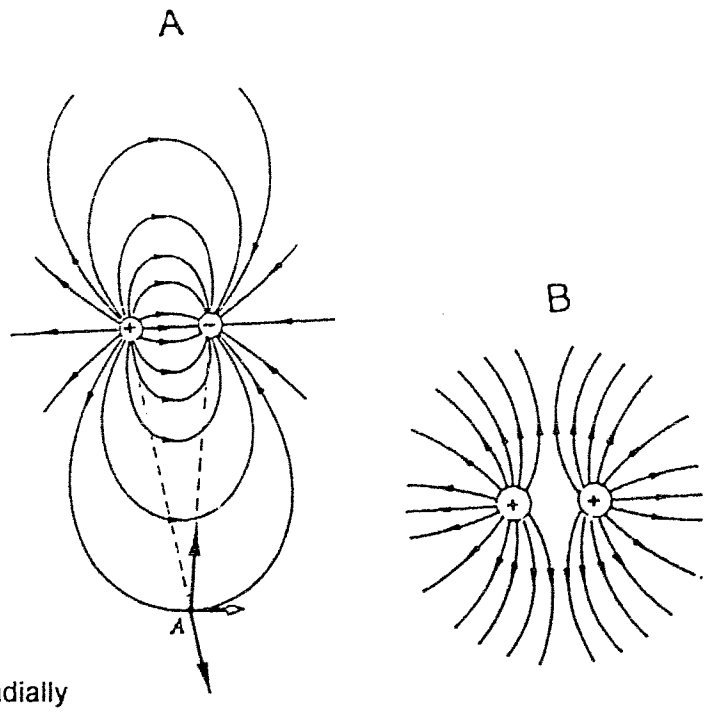

Figure A-2. Electric field lines for two simple charge distributions. (A) A negative and a positive charge. (B) Two positive charges.

While work must be done to move a positive charge against an electric field, no work is needed to move the charge in a direction perpendicular to the field. By definition, then, there is no potential difference between points A and B shown in Figure A-3, and all points on the dashed line between A and B are at the same potential. No work is done in moving a charge along such an equipotential line or plane since this motion is perpendicular to the lines of force, the electric field. Conversely, the lines of force are perpendicular to the equipotential lines. Since no work is done in moving a charge along equipotential lines, the work done in moving a charge from point A to any other point is independent of the path taken, and the static electric field is termed a

conservative field. That is, the electric potential difference between two points is a constant which is not dependent upon the path used for its computation.

Since electric potential measurements are concerned with differences in potential, the choice of a position with "zero" potential is purely arbitrary. At the atomic level, the "absolute" potential at a point is defined as the work done in moving a test charge from infinity to that point, while in electrical-circuit theory the wire attached to the ground is usually taken to have zero potential energy. In monopolar EEG recording, potential differences are recorded between an "active" electrode and a supposedly "inactive" reference electrode, often placed on the ears, mastoid, or nose. [6]

Figure A-3. Points A and B are on an equipotential line.

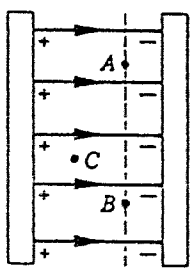

Neuronal Current Sources

[6] The assumption of an inactive reference electrode is generally not supportable, for several reasons. First, since potential fields generated by sources in the brain are confined to the head, the reference electrode must also be on the head. Little or no current flows through the volume constriction of the neck, and so there is no potential difference between the neck and the body due to the source in the head: A reference electrode anywhere below the neck will effectively be equivalent to a reference on the neck. Placing the reference on the body will have no advantage over a cephalic reference, but may have the disadvantage of introducing EKG artifact into the EEG recording (Nunez, 1981). Secondly, since scalp EPs are likely to be generated by active brain regions of substantial size, there is no point within the dimensions of the head which is far enough away from the current source to be truly indifferent (Nunez, 1981). The implications of the foregoing considerations are that the scalp recorded potential is dependent upon the locations of both the active and reference electrodes, and the potential fields recorded may be strongly influenced by the choice of reference electrode.

Electrolytic currents in the brain are established by the changes in membrane permeability associated with neuronal excitation. In the resting state, a separation of charge, carried primarily by cationic sodium and potassium and anionic chlorine ions, is maintained across the neuron membrane such that a penetrating microelectrode registers a potential difference (the resting potential) between the outside and the inside of the neuron of some 40 to 90 uV (negative inside). This charge separation is actively maintained by metabolic pumps in the neuron membrane, and passively maintained by the semipermeant properties of the membrane itself. When the membrane permeability to a particular ion species is changed, charge carried by the aforementioned ions moves across the cell membrane to restore electrical and osmotic neutrality for that particular ion. The movement of charge across the cell membrane per unit time is, by definition, electrical current, measured in units of coulombs per second or amperes.

The direction of current flow is by convention in the direction of movement of positive charge. Since the gated channels of the neuron membrane are selectively permeable to particular ions, the type of channel opened will determine the direction of current flow. When sodium channels in the cell membrane are opened at the resting potential, inward current flow results in the "depolarization" of the membrane, such that the potential difference across the cell membrane is decreased. When either potassium or chlorine channels are opened at the resting potential, osmotic and electrostatic forces act to produce outward current flow, increasing the potential difference across the cell membrane and "hyperpolarizing" the cell. These events, inward versus outward current flow, have important consequences for the excitability of the cell: hyperpolarizing the cell makes it less excitable by moving the membrane potential further away from the firing threshold, while depolarizing the cell makes it more excitable by moving the membrane potential closer to the firing threshold. Hyperpolarizing events are therefore referred to as "inhibitory", while depolarizing events are referred to as "excitatory". Inhibitory and excitatory electrical events are initiated, by chemical neurotransmitters released by a presynaptic neuron, at the postsynaptic membrane of a receiving neuron. These events are thus referred respectively as inhibitory and excitatory postsynaptic potentials (IPSPs and EPSPs).

The transmembrane current initiated at the synapse by PSPs results in (oppositely directed) intracellular and extracellular return currents which complete the circuit of current flow. For the case of an EPSP, current leaves the extracellular space for the inside of the neuron at the site of the synapse, and this site is referred to as a current "sink". To complete the circuit, current flows within the neuron (intracellular current) and back across the cell membrane into the extracellular space to return to the site of the synapse (extracellular, or "volume" current). The location at which current leaves the cell to enter the extracellular space is referred to as a current "source". In a excitatory synapse, sinks are concentrated at the synapse, while the sources are distributed along the cell membrane, with the strength of the sources decreasing in an exponential manner with distance from the synapse. The opposite configuration holds for IPSPs: a local source at the synapse and distributed passive sinks at nonsynaptic sites.

All three classes of currents, transmembrane, intracellular and extracellular, generate electrical and magnetic fields. The transmembrane current initiated by synaptic events will of course determine the magnitude and time course of the other two currents, but does not itself produce a detectable field at a distance from the active neuron. The EEG, by its nature, is sensitive to volume currents. Figure A-4 depicts an EPSP in different regions of a cortical pyramidal cell and the resultant extracellular fields encountered by a recording electrode in the surrounding volume. The electric lines of force in this diagram correspond to the path of extracellular current flow in the volume. The EEG actually measures the potential difference between two electrodes placed at different isopotential lines of this field (since, of course, no potential difference will be recorded between two electrodes on the same isopotential line). Not depicted in this figure is the effect of barriers to current flow, such as the highly resistant medium of the skull, on the potential field. Since current follows the path of least resistance, these barriers will have the effect of distorting the potential field recorded at the scalp, a major problem in the interpretation of the generators of the EEG.

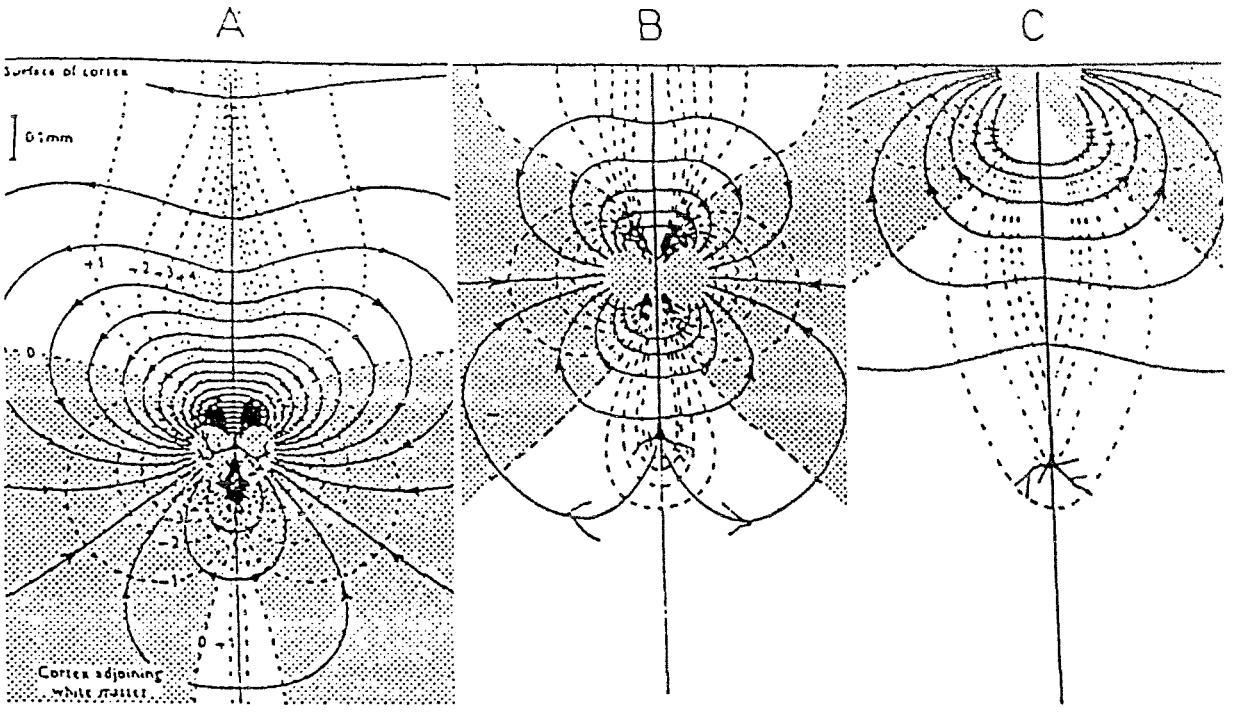

Figure A-4. Theoretical extracellular fields generated by depolarization of different parts of a pyramidal cell. (A) Depolarization of somatic region. (B) Depolarization of middle region of the apical dendrite. (C) Depolarization of the distal end of the apical dendrite. Solid lines are current flow lines. Arrows indicate the direction of flow of positive charges. The density of the lines indicates the density of current. Broken lines are voltage contours numbered on an arbitrary but linear scale with reference to the potential at a distant point. Shading indicates negative potential. (From Gabor, 1978).

Morphological Considerations

Cortical Histology

In comparison to other vertebrate brains, the human brain is distinguished especially by the large expanse and complex infolding of the neocortex. Since the EEG records activity primarily from the neocortex, its cellular organization has important implications for the interpretation of the physiological basis of the EEG.

The cerebral neocortex refers to a thin (2-4 mm) sheet of cells covering the gross aspect of most of the cerebral hemispheres except for the inferior and medial aspects of the temporal lobe. In most areas of the neocortex, six layers can be distinguished, numbered successively

from the superficial layer (layer I) beneath the pial membrane to the deepest layer above the underlying white matter (layer VI). Each layer is distinguished by the type of and components of cells contained in it. Layer I is made up largely of glial cells and axons running tangential to the cortical surface, but with relatively few neuronal cell bodies. Layers II and III are densely packed with small pyramidal cells which provide the output to other cortical areas. Layer IV contains primarily stellate cells and receives most of the thalamic input to the cortex. Layer V contains the large pyramidal cell bodies whose ascending dendrites extend up through the superficial cortical layers and whose axons provide descending output to the basal ganglia, the brainstem and the spinal cord. Layer VI contains small pyramidal cells which provide output back to the thalamus.

The six layers described above can be identified in most regions of the neocortex, although the pattern of layering varies in different cortical regions. Brodmann (1909; cited in Barr & Kiernan, 1988) identified 52 distinct cytoarchitectonic areas, but a few simple principles govern the patterning of the layers. First, the heavy thalamic input to sensory areas increases the size of layer IV in these areas. In visual cortex, this layer is so large as to be visible to the naked eye (the band of Gennari). Second, layer V becomes prominent in motor areas because of the large pyramidal cells from which the descending axons originate. Thus, the relative importance of sensory and motor connections in a region of the brain will primarily dictate the pattern of the layering of the cells.

As indicated above, cortical cells consist primarily of two types: pyramidal cells and stellate cells, distinguished on the basis of their shape, size and the pattern of dendritic ramifications into adjoining cell layers. Pyramidal cells are named for the conical shape of their cell bodies. Long (up to 0.5 mm in length) apical dendrites arise from the apex of the pyramidal cell bodies and extend toward the cortical surface at right angles to the overlying layers. Basal dendrites arise from the base of the pyramids and course laterally within their layer of origin to make contact with the dendrites and axons of stellate cells. Axons of the pyramidal cells leave the base and extend to other cortical regions or distant regions of the central nervous system. Stellate cells have a star-shaped appearance conferred by the numerous dendrites that leave at

all aspects of the cell body. These neurons have small, rounded cell bodies with short axons which terminate within cortical columns; they thus serve an interneuron role in the cerebral cortex. As described above, stellate interneurons in layer IV receive projections directly from thalamic nuclei, and project this information vertically within a cortical column to other stellate interneurons and to pyramidal cells.

Open and Closed Fields

The architecture of cortical neurons and their orientation as groups are important determinants of their extracellular fields. Lorente de No (1947) pioneered the study of extracellular potential fields in simplified model configurations of neurons. He pointed out that anatomically symmetrical neurons would exhibit a symmetrical configuration of sources and sinks that would tend to cancel each other, so that no significant extracellular field would be detectable outside of the immediate vicinity of the neuron. The dendrites of cortical stellate cells, for example, are radially distributed about the cell body; synaptic activation of the cell body would result in a central source (or sink) surrounded by a spherical distribution of sinks (or sources). The potential field in this case is equivalent to that of radially oriented source-sink configurations uniformly distributed over the surface of a sphere. In this case, both the radial and the tangential components of current flow will cancel each other and no potential field will be recorded outside of the surface of the sphere. Lorente de No (1947) termed these morphological configurations "closed field" generators. For this reason, the large population of cortical stellate cells have generally not been considered to contribute significantly to the EEG. A similar result holds for populations of neurons that are oriented in a radially symmetric fashion, a configuration seen in many subcortical structures such as the basal ganglia and some thalamic nuclei (Vaughn & Arezzo, 1988).

In contrast to the stellate cells, cortical pyramidal cells exhibit a morphological polarization that results in the generation of "open fields" that can be detected at some distance

from the site of neural activity. These cells have long apical dendrites that extend vertically to the superficial layers of the cortex, basal dendrites surrounding the cell body, and an axon that extends down to the white matter. Synaptic activity at the cell body or the dendrites would result in a superficial source (or sink, depending on the type of synaptic activity) and a deep sink (or source), a situation that resembles a simple charge dipole with a resultant potential field that can be detected well beyond the immediate vicinity of the sources and sinks. As a population, cortical pyramidal cells are oriented in parallel, so that synchronous activation would result in summation of the extracellular fields. Examples of the open and closed fields described by Lorente de No (1947) are illustrated in Figure A-5.

Figure A-5. Examples of model potential fields described by Lorente de No (1947). (From Wood & Allison, 1981).

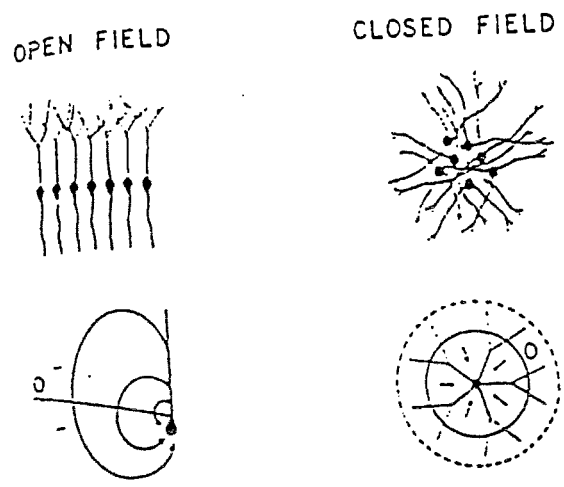

The morphological considerations described above have led to general acceptance of the pyramidal cell model of cortical field potential generation (Creutzfeldt & Houchin, 1974) which assumes that surface-recorded activity is generated primarily by synaptic activity in cortical pyramidal neurons. According to this model, the type of surface wave recorded (positive or negative) is dependent on whether (a) the synaptic activity is excitatory or inhibitory and (b) whether the active synapse is deep or superficial with respect to the cortical surface. An EPSP near the cell body of a cortical pyramidal cell would produce simultaneously a deep active current sink and a superficial passive current source in the apical dendrites. In this case a positive wave would be recorded at the cortical surface. Alternatively, an IPSP near the cell body would result in a passive current sink in the apical dendrites and a negative potential at the cortical surface. Exactly the opposite potentials would be recorded at the cortical surface with superficial synapses: An EPSP would produce a surface negativity and an IPSP would produce a surface positivity. It can be seen that while a knowledge of the configuration of sources and sinks allows prediction of the polarity of the surface potential, it is not possible to work in the opposite direction; the polarity of the surface waveform provides no information on the depth or type of synaptic activity. For example, a surface positive potential could be produced by either a deep EPSP or a superficial IPSP.

The strongest support for the dipolar model of cortical field potential generation is provided by intracranial recording studies in humans and animals. First, transcortical polarity inversions are observed with depth recordings. The evoked potential reverses in polarity as a recording electrode is inserted perpendicularly from the surface of the cortex to the underlying white matter, an observation which is consistent with the model of vertically oriented source-sink configurations. Transcortical polarity inversion is a very general finding and has been observed in the sensory cortex of all modalities (Amassian et al., 1964; Arezzo et al., 1975; Kraut et al., 1985).

A second line of evidence for the dipolar model comes from intracranial recording studies which report close correlations between the type of postsynaptic activity in cortical

pyramidal cells and the polarity of the surface evoked potential. Creutzfeldt et al. (1966) studied PSPs and EPs obtained with electrical stimulation of motor cortex in the anesthetized cat and provided evidence for many of the details of the open-field model .

Criticisms of the Open-Field Model

While most reviews of the cortical electrogenesis of evoked potentials emphasize the role of pyramidal cells, there is a paucity of direct experimental evidence for this model aside from that outlined above. Support for the model is drawn from histological, rather than electrophysiological evidence: (a) pyramidal cells constitute two-thirds of neuronal cells in the cortex; (b) the morphological asymmetry of pyramidal cells fits the criterion for Lorente de No's "open field generator"; (c) pyramidal cells are oriented in parallel to one another and their fields are likely to sum if they are synchronously active.

While the open field model predicts the observed transcortical polarity inversion of evoked potentials, there are often complex changes in evoked potential shape and latency with depth (Kraut et al., 1985; Wood, 1982). While the changes with depth can be explained within the simple open field pyramidal model, the predictions are untestable. Humphrey (1968b) criticized the model as follows: "The genesis of cortical surface potentials is usually discussed in terms of pyramidally shaped neurons, with long apical dendrites which extend upward to ramify in the superficial cortical layers. Given this cellular arrangement, and a few qualitative (and sometimes contradictory) statements about electrotonic 'conduction', the inconstant phase relations observed between EEG waves and PSPs of a certain category are easily 'explained'; one merely needs to slide the postulated site of synaptic impingement up or down the apical dendrites until PSPs of a given type would appear to generate the desired wave form at the cortical surface."

Precise information on cortical sources and sinks has only recently become available with the increasing application of the current source density technique to the laminar analysis of

cortical evoked potentials. This technique, first proposed by Pitts (1952), is based on the fact that the second spatial derivative (Laplacian) of the extracellular field potential is proportional to the current sinks and sources in the extracellular space. Assuming constant conductivity, these sink and source currents are the membrane currents which respectively leave and enter the extracellular space through the neuronal membrane.

Kraut et al. (1985) obtained depth profiles of the flash visual EP in unanesthetized monkeys. Current source density analysis of this data showed that the current sinks and sources associated with the major early components of the flash EP are mainly within lamina IVc-β, where lateral geniculate fibers terminate on stellate cells. Although the apical dendrites of layer V and VI pyramidal cells ascend through lamina IVc-β, the stellate cells probably do not synapse upon the pyramidal cells in this layer, as there is a marked decrease in spine density on the pyramidal dendrites at this layer (Lund, 1973). According to the open field model described above, the stellate cells are assumed to have a morphology which is incompatible with the generation of open fields. Kraut et al. (1985), however, propose that asymmetries in the dendritic arbor, as well as asymmetries in the pattern of synaptic input would allow for the generation of open fields.

While the hypothesis that the uniform orientation of apical dendrites of the pyramidal cells provides one anatomical substrate for EP components is valid, the data of Kraut et al. (1985) provide strong evidence that stellate cells, previously considered to be closed field generators, are in fact potent open field generators in the flash EP. Present evidence indicates that most evoked potential components are likely generated by a complex pattern of excitatory and inhibitory activities, occurring in sequence or simultaneously at different layers of the cerebral cortex (Vaughn, 1987). It seems likely that as more information becomes available with the use of the current source density technique, the interpretation of evoked potential in terms of cellular sources and sinks will greatly increase in sophistication. At present, some reviewers propose that "...it is not fruitful to discuss the differences in wiring or cytoarchitectonics between different cortical areas, but rather emphasize the general features of the cerebral cortex" (Hari &

Kaukoranta, 1985). Other reviewers insist that " .. each cortical region must be considered as a distinct generative structure whose electrogenesis is governed by its neuronal structure, connectivity, and pattern of activation...these circumstances preclude the assumption of a common cellular basis for cortical electrogenesis and complicate the specification of models for generators of surface recorded potentials" (Vaughn & Arezzo, 1988).

Physiological Considerations: Action Potentials and Postsynaptic Potentials

The modern view of central nervous system functioning holds that all signalling in nervous tissue can be regarded as changes in the resting membrane potential of neurons. These changes in the resting membrane potential are of two types, with distinct underlying mechanisms: postsynaptic potentials (PSPs) and action potentials (APs). Table A-1 provides a summary of the distinguishing physiological features of these two types of electrical events.

In terms of transmembrane current flow, the action potential is a much larger electrical signal than PSPs are (see Table A-1), and the pioneers of EEG and EP recording assumed that the gross activity of the central nervous system would be comprised primarily of the summation of propagating action potentials, in a manner analogous to the compound action potential recorded from peripheral nerves (Adrian, 1941). Eccles (1951), was the first to take the opposite position: that gross cortical potentials are composed primarily of summated PSPs in the cerebral cortex with little or no contribution from the neuronal action potentials which initiated them. A number of empirical observations provide support for Eccles' position:

1. The timing and duration of cortical EPs correspond to the timing and duration of postsynaptic, rather than presynaptic activity (Eccles, 1951; Humphrey, 1968a).
2. Unitary spikes cannot be recorded outside the cell at distances where PSPs are recorded without appreciable attenuation (Humphrey, 1968a).
3. Cortical EPs and intracellular PSPs can be recorded at levels of anesthesia sufficient to block AP generation (Amassian, Waller & Macy, 1964).

The primacy of PSPs as the basis for most EPs (except for certain short latency EPs) is now well established, but there is less consensus on an explanation of this state of affairs. Since the action potential involves substantial transmembrane current, it is not immediately obvious why it does not make a proportionate contribution to the gross EP. A number of factors contribute to this situation, and different reviewers seem to emphasize different factors.

One important factor is that the short duration (1-2 msec) APs tend to overlap much less than so the long duration PSPs (10-250 msec). Temporal synchronization is thus much more critical in the summation of APs than in PSPs. Recording from the surface of cat somatosensory cortex, Allison (1965) found that direct stimulation of the thalamocortical radiations results in a distinct sequence of potentials, including an early potential corresponding to the thalamocortical volley. However, with stimulation of the peripheral nerve, only a single broader component is recorded. APs are subject to even more temporal and spatial dispersion after initial activation of sensory cortex, making it quite unlikely that they will contribute significantly to any but the very short latency EPs.

Table A-1. Features of Synaptic and Action Potentials

Feature	Synaptic Potential	Action Potential
Amplitude	Small (100 uV to 10 mV)	Large (70 to 110 mV)
Duration	Brief to long (5 msec to 30 min)	Brief (1-10 msec)
Summation	Graded	All or none
Signal	Hyperpolarizing or depolarizing	Depolarizing
Propagation Type	Passive	Active
Propagation Speed	Fast	Slow

A second factor, emphasized by Humphrey (1968b), relates to the differences in spatial distribution of the transmembrane current flow for APs and PSPs. While more current flows across the membrane in the action potential, the portion of the membrane which is depolarized at any one time is small, and the sources and sinks of current flow are close together. The restricted size of potential fields would result in less summation between adjacent neurons and more cancellation of fields between neurons at slightly different depths. For postsynaptic potentials, however, the spatial separation between sources and sinks of current flow may involve large portions of the membrane.

A third factor is that spikes and waves differ in the manner in which they propagate through the extracellular medium. Elul (1972) argues that the extracellular medium offers much less impedance to fast voltage transients than to slow voltage transients because they can be conducted by capacitative coupling rather than actual ion flow. Thus, voltage spikes are free to propagate through brain tissue, while slow voltage transients are confined to the extracellular

space. Since by Ohm's Law the voltage drop is equal to current times resistance, the voltage drop produced by a fast voltage transient will be much smaller than the voltage drop produced by a slow voltage transient.

Finally, the closely-spaced configuration of oppositely-directed intracellular currents produced by a propagating action potential generates an extracellular field that has a much stronger dependence on distance than does the field generated by a postsynaptic potential (Barth, Sutherling & Beatty, 1986).

Source Localization

The Forward and Inverse Problems

The forward problem in EEG can be stated as thus: Given a known configuration of current flow in the brain, we would like to derive the potential field patterns that will be measured on the surface of and above the surface of the scalp respectively. The relationship between electrolytic currents in the brain and the extracerebral fields measured by EEG is described by the laws of electromagnetism, expressed mathematically by the Maxwell equations (see Hari & Ilmoniemi, 1986, for a detailed discussion of the mathematical aspects of the forward problem). As mentioned, the computational aspects of the relationship are considerably simplified by the assumption that, in the low frequency range of interest in physiological situations, all of the terms of the Maxwell equations which are time derivatives can be approximated as zero (i.e., currents are static). Assuming static currents, the electrostatic and magnetostatic formulations of the Maxwell equations can be solved independently (since they have no terms in common) to compute the electric and magnetic fields of a given current source. In contrast, in the case of rapidly time-varying currents, the electric and magnetic fields become coupled and the computation of the electromagnetic field becomes exceedingly complex.

The forward problem can therefore be solved in a relatively straightforward manner with the solution of the Maxwell equations for a given current source. However, it is actually the inverse problem[7] that pertains in the interpretation of EEG: Given a topographical pattern of extracerebral potential fields, we would like to derive the configuration of cerebral currents that gave rise to the empirical fields. It has been known from the time of Helmholtz (1853; cited in Regan, 1989) that there is no unique solution to the inverse problem, because of the principle of linear superposition of fields. Superposition refers to the fact that if a current source generates one field, and a different source generates another field, then the field due to both sources is simply the sum of the two fields. The implication for the inverse problem in bioelectromagnetism is that any given field can be generated identically by an infinite number of different configurations of sources. Since there is no unique solution, the inverse problem in EEG is considered to be an "ill-posed problem" [8].

Since there are an infinite number of possible solutions, one must ultimately appeal to information outside of the strict logic of the problem to solve an ill-posed problem. The approach taken in the bioelectromagnetic inverse problem is to use this outside information to greatly restrict the number of possible generator configurations which can give rise to empirically observed fields. There are three major types of constraints which may be imposed on the inverse problem in EEG: (1) The type of source is constrained to those capable of generating

---

[7] The bioelectromagnetic inverse problem is only one example of the more general class of inverse problems that occur in the physical sciences and in applied fields such as radar and seismology. In fact, there is a journal (*Inverse Problems*) dedicated to this general class of problems. Ill-posed problems constitute a subset of inverse problems.

[8] There are in fact three criteria which must be met to ensure that an inverse problem is "well-posed" (Balish and Muratore, 1990):

1. There must exist an inverse. In EEG the inverse is the source.

2. The inverse must be unique. This condition is not met in EEG because of superposition.

3. The inverse must be stable. EEG measurements contain an unknown amount of "noise", of instrumental and biological origin. If the inverse solution is substantially influenced by noise, it is not stable.

extracerebral fields. For theoretical and empirical reasons (discussed below) only one type of source - the current dipole - is generally considered in the inverse problem. (2) The number of sources is generally constrained to a few or only one current dipole. (3) The possible spatial locations of sources are constrained by anatomical and physiological considerations. For example, the known anatomy of sensory pathways and cerebral cortex greatly limits the number of plausible locations for dipole sources. Given these considerations, the inverse problem can be restated as that of choosing among a finite, even small, number of possible source configurations (Vaughn & Arezzo, 1988) .

Even a severely constrained inverse problem has no unique solution and can be "solved" only in an iterative, least-squares sense. The classic dipole localization method (DLM) uses such an iterative strategy. For a given instant in time, a current source configuration is chosen arbitrarily and the forward solution computed for that configuration. The surface field predicted from the forward solution is then compared to the observed field using goodness of fit statistics. The source parameters are then altered slightly and the process is repeated, using numerical minimization techniques to ensure convergence, until a goodness of fit criterion is reached. DLM was first developed for the EEG by Schneider (1972) and Henderson et al. (1975) and applied to empirical evoked potentials by Darcey et al. (1980) and Sidman et al. (1978). The method was later extended to neuromagnetic data by, among others, Okada (1985), Stok (1986) and Weinberg et al. (1987).

The classic "time-slice" DLM is generally used to estimate a single source for the empirical field at a given instant in time. The estimation of multiple sources has become more practical with the recent development of the spatio-temporal dipole model (STDM; Scherg & Von Cramon, 1985). This method uses all time points over a defined interval and applies additional constraints to reduce the number of source parameters to be estimated. The additional constraints are based on the idea that EPs involve neural tissue that remains active over some time, so that sources may change their strengths, but not their location or orientation over the

prescribed interval. The estimation of multiple sources is made feasible by the reduction in the number of source parameters.

Model of the Source: The Current Dipole

An electric "dipole" refers to the case of two equal and opposite charges which are separated by a small distance d. A "current dipole" refers to the case of a source and a sink for current flow separated by a short distance, a case which approximates the physiological situation encountered in neurons. It can be proved that for any arbitrary configuration of charges or currents which is on the whole electrically neutral, the electric field can be expressed mathematically as a multipole expansion, with a monopole, dipole, quadrupole, octupole etc. terms (Feynman, 1963). The monopole term drops out because of electrical neutrality, the contribution of the dipole term to the potential field drops off as the inverse square of distance, and the contribution of the higher order terms drop off as the inverse of increasingly higher powers of distance. The result of importance is that at measurement distances far enough away from any configuration of charges or currents which is as a whole electrically neutral, the potential field can be approximated by the dipole term of the multipole expansion. This greatly simplifies the computational aspects of electric field problems, and accounts for the importance of the electric dipole in the physical sciences, even though the simplest case of a pair of point charges or point sinks and sources (a "literal" dipole) is quite rare.

The potential Φ of a current dipole, at distances large in comparison to the length of the dipole, can be expressed quantitatively as

(1)

$$\Phi = \frac{Id \cos\theta}{4\pi\sigma r^2} \quad , \quad r >> d$$

where I = current,

d = length of dipole (distance between source and sink)

r = measurement distance from the center of the dipole

θ = angle with respect to axis of current dipole

σ = conductivity of medium

(Nunez, 1981, p. 117)

Note that equation (1) holds (the dipole approximation is valid) when the distance at which the field is measured is much larger than the length of the dipole, an assumption that is valid in the EEG since the distance between active tissue and the measuring electrode is certain to be considerably larger than the separation between sources and sinks in neurons. As a consequence, the relation between neural activity and the generated electric fields can be modeled with considerable accuracy by a current dipole model. Equation (1) can be employed to calculate the solution of the "forward problem" in EEG: Given a brain generator source which can be modeled as a current dipole, the potential field on the surface of the scalp can be calculated from knowledge of the dipole's magnitude (magnitude = dipole moment = $I * d$) and location (its depth and orientation) in the brain, and the conductivity of the intervening medium (the head).

Physiological Significance of the Dipole Model

Wood (1982) distinguishes three versions of the assumption that extracerebral fields are generated by dipoles in the brain:

Literal Dipole Assumption: The instantaneous field over the scalp (a) closely approximates that of a dipole field; because (b) it is in fact generated by a current dipole.

Equivalent Dipole Assumption (with Spatial Constraints): The instantaneous field over the scalp: (a) closely approximates that of a dipole field; (b) is generated by a spatially restricted region of current sources and sinks; and (c) has an equivalent dipole located in or near the region of sources and sinks.

Equivalent Dipole Assumption (with no Spatial Constraints): The instantaneous field over the scalp: (a) closely approximates that of a dipole field; (b) is generated by an arbitrary distribution of current sources and sinks; and (c) has an equivalent dipole that could be located anywhere relative to the distribution of current sources and sinks.

Wood (1982) points out that the requirements of the literal dipole assumption are never met in physiological situations, since a physical dipole refers to two closely spaced point sources of current having equal and opposite polarity. Neuronal sources and sinks, on the other hand, are always spatially distributed to some extent, and the fields measured by EEG are the sum of those generated by large patches of cortex. In fact, the results of DLM on their own meet the requirements of only the weakest version of the dipole assumption - the equivalent dipole with no spatial constraints. The "dipole" in the DLM is a mathematical description of a field, referring to the second term in the multipole expansion that expresses the field of any arbitrary configuration of sources. As such, the results of DLM are in fact entirely mute with respect to the actual source-sink configuration.

"Localization" of an equivalent current dipole, then, does not necessarily permit inferences concerning the "location" of the current source(s). The concept of an equivalent dipole refers to the dipole whose extracerebral field best approximates the summated fields generated

by multiple current sources. For example, the field produced by a layer or sheet of dipoles can be approximated by a single large dipole located near the center of the sheet; the latter is said to be the equivalent or resultant dipole of the former. A single equivalent dipole is obviously not a particularly useful description for distributed activity involving large regions of the brain. However, if it is known from other lines of evidence (for example, the anatomy of a sensory projection area or from intracranial recordings) that a particular evoked potential or evoked field is generated from a restricted region of the brain, then useful inferences can be made from the localization of an equivalent current dipole. Thus, information from other sources must be combined with DLM in order to meet the requirements of the spatially constrained version of the equivalent dipole assumption.

Models of the Volume Conductor

Since volume currents follow the path of least resistance, and since the media of the brain and its coverings are not uniformly conductive, the path for volume current flow between the cerebral generators and the extracerebral recording sites is not a direct one. Therefore, volume current fields present a somewhat distorted picture of the underlying generators. Accurate source localization requires that volume current distortions must be accounted by modeling the geometries and impedance characteristics of the brain and its coverings (including cerebrospinal fluid, skull, and scalp).

The most widely used model of the head for EEG inverse calculations is the three concentric spheres model, representing the brain, skull and scalp. Conductivity is assumed to be uniform within each sphere. A fourth sphere, representing the cerebrospinal fluid, may be added, but it has been found that differences in predicted surface potentials between the three and four sphere models are smaller than errors due to uncertainty in skull properties (Nunez, 1981), and the two models may be viewed as equally accurate.

Unfortunately, relatively few studies to date have directly addressed the question of accuracy of dipole localization using EEG data. Smith et al. (1985), using a four-sphere model,

localized implanted dipole sources in human epilepsy patients with an accuracy of 20 mm. In a similar study of implanted sources in epilepsy patients, Cuffin et al. (In Press) reported an average localization accuracy of 11 mm. with a four-sphere model. Cohen et al. (1990) used a four-sphere model in the first direct comparison of EEG and MEG (magnetoencephologram) localization accuracy for implanted dipole sources in human patients. This group reported an average EEG localization accuracy 10 mm - compared to an average MEG localization accuracy of 8 mm. This study is currently the subject of some controversy in the MEG community, given Cohen et al.'s (1990) conclusion that "...the MEG offers no great advantage over the EEG in localizing a dipole source."

The concentric spheres models neglect a number of factors that affect the distribution of volume currents in the head. The most important of these factors include the nonspherical geometry of the head, variations in skull and scalp thickness and foramina in the skull. In addition, very little data is presently available on the local resistance of the living skull (that is, the local resistance times the local thickness). More realistic models of the volume conductor in EEG are presently being developed. One model (Nunez, 1990) deals with local variations in skull thickness and the presence of foramina by modeling the head as a large number (1500) of finite elements. Once again, model realism is obtained at the expense of an enormous increase in computational complexity - finite element models require supercomputer resources, while the inverse calculations using the concentric spheres models can be performed on a fast personal computer.

REFERENCES

Adrian, E.D. (1941). Afferent discharges to the cerebral cortex, from peripheral sense organs. Journal of Physiology, 100, 159-191.

Allison, T. (1965). Cortical and subcortical evoked responses to central stimuli during wakefulness and sleep. Electroencephalography and clinical Neurophysiology, 18, 131-139.

Amassian, V.E., Waller, H.J. & Macy, J. (1964). Neural mechanism of the primary somatosensory evoked potential. Annals of the New York Academy of Science, 112, 5-32.

Arezzo, J., Pickoff, A. & Vaughn, H.G. (1975). The sources and intracerebral distribution of auditory evoked potentials in the alert rhesus monkey. Brain Research, 90, 57-73.

Atkinson, R.C. & Shiffrin, R.M. (1968). Human memory: A proposed system and its control processes. In: K.W. Spence & J.T. Spence (Eds.), Psychology of learning and motivation: Advances in research and theory (Vol. 2). New York: Academic Press.

Balish, M. & Muratore, R. (1990). The inverse problem in electroencephalography and magnetoencephalography. Advances in Neurology, 54, 79-88.

Barr, M.L. & Kiernan, J.A. (1988). The Human Nervous System. Philadelphia: J.B. Lippincott Co.

Barth, D.S., Sutherling, W. & Beatty, J (1986). Intracellular currents of interictal penicillin spikes: Evidence from neuromagnetic mapping. Brain Research, 368, 36-48.

Baumgartner, C., Sutherling, S.W. & Barth, D.S. (1989). Journal of Neuroscience Methods, 30, 175-184.

Brindley, G. (1960). Physiology of the retina and visual pathways (1st ed.). London: Edward Arnold.

Breitmeyer, B.G. (1984). Visual masking: An integrative approach. Oxford University Press: New York.

Butler, S.R., Georgiou, G.A., Glass, A.., Hancox, R.J., Hopper, J.M and Smith, K.R.H. (1987). Cortical generators of the C1 component of the pattern-onset visual evoked potential. Electroencephalography and clinical Neurophysiology, 68, 256-267.

Caceci, M.S. & Chacheris, W.P. (1984). Fitting curves to data. Byte (May), 340-360.

Cheyne, D.O. (1986). Magnetic and electric field measurements of brain activity preceeding voluntary movements: Implications for supplementary motor area function. Ph.D. Thesis: Simon Fraser University.

Cheyne, D.O. (1991a). MEG-EEG source modeling program. Unpublished user's manual: Simon Fraser University.

Cheyne, D.O. (1991b). Neuromagnetic fields accompanying unilateral and bilateral movements: topography and analysis of cortical sources. Electroencephalography and clinical Neuophysiology, 81,284-298.

Cohen, D., Cuffin, B.N., Yunokuchi, K., Maniewski, R., Purcell, C., Cosgrove, G.R., Ives, J., Kennedy, J. & Schomer, D. (1990). MEG versus EEG localization test using implanted sources in the human brain. Annals of Neurology, 28, 811-817.

Coltheart, M. (1980). Iconic memory and visible persistence. Perception and Psychophysics, 27, 183-228.

Creutzfeldt, O. & Houchin, J. (1974). Neuronal basis of EEG-waves. In: A. Remond (Ed.) Handbook of Electroencephalography and Clinical Neurophysiology, 2C, 5-55. Elsevier, Amsterdam.

Creutzfeldt, O.D., Watanbe, S. & Lux, H.D. (1966). Relations between EEG phenomena and potentials of single cortical cells. I. Evoked responses after thalamic and epicortical stimulation. Electroencephalography and clinical Neurophysiology, 20, 1-18. II. Spontaneous and convulsoid activity. Electroencephalography and clinical Neurophysiology, 20,19-37.

Cuffin, B.N., Cohen, D., Yunokuchi, K., Maniewski, R., Purcell, C., Cosgrove, G.R., Ives, J., Kennedy, J. & Schomer, D. (In Press). Tests of EEG localization accuracy using implanted sources in the human brain. Annals of Neurology.

Darcey, T.M., Ary, J.P. & Fender, D.H. (1980). Spatio-temporal visually evoked scalp potentials in response to partial field patterned stimuli. Electroencephalography and clinical Neurophysiology, 50, 348-355.

Dawson, G.D. (1951). A summation technique for detecting small signals in a large irregular background. Journal of Physiology, 115, 2P-3P.

DeMunck, J.C., Vign, P.C.M. & Spekreijse, H. (1991). A practical method for determining electrode positions on the head. Electroencephalography and clinical Neurophysiology, 78, 85-87.

Di Lollo, V. (1979). Luminous calibration of oscilloscopic displays. Behavior Research Methods & Instrumentation, 11, 419-421.

Di Lollo, V. (1980). Temporal integration in visual memory. Journal of Experimental Psychology: General, 109, 75-97.

Donchin, E. & Coles, M.G.H. (1988). Is the P300 a manifestation of context updating?. Behavioral and Brain Sciences, 11, 357-374.

Drasdo, N. (1980). Cortical potentials evoked by pattern presentation in the foveal region. In: C. Barber (Ed.), Evoked Potentials II. New York: Academic Press.

Duysens, J., Orban, G., Cremieux, J. & Maes, H. (1985). Visual cortical correlates of visible persistence. Vision Research, 17, 171-178.

Eccles, J.C. (1951). Interpretation of action potentials evoked in the cerebral cortex. Electroencephalography and clinical Neurophysiology, 3, 449-464.

Elul, R. (1972). The genesis of the EEG. International Review of Neurobiology, 15, 227-272.

Engel, G.R. (1970). An investigation of visual responses to brief stereoscopic stimuli. Quarterly Journal of Experimental Psychology, 22, 148-166.

Eriksen, C.W. & Collins, J.F. (1967). Some temporal characteristics of visual pattern perception. Journal of Experimental Psychology, 74, 476-484.

Fender, D.H. (1987). Source localization of brain electrical activity. In: A. Gevins and E. Remond (Eds.). Methods of analysis fo brain electrical and magnetic signals (Vol. 1, pp. 355-403).

Feynman, R.P. (1963). Lectures on Physics, Vol. 2. Paio Alto: Addison-Wesley

Finley, G. (1985). A high speed point plotter for vision research. Vision Research, 25, 1993-1997.

Gabor, A.J. (1978). Physiological Basis of Electrical Activity of Cerebral Origin. Grass Instrument Company: Quincy Mass.

Geddes, L.A. & Baker, L.E. (1967). The specific resistance of biological materials- a compendium of data for the biomedical engineer and physiologist. Medical and Biological Engineering, 5, 271-293.

Haber, R.N. (Ed., 1969). Information processing approaches to visual perception. New York: Holt, Rinehart & Winston.

Halliday, A.M. & Michael, W.F. (1970). Changes in the pattern-evoked responses in man associated with the vertical and horizontal meridians of the visual field. Journal of Physiology, 208, 499-513.

Hari, R. & Ilmoniemi, R.J. (1986). Cerebral magnetic fields. CRC Critical Reviews in Biomedical Engineering, 14, 93-127.

Hari, R. & Kaukoranta, E. (1985). Neuromagnetic studies of somatosensory system: Principles and examples. Progress in Neurobiology, 24, 233-256.

Hari, R. & Ilmoniemi, R.J. (1986). Cerebral magnetic fields. CRC Critical Reviews in Biomedical Engineering, 14, 93-127.

Henderson, C.J., Butler, S.R. & Glass, A. (1975). The localization of equivalent dipoles of EEG sources by the application of electrical field theory. Electroencephalography and clinical Neurophysiology, 39, 117-130.

Hjorth, B. (1975). An on-line transformation of EEG scalp potentials into orthogonal source derivations. Electroencephalography and clinical Neurophysiology, 39, 526-530.

Hjorth, B. (1980). Source derivation simplifies topographical EEG interpretation. American Journal of EEG Technology, 20, 121-132.

Hogben, J.H. & Di Lollo, V. (1974). Perceptual integration and perceptual segregation of brief visual stimuli. Vision Research, 14, 1059-1069.

Humphrey, D.R. (1968a). Re-analysis of the antidromic cortical response. I. Potentials evoked by stimulation fo the isolated pyramical tract. Electroencephalography and clinical Neurophysiology, 24, 116-129.

Humphrey, D.R. (1968b). Re-analysis of the antidromic cortical response. II. On the contribution of cell discharge and PSPs to the evoked potentials. Electroencephalography and clinical Neurophysiology, 25, 421-442.

Jasper, H. H. (1958). The international 10-20 system of electrode placement. Electroencephalography and clinical Neurophysiology, 10, 370-375.

Jeffreys, D.A. (1977). The physiological significance of pattern visual evoked potentials. In: J.E. Desmedt (Ed.), Visual evoked potentials in man (pp. 134-167). Oxford: Clarendon.

Jeffreys, D.A. & Axford, J.G. (1972a). Source location of pattern specific components of human visual evoked potentials. I. Component of striate cortical origin. Experimental Brain Research, 16, 1-21.

Jeffreys, D.A. & Axford, J.G. (1972b). Source location of pattern specific components of human visual evoked potentials. II. Component of extrastriate cortical origin. Experimental Brain Research, 16, 1-21.

Jeffreys, D.A. & Musselwhite, M.J. (1986). A visual evoked potential study of metacontrast masking. Vision Research, 26, 631-642.

Kahneman, D. (1967). An onset-onset law for one case of apparent motion and metacontrast. Perception and Psychophysics, 2, 577-584.

Kraut, M.A., Arezzo, J.C. & Vaughn, H.G. (1985). Intracortical generators of the flash VEP in monkeys. Electroencephalography and clinical Neurophysiology, 62, 300-312.

Lesevre, N. & Joseph, J.P. (1979). Modifications of the pattern evoked potential in relation to the stimulated part of the visual field (clues for the most probable origin of each component). Electroencephalography and clinical Neurophysiology, 47, 183-203.

Long, G.M. (1980). Iconic memory: A review and critique of the study of short-term visual storage. Psychological Bulletin, 88, 785-820.

Lorente de No, R. (1947). A Study of Nerve Physiology: Part 2, Vol. 132. New York: Rockefeller Institute.

Lovegrove, W., Bowling, A. & Gannon, S. (1981). Orientation specificity in the visual persistence for gratings and checker boards. Vision Research, 21, 1239-1240.

Lund, J.S. (1973). Organization of neurons in the visual cortex, area 17, of the monkey (Macaca mulatta). Journal of Comparative Neurology, 147, 455-496.

Maier, J., Dangelie, G., Spekreijse, H. & van Dijk, B.W. (1986). Principal component analysis for source locations of VEPs in man. Vision Research, 27, 165-177.

Meyer, G.E., Lawson, R. & Cohen, W. (1975). The effects of orientation-specific adaptation on the duration of short-term visual storage. Vision Research, 15, 569-572.

Meyer, G.E. & Maguire, W.M. (1977). Spatial frequency and the mediation of short-term visual storage. Science, 198, 524-525.

Neisser, U. (1967). Cognitive Psychology. New York: Appleton-Century-Crofts.

Nunez, P. (1981). Electric Fields of the Brain: The Neurophysics of EEG. New York: Oxford University Press.

Nunez, P.L. (1990). Localization of brain activity with electroencephalography. Advances in Neurology, 54, 39-65.

Okada, Y. (1985). Discrimination of localized and distributed current dipole sources and localized and single multiple sources. In: H. Weinberg, G. Stroink & T. Katila (Eds.), Biomagnetism: Applications and Theory. New York: Pergamon Press, pp. 266-272.

Pitts, W. (1952). Investigations on synaptic transmission. In: H. von Foerster (Ed.) Cybernetics, Trans. 9th Conf., Josiah Macy: New York.

Plonsey, R. & Heppner, D.B. (1967). Considerations of quasi-stationarity in electrophysiological systems. Bulletin of Mathematical Biophysics, 29, 657-664.

Regan, D. (1989). Human Brain Electrophysiology: Evoked Potentials and Evoked Magnetic Fields in Science and Medicine. New York: Elsevier.

Riemslag, F.C.C., Spekreijse, H. and Van Wessem, Th.N. (1985). Responses to paired onset stimuli: Implications for the delayed evoked potentials in multiple sclerosis. Electroencephalography and clinical Neurophysiology, 62, 155-166.

Sakitt, B. (1975). Locus of short-term visual storage. Science, 190, 1318-1319.

Sakitt, B. (1976). Iconic memory. Psychological Review, 83, 257-276.

Sakitt, B. & Long, G.M. (1978). Relative rod and cone contributions in iconic storage. Perception and Psychophysics, 23, 527-536.

Sakitt, B. & Long, G.M. (1979). Spare the rod and spoil the icon. Journal of Experimental Psychology: Human Perception and Performance, 5, 19-30.

Scherg, M. (1989). Fundamentals of dipole source analysis. Advances in Audiology, 6, 1-28.

Scherg, M. & Von Cramon, D. (1985). Two bilateral sources of the late AEP as identified by a spatio-temporal dipole model Electroencephalography and clinical Neurophysiology, 62, 32-44.

Schneider, M.R. (1972). A multistage process for computing virtual dipolar sources of EEG discharges from surface information. IEEE Transactions on Biomedical Engineering, BME-19, 1-12.

Sidman, R.D., Giambalvo, V., Allison, T. & Bergey, P. (1978). A method for localization of sources of human cerebral potentials evoked by sensory stimuli. Sensory Processes, 2, 116-129.

Smith, D.B., Sidman, R.D., Flanigin, H., Henke, J. & Labiner, D. (1985). A reliable method for localizing deep intracranial sources of the EEG. Neurology, 35, 1702-1707.

Spekreijse, H., van der Tweel, L.H. & Zuidema, T. (1973). Contrast evoked responses in man. Vision Research, 13, 1577-1601.

Sperling, G. (1960). The information available in brief visual presentations. Psychological Monographs: General and Applied, 74, 1-29.

Sperling, G. (1963). A model for visual memory tasks. Human Factors, 5, 19-31.

Sperling, G. (1971). Information retrieval from two rapidly consecutive stimuli: New analysis. Perception and Psychophysics, 9, 89-91.

Stok, C.J. (1986). The inverse problem in EEG and MEG with application to the visual evoked responses. Ph.D. Dissertation, University of Twente.

Teller, D.Y. (1984). Linking propositions. Vision Research, 24, 1233-1246.

Turvey, M.T. (1973). On peripheral and central processes in vision: Inferences from an information-processing analysis of masking with patterned stimuli. Psychological Review, 80, 1-52.

Turvey, M.T. (1978). Visual processing and short-term memory. In: W.K. Estes (Ed.), Handbook of learning and cognitive processes (Vol. 5). Hillsdale, New Jersey: Erlbaum.

Uttal, W.R. (1981). A taxonomy of visual processes. Hillsdale, New Jersey: Erlbaum.

Vaughn, H.G. (1987). Topographic analysis of brain electrical activity. In: R.J. Ellington, N.M.F. Murray & A.M. Halliday (Eds.), The London Symposia (EEG Suppl. 39), 137-142. Elsevier: Amsterdam.

Vaughn, H.G. & Arezzo, J.C. (1988). The neural basis of event-related potentials. In: Picton, T.W. (Ed.), Handbook of Electroencephalography and Clinical Neurophysiology. Volume 3: Human Event-Related Potentials. Elsevier: New York.

Van der Tweel, L.H., Estevez, O. & Cavonius, C.R. (1979). Invariance of the contrast evoked potential with changes in retinal illuminance. Vision Research, 19 1283-1287.

Weinberg, H., Brickett, P., Coolsma, F. & Baff, M. (1987). Magnetic localization of intracranial dipoles: Simulation with a physical model. Electroencephalography and clinical Neurophysiology, 64, 159-170.

Wood, C.C. (1982). Application of dipole localization methods to source identification of human evoked potentials. Annals New York Academy of Sciences, 388, 139-155.

Wood, C.C. and Allison, T. (1981). Interpretation of evoked potentials: A neurophysiological perspective. Canadian Journal of Psychology, 35, 113-134.